Spring 2016

Alternatives to Charcoal for Improving Chronometric Dating of Puget Sound Archaeological Sites

James W. Brown
Central Washington University, brownjam@cwu.edu

ALTERNATIVES TO CHARCOAL FOR IMPROVING CHRONOMETRIC DATING OF PUGET SOUND ARCHAEOLOGICAL SITES

A Thesis

Presented to

The Graduate Faculty

Central Washington University

In Partial Fulfillment

of the Requirements for the Degree

Master of Science

Cultural and Environmental Resource Management

---

by

James W. Brown

June 2016

CENTRAL WASHINGTON UNIVERSITY

Graduate Studies

We hereby approve the thesis of

James W. Brown

Candidate for the degree of Master of Science

APPROVED FOR THE GRADUATE FACULTY

_____ _____
Dr. Steven Hackenberger, Committee Co-Chair

_____ _____
Dr. Patrick T. McCutcheon, Committee Co-Chair

_____ _____
Dr. James C. Chatters

_____ _____
Dean of Graduate Studies

ABSTRACT

ALTERNATIVES TO CHARCOAL FOR

IMPROVING CHRONOMETRIC DATING OF PUGET SOUND

ARCHAEOLOGICAL SITES

by

James W. Brown

June 2016

Radiocarbon dating of archaeological sites in the Puget Lowlands can be problematic. Dating specific cultural events associated with features and sites is difficult due to the ubiquity of charcoal in forest soils and poor preservation of bone in acidic soils. These conditions have impeded the development of regional cultural chronologies. The lack of dates for critical time periods also inhibits testing processual models of cultural change. Evidence for the timing and rate of ecological, economic, and political change is critical for testing evolutionary models in the Pacific Northwest (PNW).

Radiocarbon dating highly burned bone (calcined bone) and luminescence dating fire-modified rock from cooking features will improve age estimates for features and sites. Calcined bone survives well in archaeological sites with acidic soils that are common in the PNW. Luminescence dating can be applied to fire-modified rock recovered particularly from food processing features.

This study, conducted in collaboration with the DirectAMS and the University of Washington Luminescence Laboratory, summarizes tests designed to compare dates for paired samples of charcoal, calcined bone, and fire-modified rock. The comparisons are based on a model that includes both the nature of target events and properties of the dated material. Test

results show the accuracy and precision of radiocarbon dates for calcined bone and substantiate the utility of luminescence dates.

As possible, two or more of the dating methods should be used together to assign age estimates for features and sites. Within the next 20 years, we may have accumulated sufficient chronometric dates to better outline cultural chronologies for the Puget Sound. More complete chronometric databases and cultural outlines will then better support tests of processual models of cultural changes in the Pacific Northwest.

ACKNOWLEDGEMENTS

I would like to thank my committee for the continual help and support in bringing this project further. This study is a research initiative of DirectAMS, which funded all radiocarbon dating. Dr. James K. Feathers at the University of Washington Luminescence Laboratory for allowing me to intern in his laboratory. Sources of funding for this research include Office of Graduate Studies, Central Washington University Mt. Rainier Field School, Office of Undergraduate Studies, the Science Honors Research Program, and the College of the Sciences. Individuals and organizations contributing samples include Greg Burtchard of Mount Rainier National Park, the Jamestown S'Klallam Tribe, and the Burke Museum. Additional thanks go to The Bray Family, Edgar Huber and Statistical Research Inc. for the funding of the luminescence dates for the Bray Site.

Additional thanks go to my committee: Dr. Hackenberger, Dr. McCutcheon, and Dr. Chatters. I appreciate all the mentorship and guidance through all these years. I hope to work with you all in the future.

To my parents, thank you for instilling me with the drive to get where I am. None of this would have been possible without your support.

And to my cohort and friends, thank you for going with me to get coffee and talking this process through. For being able to talk each other through moments of frustration and annoyance.

Any errors in description or interpretation are solely the responsibility of the author.

TABLE OF CONTENTS

Chapter		Page
I	INTRODUCTION	1
	Problem	3
	Purpose	5
	Significance	6
II	STUDY AREA	7
	Biophysical	7
	Cultural Context	10
III	LITERATURE REVIEW	15
	Radiocarbon Dating and Thermoluminescence Dating	15
	Calcined Bone	17
	Resource Intensification	20
IV	CHRONOMETRIC HYGIENE	25
V	ARTICLE	30
	Abstract	32
	Introduction	33
	Theory	38
	Materials & Methods	40
	Results	45
	Discussion & Conclusion	59
	Acknowledgements	60
	BIBLIOGRAPHY	61
	APPENDIXES	71
	Appendix A—DirectAMS Laboratory Protocol	71
	Appendix B—Radiocarbon Calibration Data	74
	Appendix C—Thermoluminescence Pottery Procedure	90
	Appendix D—Thermoluminescence FMR Procedure	95
	Appendix E—Luminescence Results	98

LIST OF TABLES

Table		Page
1	Study Sites	8
2	Cultural Chronologies of the Northwest Coast and Columbia Plateau	11
3	Count of Material Types of Radiocarbon Dates from Western Washington	26
4	Radiocarbon Dates of Western Washington by Material Types	34
5	Study Sites	41
6	Results of Radiocarbon and Luminescence Dates	46
7	Identified Charcoal-Calcined Bone Match Pairs	56
8	Identified Charcoal-FMR Match Pairs	58

LIST OF FIGURES

Figure		Page
1	Study area	7
2	Distribution of radiocarbon dates by county	27
3	Radiocarbon date curve of western Washington	28
4	Frequency of radiocarbon dates for western Washington	29
5	Accurate medium model	39
6	Map of study area	41
7	Calibrated age ranges of radiocarbon dates and two sigma age ranges of luminescence dates from the bray site earth oven features	49
8	Calibrated age ranges of radiocarbon dates and two sigma age ranges of luminescence dates from the sunrise ridge borrow pit site 30N features	50
9	Calibrated age ranges of radiocarbon dates and two sigma age ranges of luminescence dates from the sunrise ridge borrow pit site feature AA	51
10	Calibrated age ranges of radiocarbon dates and two sigma age ranges of luminescence dates from the sunrise ridge borrow pit site feature AD	52
11	Calibrated age ranges of radiocarbon dates and two sigma age ranges of luminescence dates from the sunrise ridge borrow pit site feature R	53
12	Calibrated age ranges of radiocarbon dates from the fryingpan creek rockshelter feature 1	54
13	Calibrated age ranges of radiocarbon dates from the Sequim bypass site	55

CHAPTER 1

INTRODUCTION

In the Pacific Northwest (PNW) of North America, much of the extant radiometric chronological record has been built using charcoal and marine shell (see Table 3 in Chapter 5). Outside of shell midden deposits, conditions do not preserve organic materials such as bone. Otherwise, charcoal in the PNW is ubiquitous in the soils due to the wide extent of coniferous forests that have succumbed to burning. Dating charcoal is problematic due to the unknown event in which wood material is burned and/or how it was deposited in an archaeological context. Thus, a radiocarbon assayed fragment of charcoal found in association with artifacts cannot be assumed to be of the same age as when the organic material died and when it was deposited without making a bridging argument that connects these two events (Dean 1978).

The event typology developed by Dean defines the event types as the dated event, dated reference event, target event, and the bridging event. Recent studies have reduced the number of event types by combining the dated event and the dated reference event, this research uses the combined event typology of Richter (2007; Richter et al. 2009). The dated event is calculated as the event tied to the age of a material. For example, a charcoal date for a group of tree-rings is an event associated with the death of those rings. The target event is the cultural event to which the age is estimated. A bridging event is the event that links the dated and target events (See Figure 5 in Chapter 5).

Efforts need to be focused on the chronometric dating of materials that have better defined bridging events, such as culturally modified bone and/or fire-modified rock. Charcoal

often lacks accuracy due to the old-wood effect and the possibility of the dated event being caused by natural burning. Due to the acidic nature of the soils in the PNW little to no bone remains in non-shell midden deposits. Where bone does exist in the absence of neutralizing shell deposits, it is either calcined and/or charred. Charred bone is suspect as a medium in radiocarbon dating due to the potential for environmental contamination of the organic fraction and the difficulty of removing said contamination without also removing heat-damaged bone proteins.

Two alternatives are available in chronometric dating, calcined bone, and fire-modified rock. The remnants of calcined bone are a recrystallized inorganic fraction. The association of calcined bone to cultural contexts lends credibility to the accuracy of calcined bone as a medium in the radiocarbon dating of archaeological deposits. Due to the carbon content of calcined bone being an admixture of carbon from the death of the animal and the fuel source this means that calcined bone would be affected by old carbon. Fire-modified rock (FMR) is the heated remains of hot-rock cooking. FMR in association with a charcoal and burned bone context is an accurate medium in the luminescence dating of hearth features. Luminescence dating of FMR is highly accurate but lacks precision due to the large standard error associated with the technique.

Cultural materials such as calcined bone and fire-modified rock are considered to be more accurate due to these materials having a closer association with a cultural event such as the use of a hearth feature. The dating of more accurate media in the PNW is not the only requirement for developing a more refined chronology, but we must resolve the way in which archaeologists in the PNW utilize chronometric dates. Archaeologists in this region lack a model that integrates the dated and cultural event with a well-articulated bridging event (Dean 1978). Development of a model that utilizes more accurate media (see Figure 5 in Chapter 5), such as

culturally modified bone (calcined bone) and fire-modified rock, and tracks the difference of dated versus target events will enable archaeologists to employ greater quantities of accurate chronometric dates in describing cultural change in the PNW.

Utilization of a model that defines the accuracy of materials in chronometric dating is necessary to refine the chronological record of the PNW. Clearly articulating what is actually measured (dated event) and what archaeologists want to know the age of will help target those artifacts that provide a clear path for bridging the two events. More accurate and precise chronologies will provide a timeline that will help us better describe and explain cultural change. Two types of significant cultural change in the PNW are the development of broad-spectrum foraging (8000-6000 B.P.) (Chatters et al. 2011; Mack et al. 2010) and resource intensification (3500-2500 B.P.) (Ames 2002; Chatters 1995; Croes and Hackenberger 1998; Matson 2008; Sheldon et al. 2013). The samples analyzed in this study are especially important for examining questions about the timing and rate of resource intensification.

Problem:

.

Steps must be taken to develop a model of the accuracy of media for chronometric dating. To develop this model, I have conduct a series of dates using radiocarbon and luminescence methods. Using these dates, I examine the relationship of precision and accuracy of charcoal, calcined bone, and fire-modified rock.

Through a series of charcoal-calcined bone matched-pair samples this research aims to show the validity of calcined bone as a medium for radiocarbon dating. Calcined bone survives well in the soils of the PNW due to the processes the bone undergoes during burning with the removal of the organic fraction (Brain 1981; Johnson 1989; Kiszley 1973; McCutcheon 1992;

Shipman et al. 1984). The carbon that remains in calcined bone is a minimal amount found within the mineral apatite structure mixed with carbon from the fuel source (Huls et al. 2010; Snoeck et al. 2014; Van Strydonck et al. 2010; Zazzo et al. 2009; Zazzo et al. 2012). Recent studies in the Old World have shown calcined bone to be a viable medium for the dating of archaeological sites (Lanting and Brindley 1998; Lanting et al. 2001; Naysmith et al. 2007; Zazzo and Saliege 2011; Zazzo et al. 2013). Calcined bone as a form of culturally modified bone does not have a direct correlation between the dated event and the cultural event. In the framework of Dean's (1978) event typology, the bridging event is the time between the death of the animal and the burning of the bone. This bridging event makes calcined bone a more accurate medium then charcoal.

Through a series of charcoal-calcined bone-FMR matched-pairs this research aims to show the validity of FMR as a medium for dating Holocene deposits in the PNW. FMR is a prime material because it preserves better then charcoal and bone. When discovered in hearth contexts it is clearly indicative of a cultural event. The bridging event associated with FMR is the heating of the rock to 500 °C and the last use of the hearth, which is believed to be brief enough that it is of little issue (Richter 2007, Richter et al. 2009) providing FMR to be the most accurate medium. However, due to the nature of luminescence dating with the reporting of large errors, the precision of FMR can be of issue. FMR has been shown to be a viable medium for dating using luminescence dating throughout the world (Aitkens 1985, 1998; Feathers 2003; Wintle 2008). Luminescence dating has been shown as a valid technique in the chronometric dating of old archaeological deposits (Liritzis et al. 2013). In particular, there is significant evidence of luminescence dating being applied to considerably ancient deposits. This research seeks to show

the validity of luminescence dating of FMR as an accurate medium in the dating of Holocene deposits throughout the PNW.

Purpose:

Development and implementation of accelerator mass spectrometry (AMS) in radiocarbon dating (Taylor and Bar-Yosef 2014) and the development of luminescence dating (Aitkens 1985) have made it possible to utilize these materials to date archaeological deposits. There has not yet been adequate work undertaken on the techniques used to develop accurate chronometric dating of PNW sites. The purpose of this thesis is twofold: 1) develop a model that identifies the event typology of media that provide more accurate chronometric dates by furthering the concept of the bridging events for charcoal, calcined bone, and fire-modified rock, and 2) conduct a series of radiocarbon and luminescence dates to produce accurate age estimates of sites without reliable charcoal or shell dates, which would ultimately allow us to evaluate the timing of cultural change in the PNW. This purpose will be achieved with the following objectives:

1) Develop a model of accurate media that is used in identifying contexts and samples for sampling. The model compares the relation of radiocarbon and luminescence dating in the framework of Dean's (1978) event typology.
2) Provide evidence for the reliability of calcined bone as material for the dating of archaeological sites in the mesic environment of the PNW.
3) Provide evidence for the reliability of fire-modified rock as a material for luminescence dating of Holocene age sites in the PNW.

4) Use these chronometric techniques to analyze the use of the accurate medium model in the context of cultural change in the PNW.

Dating techniques are limited without adequate research on the contexts of cultural change, such as: peopling of the new world, Pleistocene/Holocene Epoch technological changes, shifts in settlement and subsistence patterns, and the timing of contact. Thus, the sample selection, dating results, and interpretation utilizes the following research questions:

1) How reliable are calcined bone and fire-modified rock for the chronometric dating of archaeological deposits in the PNW? (Objectives 2 and 3)
2) What relationship of event typology is there between radiocarbon and luminescence dating of shared contexts? (Objective 1)
3) How does the development of a refined event typology model affect the understanding of cultural change in the PNW? (Objective 4)

Significance:

This research generates a new set of accurate chronometric dates for four sites. Comparisons of different types of chronometric dates demonstrates that archaeologists in the region should feel more confident in these dating methods. Future work with all three types of dating methods will lead to the refinement of the chronological record of the PNW. With a better chronological record archaeologists will then be able to resolve broader questions about cultural evolution in the region. The development of larger quantities of accurate and precise chronometric dates will aid in determining the tempo of cultural change, for example punctuated or gradual evolution (Chatters and Prentiss 2005; Dunnell 1980; Eldredge and Gould 1972).

CHAPTER 2

STUDY AREA

The study area in this thesis is the west side of the Cascade Range of Washington (Figure 1). Within this area, I have identified four archaeological sites (Table 1. Study Sites) that meet the criteria of containing discrete cultural contexts in the form of hearth features. Establishing the PNW as the study area of this research is in reference to the Northwest Coast culture area (Ames and Maschner 1999; Matson and Coupland 1995). The PNW is comprised of multiple geographic regions that share similar ecosystems.

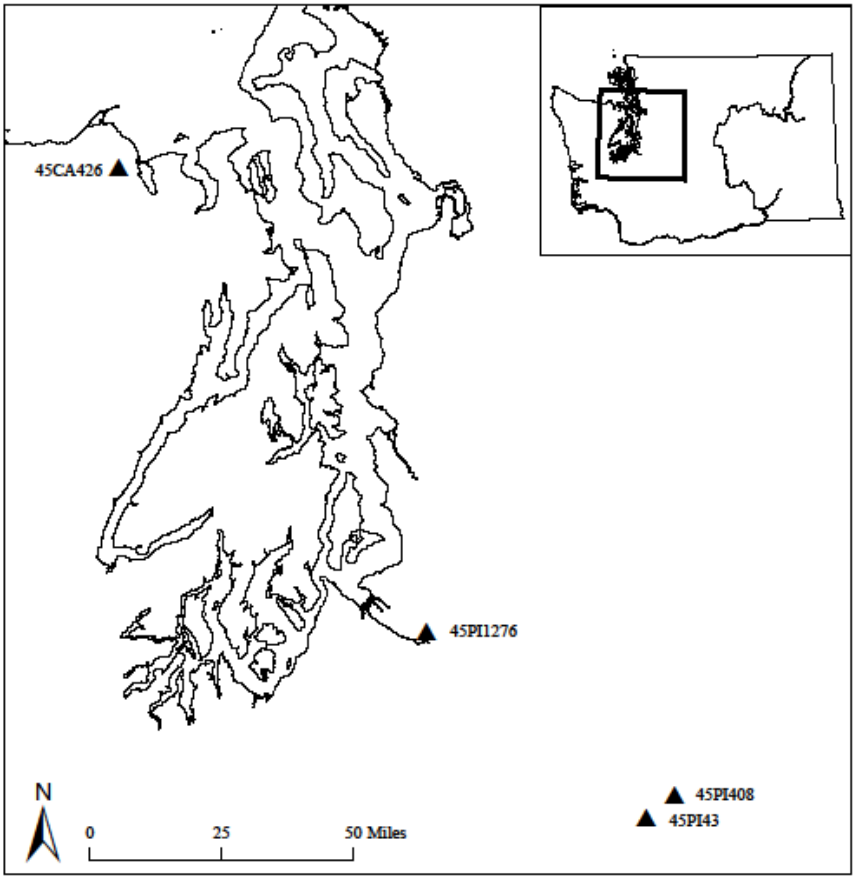

Figure 1. Study Area

Table 1. Study Sites

Site Number	Site Name
Charcoal/Calcined Bone/FMR	
45PI408	Sunrise Ridge Borrow Pit
45PI1276	Bray
Charcoal/Calcined Bone	
45CA426	Sequim Bypass
45PI43	Fryingpan Creek Rockshelter

Biophysical

The four study sites are located within the physiographic regions of the Puget Lowlands, Southern Cascades, and Olympic Peninsula. The climate of the Southern Northwest Coast is typically characterized as wet, cool winters and dry, warm summers. The climate of this region can be attributed to the interplay between the maritime setting of the coast and the continental landmasses of the Washington Cascades causing high annual rainfall and cooler temperatures (Franklin and Dyrness 1988). The average temperature for this region during the winter is around 40°F and during the summers around 65°F; with an average annual rainfall for Seattle of 888 mm (Franklin and Dyrness 1988).

Hallet et al. (2003) and Walsh et al. (2015) summarize environmental and climatic histories of the PNW. In the PNW around 14,000 B.P. the region was covered by Pleistocene glaciers across the lowlands, with a mesic forest covering much of the region south of the glacial advance. Starting 12,900-11,600 B.P. was the Younger Dryas period with a peak cooling in the climate with no new glacial advances. From 10,000-8000 B.P., the glaciers begin to recede. Around 8000 B.P. the hypsithermal began; this was a period of warm and dry temperatures above today's climate which lasted till 5000 B.P. Around 5000 B.P. the Neoglaciation began, this was characterized by an advance of mountain glaciers which led to a decrease in temperature, and this decrease brought the climate to relatively modern climate. The Neoglaciation continued to 3000 B.P. when the Medieval Warming Period began, which increased the temperature of the region, this warming occurred from 2000-900 B.P. Following the Medieval Warm Period was the Little Ice Age, which occurred from 650-150 B.P., during this period there was an advance of the mountain glaciers with a drop in temperature. Following the termination of the Little Ice Age the temperature of the region established modern climatic trends.

The Northwest Coast contains some of the most heavily forested regions in the United States (Franklin and Dyrness 1988). The forests of the Northwest Coast are dominated by douglas-fir with western hemlock and western red cedar (Franklin and Dyrness 1988). The abundance and longevity of the coniferous forests in the Northwest Coast contribute to soils that are slightly too moderately acidic.

On the Northwest Coast, the climate and coniferous forests have an effect on the preservation of bone in buried archaeological contexts. Heavy precipitation causes a buildup of carbonic acids in soil through the seeping of rainwater into the ground. The coniferous forests of

the region contribute to the development of humic acids within the soils. The buildup of carbonic and humic acids contribute to the degradation of unburned bone over time. However, the structure of calcined bone causes it to be less susceptible to the carbonic acid (Taylor and Bar-Yosef 2014). Additionally, the forests of the Northwest Coast pose an issue in that the dense forests of the region draw skepticism to the radiocarbon dating of charcoal due to the non-cultural burning of the forests and the depositing of new wood into cultural contexts (Olsen et al. 2012, Walsh et al. 2015).

Cultural Context

Chronological assays are only relevant if placed in cultural contexts and inversely cultural materials only have meaning if they can be placed in time. The cultural chronology of the Northwest Coast and Columbia Plateau Culture Areas (Ames and Maschner 1999; Matson and Coupland 1995) spans the past 13,000 years. Table 2. Cultural Chronologies of the Northwest Coast and Columbia Plateau shows the cultural sequences for the Northwest Coast and the Columbia Plateau. Both regions contain many differing chronologies, however, I have included here the most pertinent chronologies to the regions included in this study. The Columbia Plateau is included here because archaeological sites that are located in the Cascade Range share similar typologies to those of the Coast and the Plateau.

Table 2. Cultural Chronologies of the Northwest Coast and Columbia Plateau

<table>
<tr><th></th><th>Northwest Coast
(adapted from Carlson 1983 and Croes et al. 2008)</th><th>Columbia Plateau
(adapted from Ames et al. 1998)</th></tr>
<tr><td>0 cal BP</td><td rowspan="3">Late, San Juan Phase
(1500 cal BP -Contact)</td><td rowspan="5">Period III
(4000 cal BP-Contact)</td></tr>
<tr><td>1000 cal BP</td></tr>
<tr><td>2000 cal BP</td><td>Marpole Phase
(2500-1500 cal BP)</td></tr>
<tr><td>3000 cal BP</td><td rowspan="2">Locarno Beach Phase
(3500-2500 cal BP)</td></tr>
<tr><td>4000 cal BP</td></tr>
<tr><td>5000 cal BP</td><td rowspan="4">St. Mungo, Mayne Phase
(4500-3500 cal BP)

Olcott Phase, Old Cordilleran Tradition
(9,000-4500 cal BP)</td><td rowspan="2">Period II
(6500-4000 cal BP</td></tr>
<tr><td>6000 cal BP</td></tr>
<tr><td>7000 cal BP</td><td rowspan="5">Period IB
(11,000-6500 cal BP)</td></tr>
<tr><td>8000 cal BP</td></tr>
<tr><td>9000 cal BP</td><td rowspan="3">Western Stemmed Tradition
(11,000-9,000 cal BP)</td></tr>
<tr><td>10,000 calBP</td></tr>
<tr><td>11,000 calBP</td></tr>
<tr><td>12,000 calBP</td><td rowspan="2">Paleoindian
(13,000-11,000 cal BP)</td><td rowspan="2">Paleoindian/Period IA
(13,000-11,000 cal. BP)</td></tr>
<tr><td>13,000 calBP</td></tr>
</table>

On the Coast, a total of seven cultural phases are identified (Table 2) (Carlson 1983, Croes et al. 2008). Evidence of Paleoindian occurs from 13,000-11,000 cal B.P. (Table 2). The occupation on the Coast by Paleoindian is minimal; only isolated projectile points have been identified in the region. The Western Stemmed Tradition occurs from 11,000-8000 cal B.P. (Table 2). Few sites have been identified on the Coast dating to this period, sites that have been identified characterize the phase as a highly mobile-forager system (Chatters et al. 2011). The Olcott Phase occurred from 9,000-4500 cal B.P. (Table 2) and is characterized by leaf-shaped projectile points (Kidd 1964). To date the Olcott Phase is identified as a regional variation of other phases grouped under the Old Cordilleran Tradition (OCT), phases of the OCT are characterized by a mobile-forager system (Butler 1961, Mack et al. 2010, Chatters et al. 2011).

From 4500-3500 cal B.P. the St.Mungo or Mayne Phase occurred (Table 2). The Mayne Phase is characterized by a mobile-forager system that exhibits a change in projectile point styles from the preceding Olcott Phase (Carlson 1983). Projectile points in the Mayne Phase have been described as being similar to the preceding Olcott Phase in that the projectile points of the Mayne Phase are small leaf-shaped points (Carlson 1983). It is during the Mayne Phase that early evidence of shell middens are established on the Central Coast (Carlson 1983). Following the Mayne Phase is the Locarno Beach Phase occurring 3500-2500 cal B.P. This phase is characterized by a transition from a mobile-forager system to a semi-sedentary collector system (Carlson 1983). On the Coast, it is often the Locarno Beach Phase that is interpreted as coinciding with the start of resource intensification (Ames and Maschner 1999; Matson and Coupland 1995, Chatters and Prentiss 2005). The Marpole Phase occurs from 2500-1000 cal B.P. is characterized as a semi-sedentary collector system with the establishment of the ethnographic Northwest Coast Pattern (Carlson 1983). The distinction of difference between the Locarno

Beach Phase and the Marpole Phase is that the Locarno Beach Phase is characterized by a transition to a semi-sedentary collector system, and the Marpole Phase is characterized by the semi-sedentary collector system becoming widespread throughout the Coast. The most recent cultural phase on the Coast is the Late Phase or San Juan Phase that occurs from 1000 cal B.P. to contact, this phase is when European contact occurs, and the demographics of the region are widely devastated by disease (Carlson 1983).

In the Columbia Plateau Culture Area, a similar chronology occurs but with fewer phases (Table 2). The Paleoindian/ Period IA culture has been documented in Columbia Plateau as occurring from 13,000-11,000 cal B.P. (Ames et al. 1998). From 11,000-6500 cal B.P. is Period IB which is comprised of stemmed and foliate projectile point styles; this phase is characterized by a broad spectrum mobile-forager system (Rice 1972, Chatters et al. 2011). In different parts of the Plateau, this period is referred to as the Windust phase and Cascade phase (Leonhardy and Rice 1970). The earlier of these two is the Windust Phase (11,000-9000 cal. B.P.), which is a regional manifestation of the Western Stemmed Tradition (Rice 1972). This period is characterized by large stemmed projectile points (Rice 1972). The Cascade Phase (8000-6500 cal. B.P.) of the Plateau is a regional manifestation of the Old Cordilleran Tradition (Butler 1961). This period is characterized by large leaf-shaped projectile points (Butler 1961). Both of these archaeological phases share similar settlement and subsistence strategies in the form of highly mobile hunter-gatherers (Butler 1961). From 6500-4000 cal B.P. is Period II, this period is characterized by the development of one or more types of collector strategies and the development of semi-subterranean housepits (Ames et al. 1998, Chatters 1995). The final archaeological period on the Plateau is Period II, which occurred 4000 cal B.P. to contact. This period is characterized by a semi-sedentary collector system that establishes the ethnographic

present of the Columbia Plateau Pattern (Ames et al. 1998). During this period is when resource intensification is believed to occur on the Plateau with a heavy reliance on fishing, storage, and processing of plant resources (Ames et al. 1998).

CHAPTER 3

LITERATURE REVIEW

The following section will review the research pertinent to this thesis. I have divided this section based upon my objectives as outlined in Chapter 1.

Radiocarbon Dating and Thermoluminescence Dating:

Taylor (1987; Taylor and Bar-Yosef 2014) has reviewed the development and application of radiocarbon dating in archaeology. The earliest work in radiocarbon utilized the beta-counting method that produced low precision radiocarbon dates. It was not until 1977 that the accelerator mass spectrometer (AMS) was employed in the use of radiocarbon dating (Muller 1977). This innovation allowed for the refinement of radiocarbon dating by producing dates that are highly precise. This revolution has enabled the study of media that were previously considered unreliable and/or not usable. Through the development of AMS technology and the implementation of it in radiocarbon dating, the standard of dating archaeological deposits has become AMS radiocarbon dating. However, many of the dates that have been produced have not taken into consideration the accuracy of the material in the dating of cultural events. Thus, the materials used in radiocarbon dating require the consideration of accuracy in radiocarbon dating.

Multiple syntheses have discussed the development and history of luminescence dating throughout the world (Aitkens 1985, Berger 1988, Wintle 1993). Feathers (1997) has developed a synthesis and analysis of luminescence dating pertaining to its application in North America. Luminescence dating encompasses three techniques: thermoluminescence, optically-stimulated luminescence, and infrared stimulated luminescence. These techniques did not gain traction in the dating of archaeological deposits until Aitken's (Aitken et al. 1964, 1968) and Mejdahl's

(1969) works developing the validity of the dating technique. The dating of sediments in luminescence dating has come to dominate the field, however, heated lithics and ceramics are commonly used (Feathers 1997). Luminescence dating is argued to contain three advantages over other dating techniques: 1) the materials are abundant within archaeological deposits, 2) the date range that is covered is extensive (approximately 100,000), and 3) most importantly it directly dates cultural events (Feathers 1997). The direct dating of cultural events indicates that luminescence dating provides accurate dates, however, what is problematic is that the technique provides highly accurate dates with low precision. The reporting of luminescence dates come with 1-sigma errors of 100+ years. A large error term makes it very difficult to apply luminescence dates to the analysis of cultural change that occurs over centuries.

Very few studies (Gardener et al. 1987; Smith et al. 1997; Stuiver 1978) have attempted a comparison of radiocarbon dating to luminescence dating. None of the studies identified (Gardener et al. 1987; Smith et al. 1997; Stuiver 1978) directly analyzes the relationship between the dated events of radiocarbon and luminescence dating. However, Dean (1978) developed a model depicting the relationship of dendrochronology, archaeomagnetism, and radiocarbon dating.

Dean's (1978) model compares the three techniques to each other for their dated events, dated reference events, target events, and bridging events. The dated event is the event that the technique calculates. The dated reference event often coincides with the dated event, often these two events are considered the same. The target event is the point at which the date is to be applied, for instance the use of a cultural feature. The bridging event is the event that links the dated event and the target event. Dean's (1978) model has been modified through the use of different dating techniques (Richter 2007; Richter et al. 2009; Dykeman et al. 2002; Yang et al.

2005; Benea et al. 2007; Feathers 2009). These models (Richter 2007; Richter et al. 2009; Dykeman et al. 2002; Yang et al. 2005; Benea et al. 2007; Feathers 2009) have explored the implications of Dean's (1978) model with luminescence dating. The primary focuses of these applications have been on the luminescence dating of lithics (Richter 2007; Richter et al. 2009) and pottery (Dykeman et al. 2002; Yang et al. 2005; Benea et al. 2007; Feathers 2009).

Calcined Bone:

The two primary components of research centered on calcined bone are the diagenetic processes that bone undergoes in the process of calcination and the attempts at radiocarbon dating calcined bone throughout the world. Bone, when burned to 600 °C, undergoes a number of changes; the most important change from the standpoint of this research is the recrystallization of the inorganic apatite structure at the molecular scale (McCutcheon 1992). A number of analyses have been conducted to understand what happens to bone when it is burned (Brain 1981; Johnson 1989; Kiszley 1973; McCutcheon 1992; Shipman et al. 1984). Many of these studies imply that the changes are a series of stages, however, it is best to think of these as a continuum and that the changes occur along this continuum as the temperature increases.

Brain (1981) identifies two changes where initial charring of bone occurs when the collagen becomes carbonized followed by the bone becoming white and chalky or calcined. Johnson (1989) identifies four stages of change as bone is burned. The first of Johnson's (1989) stages is unburned bone, which is attributed to no thermal alteration. Johnson (1989) follows unburned bone with a scorched stage that is characterized by superficial burning. The third stage that Johnson (1989) has is a charred stage that the bone is completely blackened throughout. The fourth stage is calcined, which is characterized by the loss of all organic material. At this stage the bone has become blue-white (Johnson 1989).

Kiszley (1973) identifies three stages of burning; these stages are more characterized by the changes that bone undergoes while being burned. Kiszley's (1973) stages are: first the loss of water between 137-220 °Celsius, second the organic matter begins to liquefy and decompose from 220-380 °Celsius, and third all organic matter is burned away at 600 °C. Shipman (1984) conducted an experiment by burning bone in a muffle furnace. This experiment found that the color of bone was a poor indicator of the precise temperature that bone was heated at due to change in the color of bone diagenetically. Shipman (1984) does, however, conclude that the color of bone can be used to indicate a range of temperature to which bone was heated as long as there was no diagenetic alteration.

McCutcheon (1992) conducted similar experiments that identified three classes of change; the first of these classes is a loss of water and some carbonization of the organic matter with color changing as the temperature range varied between 20-340 °C. The second class ranging from 340-600 °C is characterized by the complete loss of organic matter (McCutcheon 1992). The third class ranges from 650-950 °C and is characterized by a change in the crystal size of the inorganic fraction (McCutcheon 1992).

All of these studies (Brain 1981; Johnson 1989; Kiszley 1973; McCutcheon 1992; Shipman et al. 1984) identify varying stages of change in bone as it undergoes burning with some reference to the change in bone chemistry. Taylor and Bar-Yosef (2014) have identified elements of bone chemistry that include the isotopic uptake of carbon in calcined bone from the fuel source used in the burning process. This uptake has the possibility to distort the age of the calcined bone in an older direction due to the "old wood" effect (Olsen et al. 2013; Taylor and Bar-Yosef 2014). However, Taylor and Bar-Yosef (2014) do note that if the fuel (wood/charcoal) and the calcined bone are of similar ages, then the isotopic uptake of carbon

from old wood is not a concern. Further work has been conducted on the chemistry of calcined bone that identifies the effects of isotopic exchange between the bone and the fuel source (Huls et al. 2010; Snoeck et al. 2014; Van Strydonck et al. 2010; Zazzo et al. 2009; Zazzo et al. 2012). These recent works have analyzed the isotopic exchange between charcoal and calcined bone in experimental settings and determined that when a carbon source of significantly old age is used as a fuel source it can skew the age of the calcined bone older (Huls et al. 2010; Snoeck et al. 2014; Van Strydonck et al. 2010; Zazzo et al. 2009; Zazzo et al. 2012). It thus results in an "old wood" effect within the bone itself (Olsen et al. 2013).

Few studies have addressed the radiocarbon dating of calcined bone (Lanting and Brindley 1998; Lanting et al. 2001; Naysmith et al. 2007; Zazzo and Saliege 2011; Zazzo et al. 2013). Lanting and Brindley (1998) compared cremated bone (calcined bone) to charcoal from archaeological sites in Ireland. The results from this study indicate samples of cremated bone and charcoal did appear to provide similar ages (Lanting and Brindley 1998). The authors of this study concluded that carbonate within the inorganic apatite structure of the bone was a reliable material for the dating of their sites (Lanting and Brindley 1998).

Zazzo and Saliege (2011) radiocarbon dated calcined bone from archaeological sites in North Africa and the Middle East. This study looked at a comparison of carbonate and apatite dates from the calcined bone. They have greater variation in their dates with the carbonate dates appearing significantly younger and the apatite dates appearing older.

Resource Intensification:

In the PNW of North America, the development of logistical settlement strategies with task-specific field camps, evidence for food storage in the form of large fire-pit and storage features, and the seasonal and habitat displacement of food species appear in the archaeological

record approximately 3500 B.P., these phenomena are associated with collector strategies and resource intensification (Kramer 2000; Thoms 1989). In addition, to the appearance of large fire-pit and storage features there is the development of logistical settlement strategies with task-specific field camps.

To establish the foundation works of resource intensification we first look back to Binford's (1980) modeling of the forager-collector system. The two systems are modeled off of the ethnographic cultures the Nunamiut Eskimo of Alaska and the Kalahari San from Africa (Binford 1980). The forager model is based upon the Kalahari San and depicts a highly mobile group that map onto their environment moving seasonally to resource patches (Binford 1980). The collector model is based upon the Nunamiut Eskimo and depicts a semi-sedentary to a sedentary population that has a logical subsistence pattern using satellite resource procurement and processing sites (Binford 1980). Binford (1980) does not refer to the forager-collector system as a dichotomy but instead as two points upon a spectrum that within the archaeological record can exhibit greater degrees of variation. The system does not take into account a temporal scale; instead, the model is strictly spatial (Binford 1980). The forager-collector system was developed as a way to compare settlement and subsistence patterns spatially, however, it was Northwest Coast archaeologists (Chatters 19995; Schalk and Cleveland 1983) that converted the idea into a diachronic view of the forager-collector system

Schalk and Cleveland's (1983) Lyons Ferry Report builds upon Binford's (1980) model to develop a diachronic model for the PNW. The model that Schalk and Cleveland (1983) developed centers around two phases of subsistence and settlement patterns: broad-spectrum foraging and semi-sedentary foraging. According to Schalk and Cleveland (1983), the broad-spectrum foraging system occurred from 11,000 B.P. to 4000-3000 B.P. this system is similar to

Binford's (1980) forager model due to the high mobility and impermanence of forager groups. After the broad-spectrum foraging system, a semi-sedentary foraging system developed that is similar to Binford's (1980) collectors; the shift to the semi-sedentary foraging system occurred around 4500-2500 B.P. (Schalk and Cleveland 1983). The transition to the semi-sedentary foraging system according to Schalk and Cleveland (1983) is manifested in the archaeological record of the PNW as the appearance of house pits, storage pits, increased assemblage diversity, and increased inter-site variability.

Chatters (1987) was one of the first to use models of assemblage structure to identify transitions from foraging to collecting strategies on the Upper to Middle Columbia River. By the mid 1990's, Chatters (1995) shared the first Plateau wide synthesis of the timing and rate of these transitions.

Resource intensification is part of an explanation for the transition from foraging to collecting strategies. A general definition of resource intensification is that an increased labor input results in an increased output of resource procurement and processing (Ames 2002; Chatters 1995; Chatters and Prentiss 2005; Croes and Hackenberger 1998; Matson 2008; Sheldon et al. 2013). The activities of resource procurement and processing appear to occur in the lowland and upland environments with semi-sedentary villages occurring on the coast. The timing of occupation at these coastal sites is better documented (Ames 2002; Chatters 1995; Croes and Hackenberger 1998; Matson 2008; Sheldon et al. 2013) than the timing of occupation of the lowland and upland sites.

Interpretation of the archaeology of the PNW assumes that resource intensification is a shift that occurs (Ames and Maschner 1999; Matson and Coupland 1995). It is believed that resource intensification causes a transition in the settlement and subsistence patterns (Ames and

Maschner 1999; Chatters 1995; Croes and Hackenberger 1988; Matson and Coupland 1995). If we are to assume that a shift occurred, then it is necessary that archaeologists have an accurate understanding of the timing of resource intensification.

Historically, resource intensification has been heavily discussed by archaeologists on the Coast and Plateau (Ames 2002; Chatters 1995; Croes and Hackenberger 1998; Matson 2008; Matson and Coupland 1995; Sheldon et al. 2013) as the transition between a mobile forager system and a semi-sedentary collector system. This region-wide discussion has led to varying definitions of resource intensification. A definition of resource intensification comes from work done on the Columbia Plateau, Thoms (1989) defines resource intensification as a response to population growth that forces an increased use of previously unused food resources. The schools of thought for resource intensification theory are economic (Croes and Hackenberger 1988, Coupland 1988, Huelsbeck 1988, Mitchell and Donald 1988, Wessen 1988), social (Ames 1991, 1994, 1996; Hayden 1995, 2001; Maschner 1991), and macroevolutionary (Chatters 2009, Chatters and Prentiss 2005, Prentiss 2009, 2011; Prentiss et al. 2005, 2014) theories.

The application of economic models to resource intensification is based on economic factors as the mechanism for resource intensification and culture change (Croes and Hackenberger 1988). The economic factors utilized in these models are descriptive of elements within the subsistence systems, such as caloric input and output, meat weight of animals, and timing of resource acquisition (Croes and Hackenberger 1988). Other economic models include resource depression models and optimal foraging theory models (Bettinger et al. 2015; Butler 2000; Butler and Campbell 2004; Campbell and Butler 2010; Lupo 2007; Lyman 2003a, 2003b).

In contrast, the application of social models to resource intensification is based upon social complexity being the mechanism for resource intensification and culture change (Ames

1996). The social complexity has been characterized as manifesting in past human cultures as social hierarchy, complex kinship systems, warfare, and slavery (Ames 1996). Research focusing on the social attributes of prehistoric cultures are often more anthropological analyses of ephemeral artifact types, such as baskets and ornamentation, with a reliance on ethnographic analogy to infer social complexity.

Recent research in the PNW has been developed using a macroevolutionary framework (Chatters 2009, Chatters and Prentiss 2005, Prentiss 2009, 2011; Prentiss et al. 2005, 2014). Macroevolution in archaeology has been based upon Eldredge's (1989) organismic macroevolution, which can be summarized as the accumulation of phenotypic variation over time (Prentiss et al. 2015). A macroevolution framework has developed out of the many branches of Darwinian archaeology. Under this framework, the cultural systems identified by anthropologists are considered the byproduct of overall cultural change (Prentiss et al. 2015). Based on the analysis of cultural change through the smallest cultural units of memes and the phenotypic manifestations of artifacts that larger cultural systems such as subsistence can be inferred (Prentiss et al. 2015).

These schools of thought differ in the mechanism for resource intensification. This difference in mechanism means that an economic standpoint argues that the people made a choice in selecting resources that would allow for populations to increase and the development of social complexity. Social arguments essentially approach the idea from the opposite end; that social complexity developed first requiring people to select different resources based upon their social status. A macroevolutionary approach would view resource intensification as a byproduct of the overall change of artifacts. Chatters (2009) notes the development of pit-cooking of geophytes in the PNW as coinciding with the emergence of collector strategies.

CHAPTER 4

CHRONOMETRIC HYGIENE

Throughout the world systematic analysis of chronometric dates has been conducted to evaluate the validity and significance of individual ages (Hunt and Lipo 2007, Nolan 2012, Wilmshurst et al. 2011). Many of these studies have utilized a hygiene protocol to determine the validity of established radiocarbon chronologies (Hunt and Lipo 2007, Nolan 2012, Wilmshurst et al. 2011). Based upon these works, I have identified patterns within the radiocarbon record of Western Washington using data collected from the Canadian Archaeological Radiocarbon Database 2.0 (CARD). In the context of this research, chronometric hygiene is being applied to identify issues in a prior sampling of radiocarbon samples to show that many, if not most of the radiocarbon record of Western Washington, lacks any form of accuracy in the dating of cultural events. This focus on the deficit of accurate dating leads this analysis to examine the material types and the distribution of radiocarbon dates temporally and spatially to understand if archaeologists of the PNW can accurately interpret anything about periods of cultural change.

Paramount to any discussion of chronometric hygiene is the understanding of sample context and association. The prime context for drawing samples for radiocarbon dating are discrete cultural features such as hearths, earth ovens, or housepit floors. By drawing samples from a discrete cultural feature then the association with faunal remains and lithics is a strong association.

Analysis of the radiocarbon data shows that there is a significant bias in the materials dated, as somewhat expected the most common medium for radiocarbon dating in Western Washington is charcoal (Table 3). Two issues are brought forth based upon the represented material types (Table 3). 1) that there is an over-reliance on charcoal in the PNW even though

the region is heavily forested and known to be subject to natural fires, and 2) that there are materials dated that can be problematic and should be avoided, in particular: wood, organic soil, plant remains, charred bone, and unknown (Table 3). However, this last issue is heavily context dependent for wood and plant remains, if they are recovered from a context such as a wet site where basketry and wood tools can be recovered. There are circumstances in which dating of these materials are acceptable. However, the inclusion of these materials brings into question the nature of them being anthropogenic. The anthropogenic nature of these materials is called into question because the connection to a cultural event is lacking and many of these materials could be naturally occurring in the soils.

Table 3. Count of Material Types of Radiocarbon Dates from Western Washington

Material	Count
Charcoal	353
Marine Shell	31
Wood	12
Charred Wood	10
Faunal Bone	5
Freshwater Shell	4
Organic Soil	4
Plant Remains	3
Charred Bone	2
Unknown	22

The distribution of dates by county (Figure 2) indicates a discrepancy in the distribution of dates by county, the county with the highest percentage of dates is King County. The more populace counties are the ones that have more documented radiocarbon dates. Also, a connection can be made that the counties with universities also have more documented radiocarbon dates. This discrepancy in the spatial distribution of dates is a function of archaeological research conducted through cultural resource management projects and universities. Identification of this

spatial discrepancy shows that not all regions of Western Washington are equally represented, meaning that portions of the record are not represented equally.

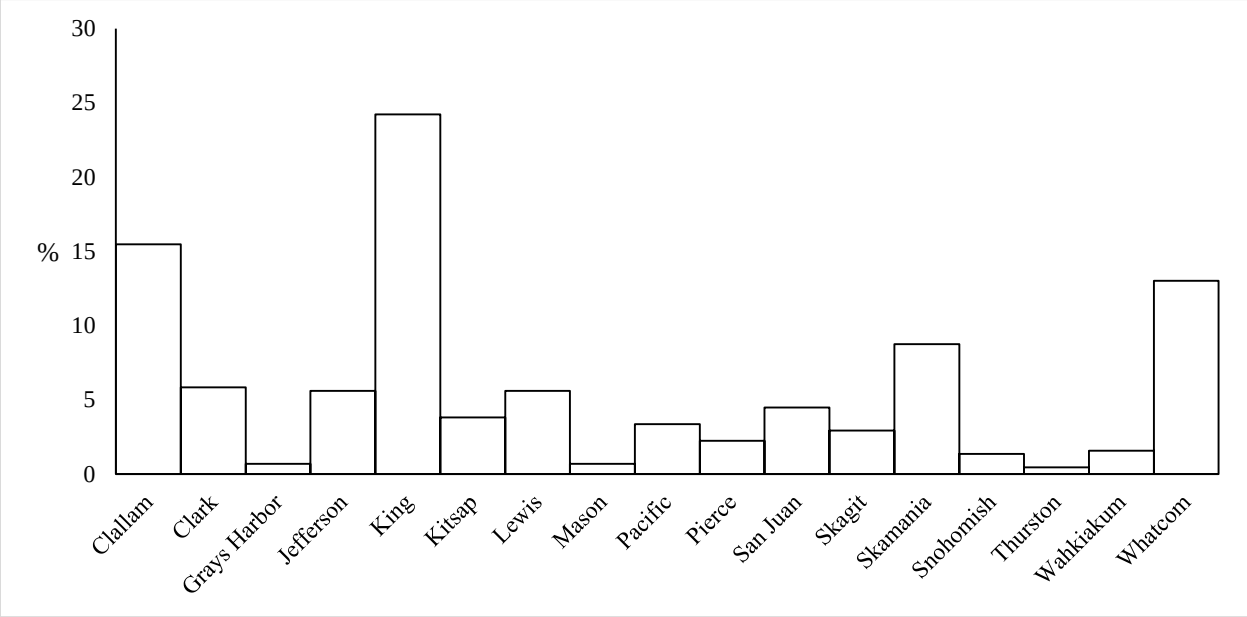

Figure 2. Distribution of Radiocarbon Dates by County

The temporal distribution of radiocarbon dates (Figure 3) shows that the frequency of dates decreases the older the dates are. The majority of dates are earlier than 4000 B.P. and after 4000 B.P. the dates decrease significantly. Radiocarbon dates attributed to the Early Holocene are extremely sparse and inconsistent. The increase in radiocarbon dates starting in the late Holocene can be seen as a function of increasing population size leaving a more significant remnant on the landscape. This discrepancy in the frequency of dates based upon time period indicates that the record for the early Holocene is extremely sparse and requires significantly more dating to understand any patterns of cultural change.

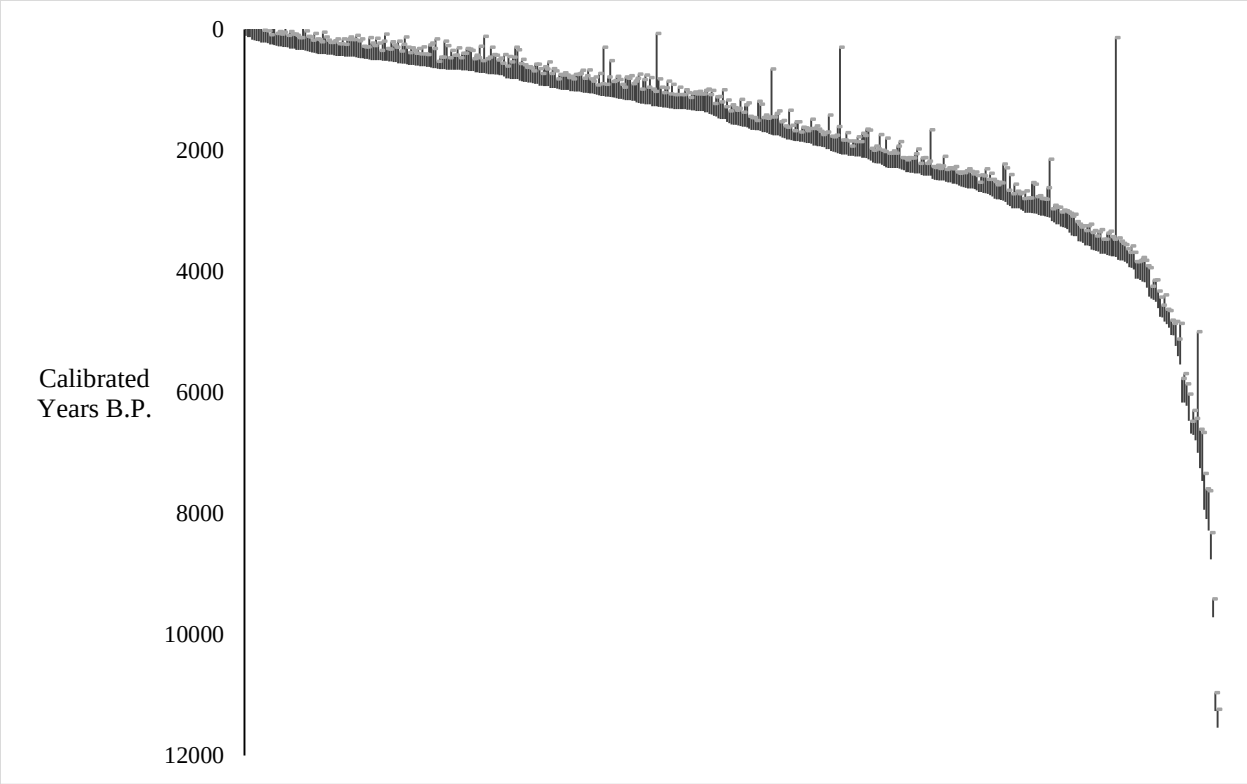

Figure 3. Radiocarbon Date Curve of Western Washington

A histogram of the uncalibrated dates by 500-year intervals (Figure 4) show that there is a significant decrease in radiocarbon dates over time. Between 4500 and 11,500 B.P. there are a minimal number of dates. 1500-4500 B.P. there is a gradual increase in radiocarbon frequency. Between 500-1000 B.P. is the most significant increase in radiocarbon date frequency. This increase in radiocarbon dates can be attributed to being a function of the increase in population size.

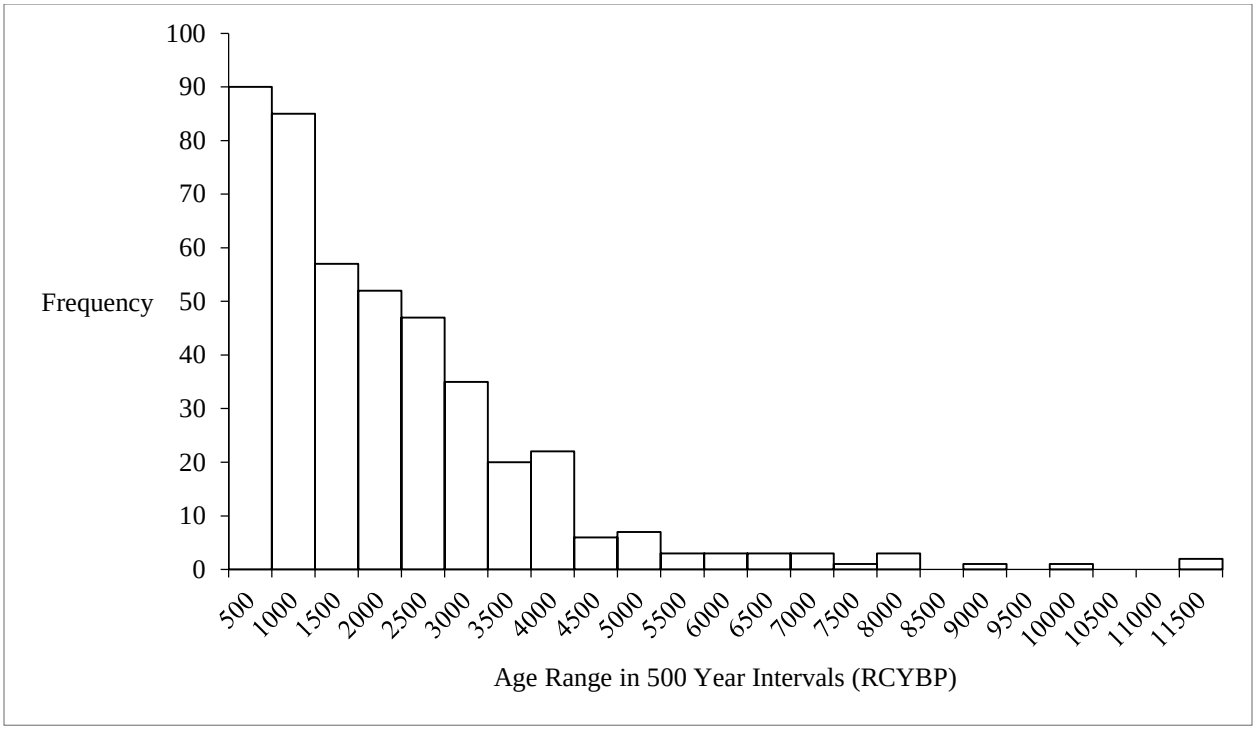

Figure 4. Frequency of Radiocarbon Dates for Western Washington

CHAPTER 5

ARTICLE

ALTERNATIVES TO CHARCOAL FOR IMPROVING CHRONOMETRIC DATING OF PUGET SOUND ARCHAEOLOGICAL SITES

The student coauthors this manuscript with the committee, and it will be submitted to the *Advances in Archaeological Practice*. The manuscript begins on the next page and will be the version submitted; the final manuscript (if accepted) may result in differences based the results of editorial and blind peer reviews.

ALTERNATIVES TO CHARCOAL FOR IMPROVING CHRONOMETRIC DATING OF PUGET SOUND ARCHAEOLOGICAL SITES

James W. Brown[1], Steven Hackenberger[1,2], Patrick T. McCutcheon[1,2], and James C. Chatters[3]

[1] Cultural and Environmental Resource Management Program, Central Washington University, Ellensburg, Washington, USA

[2] Department of Anthropology and Museum Studies, Central Washington University, Ellensburg, Washington, USA

[3] Applied Paleoscience

Contact information:

James Brown, M.S.

Cultural and Environmental Resource Management Program

Central Washington University

400 E. University Way

Ellensburg, WA 98926-7544

USA

E-mail: brownjam@cwu.edu

ABSTRACT:

Chronometric dating is problematic in non-midden sites of the Pacific Northwest (PNW). Charcoal is ubiquitous in forest soils and unburned bone readily dissolves. This fact impedes the development of regional chronologies and understanding of the processes of cultural change that were so important to the development of PNW cultures. To alleviate this deficiency, research has been conducted in conjunction with DirectAMS and the University of Washington Luminescence Laboratory to test the validity of charcoal, calcined bone, and fire-modified rock, through the use of radiocarbon dating and thermoluminescence dating. Calcined bone survives well in archaeological sites with acidic soils that are common to archaeological contexts in the PNW and has been found in the Old World to provide accurate radiocarbon dating. Luminescence dating can be applied to fire-modified rock recovered particularly from food processing features. These two dating techniques have been applied to resource intensification models to show the significance of "chronometrically clean" dates.

1. INTRODUCTION

In the Pacific Northwest (PNW) of North America, much of the extant radiometric chronological record was measured from charcoal and marine shell found in association with archaeological deposits. Outside of shell midden deposits, preservation conditions strip much of the organic matter left by past people. Charcoal in the PNW is ubiquitous in the soils due to the wide extent of coniferous forests that have succumbed to burning. The ubiquity of charcoal is problematic due to the ambiguous nature of when the organic (wood) material was burned and when it was deposited in archaeological deposits. Thus, a radiocarbon assayed fragment of charcoal found in association with artifacts cannot be assumed to be of the same age as when the organic material died and when it was deposited without making a bridging argument that connects these two events (Dean 1978).

An over-reliance on charcoal has presented a problem for archaeologists everywhere as it can attribute inaccurate dates to events (Dean 1978). This is certainly true in Western Washington (1)Table 4). The event typology developed by Dean (1978) for chronometric analysis defines four types of events related to any age measurement: the dated event, dated reference event, target event, and bridging event. Recent studies (Richter 2007, Richter et al. 2009) have reduced the number of event types by combining the dated event and the dated reference event, leaving the dated event, the target event, and the bridging event. This research uses this combined event typology of Richter (2007; Richter et al. 2009). The dated event is the event to which the technique calculates, for example the age of death for living tissue. The target event is the event to which the date is applied. In an archaeological case it is a cultural or human behavioral event. Lastly, the bridging event is the event that links the dated and target events.

Table 4. Radiocarbon Dates of Western Washington by Material Types

Material	Count
Charcoal	353
Marine Shell	31
Wood	12
Charred Wood	10
Faunal Bone Collagen	5
Freshwater Shell	4
Organic Soil	4
Plant Remains	3
Charred Bone	2
Un-reported	22

The issue with charcoal in environments like that of western Washington is that the dated event—death of wood—and the target event may not be easily linked outside of discrete, incontrovertible features. Charcoal from an archaeological stratum may come from a forest fire that occurred long before or long after the cultural event took place. The old wood problem, especially acute where trees live for hundreds of years, adds to this potential gap.

To alleviate the problem of poorly dated archaeological deposits, caused by a reliance on charcoal, an emphasis needs to be placed on the chronometric dating of more accurate media that have a defined bridging event. In this research, an accurate medium is a material for use in chronometric dating that has a clearer relationship, or bridge, between the dated and target events.

Accurate media are rare in the conifer forest regions. For example, due to the acidic nature of the soils in the PNW little to no bone remains in non-shell midden deposits. Where bone does exist in the absence of neutralizing shell deposits, it is either calcined or charred. Charred bone is suspect as a medium in radiocarbon dating due to the potential for environmental contamination of the organic fraction and the difficulty of removing said contamination without also removing heat-damaged bone proteins. Two candidates for an

accurate medium are, therefore, available in chronometric dating, calcined bone, and fire-modified rock.

Calcined bone consists of a recrystallized inorganic fraction of the bone (Brain 1981; Johnson 1989; Kiszley 1973; McCutcheon 1992; Shipman et al. 1984). The carbon in this recrystallized matrix is an admixture of carbon from the death of the animal and the fuel source (Huls et al. 2010; Snoeck et al. 2014; Van Strydonck et al. 2010; Zazzo et al. 2009; Zazzo et al. 2012). The association of calcined bone with cultural contexts lends credibility to the accuracy of calcined bone as a medium in the radiocarbon dating of archaeological deposits. One limitation, however, is that, because of its inclusion of carbon from fuel wood, it may also be partially subject to the old wood effect.

Calcined bone survives well in the soils of the PNW due to the processes the bone undergoes during high temperature burning that completely removes the organic fraction (Brain 1981; Johnson 1989; Kiszley 1973; McCutcheon 1992; Shipman et al. 1984). The carbon that remains in calcined bone is a minimal amount found within the mineral apatite structure mixed with carbon from the fuel source (Huls et al. 2010; Snoeck et al. 2014; Van Strydonck et al. 2010; Zazzo et al. 2009; Zazzo et al. 2012). Recent studies in the Old World have shown calcined bone to be a viable medium for the dating of archaeological sites (Lanting and Brindley 1998; Lanting et al. 2001; Naysmith et al. 2007; Zazzo and Saliege 2011; Zazzo et al. 2013). Through a series of match-paired samples, this study attempts show the validity of calcined bone as a medium for radiocarbon dating. Calcined bone as a form of culturally modified bone does not have a direct correlation between the dated event and the cultural event. In the framework of Dean's (1978) event typology, the bridging event is the time between the death of the animal and

the burning of the bone. This bridging event makes calcined bone possibly a more accurate medium then charcoal.

Fire-modified rock (FMR) is the heated remains of cooking fires, usually the result of hot-rock cooking. Using luminescence dating, this medium can provide a date for the last extreme heating of the rock, a phenomenon directly linked to the target event. FMR in association with cultural materials is thus an accurate medium in the luminescence dating of hearth features. Luminescence dating does, however, lack precision as indicated by the large standard error associated with the technique.

The bridging event associated with FMR is the relationship between the heating of the rock to 500 °C and the last use of the hearth, which is believed to be brief enough that it is of little issue (Richter 2007, Richter et al. 2009) providing FMR as the most accurate medium as defined here. However, due to the large standard errors associated with luminescence dating the precision of such dating of FMR can be of issue, depending on the resolution required to solve a particular chronological problem. For instance, if increased chronological resolution (narrower time range) is desired, then luminescence dates may not be appropriate. On the other hand, if a shorter bridging event is required where the target and dated event are sure to be closely associated, then luminescence dates would be preferable.

FMR has been shown to be a viable medium for dating using luminescence dating throughout the world (Aitkens 1985, 1998; Feathers 2003; Wintle 2008). Luminescence dating has been shown as an accurate technique in the chronometric dating of old archaeological deposits (Liritzis et al. 2013). In particular, there is significant evidence of luminescence dating being applied to considerably ancient deposits. This research seeks to determine the validity of

luminescence dating of FMR as an accurate medium in the dating of Holocene-aged deposits throughout the PNW.

Cultural materials such as calcined bone and fire-modified rock are considered to be more accurate due to these materials having a closer association with a cultural event such as the use of a hearth feature. The dating of more accurate media in the PNW is not the only requirement for developing a more refined chronology, but we must resolve the way in which archaeologists in the PNW utilize chronometric dates. Archaeologists in this region lack a model that integrates the dated and cultural event with a well-articulated bridging event (Dean 1978). Development of a model that utilizes more accurate media, such as culturally modified bone (calcined bone) and fire-modified rock, and tracks the difference of dated versus target events will enable archaeologists to employ greater quantities of accurate chronometric dates in describing cultural change in the PNW.

Clearly articulating what is actually measured (dated event) and what archaeologists want to know the age of will help target those artifacts that provide a clear path for bridging the two events, which will produce a more accurate and precise chronology Use of these materials will enable the development of a more refined chronology in the PNW. A refined chronology will provide a better understanding of the timing of cultural change. Archaeologists have identified two particular time periods of significant cultural change in the PNW that require chronological refinement: the mid-Holocene shift in settlement and subsistence patterns known as resource intensification (Ames 2002; Chatters 1995; Croes and Hackenberger 1998; Matson 2008; Sheldon et al. 2013), and the late Pleistocene-early Holocene transition (Chatters et al. 2011; Mack et al. 2010). By developing an analytical model for selecting accurate media and then employing it to define a technique for selecting samples from a series of archaeological sites, we

will determine a coarse for refining these critical chronological periods test the usability of the model in dating archaeological deposits with a series of radiocarbon and luminescence dates. To display the accuracy of the different media, we present a comparison of charcoal, calcined bone, and FMR pairings. These pairings are all drawn from discrete cultural features in which the dated media should be of similar ages, if the media are accurate to the cultural event.

2. THEORY

Event Typology:

In chronometric dating, there is inherent variation in dates when comparing different media due to the events that each corresponds with. Evaluating different dating techniques and their relationships with the interpretation of prehistoric human behavior patterns has been considered in the framework of event typology models (Dean 1978; Dincauze 2000; Richter et al. 2009). In particular, Dean's (1978) model established the event typologies. Dean's (1978) event typology is the dated event, dated reference event, target event, and bridging event. Richter et al. (2009) adapts the earlier model (Dean 1978) and simplifies it to contain three events. These events are the dated event, bridging event and cultural (target) event.

This research posits a comparison based upon media corresponding to the applicable dating techniques within a common human behavior. The model developed herein (Figure 5) is an adaptation of Dean (1978) and Richter (2007, Richter et al. 2009) with the emphasis on thermoluminescence and radiocarbon dating.

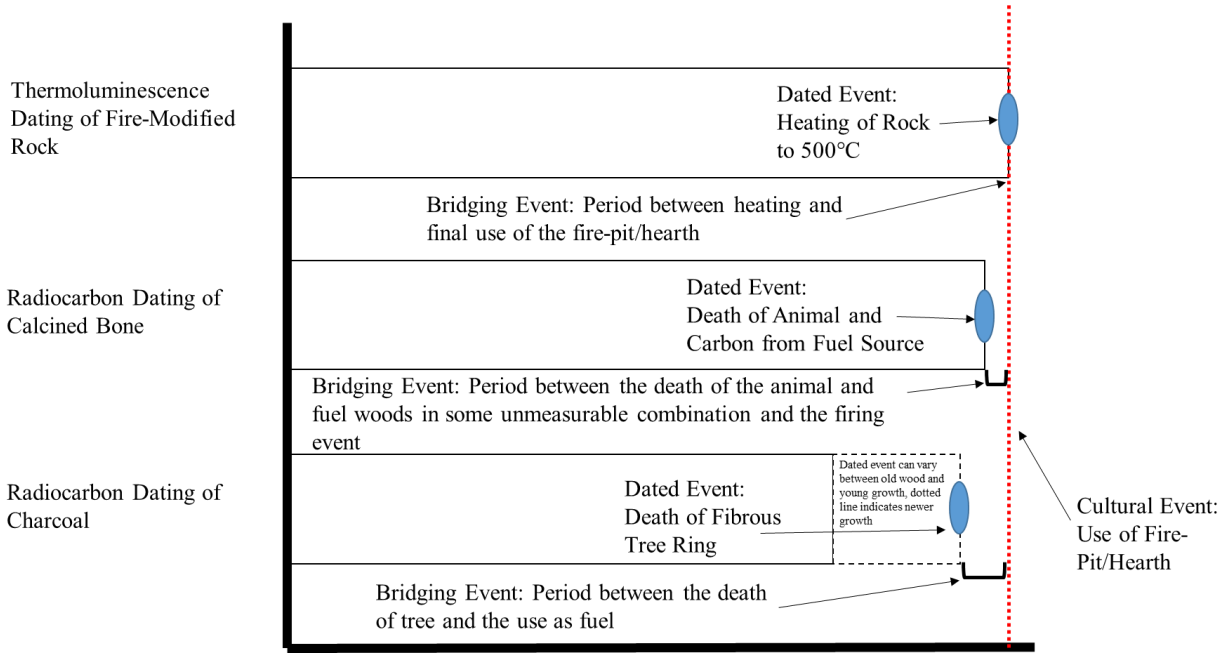

Figure 5. Accurate Medium Model Adapted from Dean (1978) and Richter et al. (2009)

This model shares a common *cultural event* in the form of the use of a fire-pit or hearth feature. For the luminescence dating of FMR the *dated event* is the heating of the rock to 500 °C (Dunnell and Feathers 1995; Rhodes et al. 2009), often this event should be near to concurrent with the *cultural event* because the heating of the FMR is directly related to the cultural use of the FMR. The *bridging event* for the FMR would be the period between the heating of rock and the final use of the feature, with the errors inherent in TL dating a *bridging event* would be minimal when considered at a two sigma age range.

Radiocarbon dating often considers the *dated event* to be a death event due to the carbon reservoir beginning to deplete upon the death of the specimen (Taylor 1997; Taylor and Bar-Yosef 2014). This holds true for charcoal in that the *dated event* is the death of the individual tree ring and/or yearly growth (Taylor 1997; Taylor and Bar-Yosef 2014). Inherent in the radiocarbon dating of charcoal is the issue of the "old wood" effect (Olsen et al. 2013; Taylor

and Bar-Yosef 2014), which can cause significant discrepancy between the *dated event* and the *cultural event*. Additionally, there is the problem that the association of charcoal with the surrounding matrix and associated artifacts is an assumption. *The bridging event* for charcoal can be problematic if the charcoal is not retrieved from a distinct cultural feature. In the case that charcoal *is* recovered from a feature, the *bridging event* would be the period of time between the death of the tree ring or annual growth and the use of the wood as a fuel source (Dean 1978; Taylor 1997; Richter et al. 2009). In the case of calcined bone, the relationship can be more complex. The *dating event* for calcined bone is an admixture of the carbon from the death of the animal plus the carbon from the fuel source that is introduced into the apatite matrix as part of an ionic exchange between the bone apatite and the fuel source (Huls et al. 2010; Snoeck et al. 2014; Van Strydonck et al. 2010; Zazzo et al. 2009; Zazzo et al. 2012). With the use of calcined bone, a *bridging event* would be the period of time between the death of the animal and the fuel source to the firing of the bone.

3. MATERIAL & METHODS

Materials:

We conducted a series of paired radiocarbon and luminescence analyses from previously excavated sites in the PNW. The selection criteria for sites and pairings were that samples must be recovered from discrete cultural features (either hearth/oven or a housepit floor) and that charcoal, calcined bone, and FMR were identified and recovered together from said feature. In these pairings, the charcoal dates is considered the control, notwithstanding the old wood issue, and that if suitable as alternative dating media, calcined bone and FMR should produce statistically similar results.

Samples were gathered from four archaeological sites (Table 5), two of these sites contain charcoal/calcined bone/FMR triplets, and two of the sites contain charcoal/calcined bone

matched-pairs. The sites are located in the vicinity of Puget Sound in the State of Washington (Figure 6).

Table 5. Study Sites

Site Number	Site Name
Charcoal/Calcined Bone/ FMR	
45PI408	Sunrise Ridge Borrow Pit
45PI1276	Bray
Charcoal/Calcined Bone	
45CA426	Sequim Bypass
45PI43	Fryingpan Creek Rockshelter

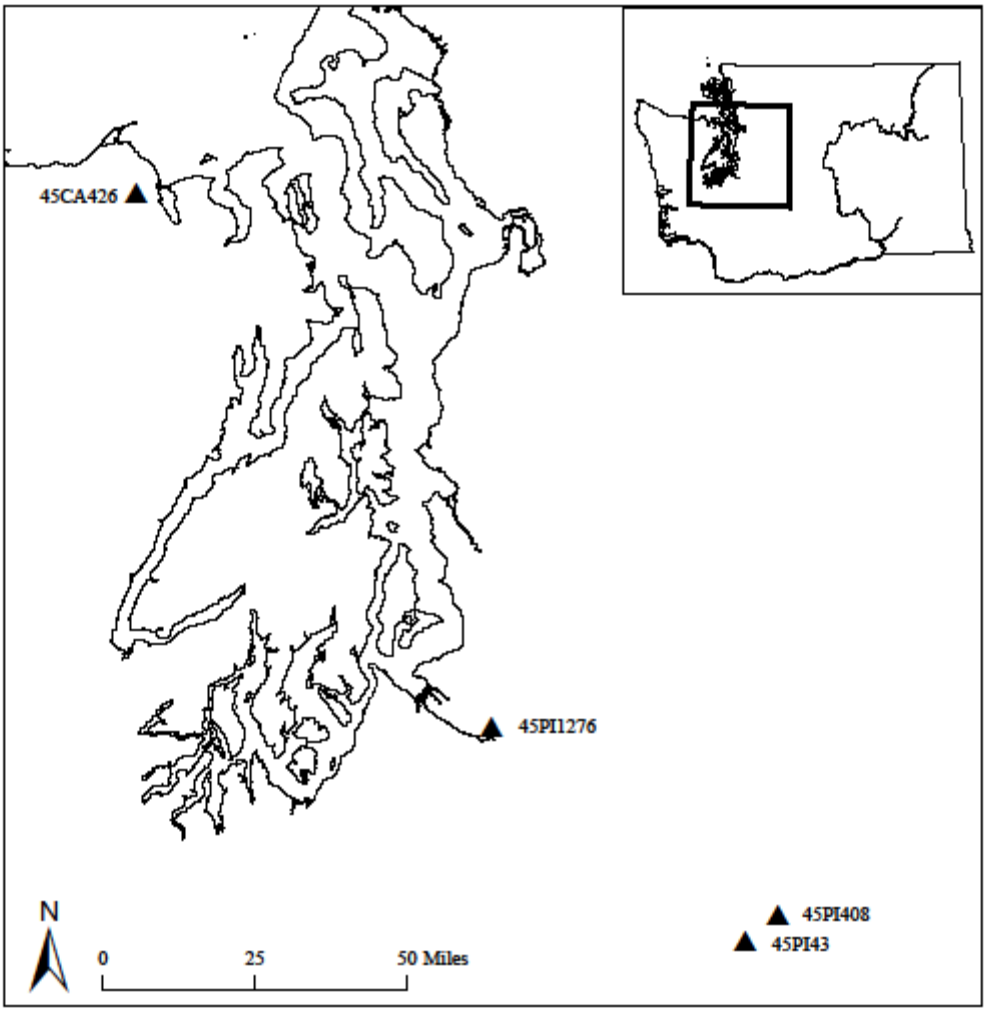

Figure 6. Map of Study Area

Site Background:

Sunrise Ridge Borrow Pit:

The Sunrise Ridge Borrow Pits Site is located in the Mount Rainier National Park. A series of field schools excavated the site between 2011-2013 as a cooperative effort between Central Washington University and Mount Rainier National Park (McCutcheon et al. In Prep). The site was excavated by students of the field schools under the supervision of teaching assistants and Dr. Patrick T. McCutcheon. In total there were four separate excavation blocks: the 30N area, 60.5N area, 71.5N area, and the 64N area (McCutcheon et al. In Prep). A series of hearth features were identified throughout the site in addition to a pit feature and large burned log feature (McCutcheon et al. In Prep). In total for chronometric dating there was: eight samples of charcoal, five samples of calcined bone, and six samples of FMR. These samples were drawn from four discrete cultural features. One from the 60.5N area, one from the 30N area, and two from the 71.5N area. Five match-pairs of charcoal-calcined bone and six charcoal-FMR match-pairs were identified for dating.

Bray Site:

The Bray Site is located in an agricultural field on a glacial outwash terrace overlooking the confluence of the Puyallup and the White Rivers. The Bray Site was previously excavated in the 1990s by amateur archaeologist, Bruce Gustafson. Work in 2012 was conducted at the Bray Site under the direction of Dr. James C. Chatters and a crew of volunteers from Central Washington University. The site is described as what appears to be a plant processing encampment that contains large earth oven features along the eastern side of the site boundary (Chatters and Sheldon 2012). From this site we have dated two samples of charcoal, two samples

of calcined bone, and two samples of FMR. Thus, resulting in two pairings of charcoal, calcined bone, and FMR.

Sequim Bypass:

The Sequim Bypass site is located south of Sequim, Washington in the vicinity of the State Route 101 bypass (Morgan 1999). Archaeological and Historical Services conducted data recovery excavations from 1996 to 1997. Two housepit structures were identified within the site containing hearth features. A single match-pair of charcoal, calcined bone, and FMR were selected from one of these hearth features. However, at this time the luminescence date on the FMR is yet to be completed and so the dates are treated as a match-pair of charcoal and calcined bone. The charcoal dated from this site was conducted as part of earlier analysis associated with the data recovery (Morgan 1999).

Fryingpan Creek Rockshelter:

The Fryingpan Creek Rockshelter is located at 5400 feet on Mount Rainier; the rockshelter is located northeast of Fryingpan Glacier and south of Goat Island Mountain in the eastern half of Mount Rainier National Park (Lubinski and Burtchard 2005). The site was investigated in 1964 and 2001. In 1964 David Rice and Charles Nelson opened a single unit in the rockshelter (Lubinski and Burtchard 2005). The site was revisited in September of 2001 by Greg Burtchard. In 2001 two charcoal-stained pit features were uncovered in the eastern wall of the original 1964 excavation (Lubinski and Burtchard 2005). From this site two samples of charcoal had been previously dated as part of earlier work (Lubinski and Burtchard 2005) and three samples of calcined bone were dated. Thus, resulting in two pairings of charcoal and calcined bone from within a single feature. For Fryingpan Creek Rockshelter only charcoal and calcined bone were selected because FMR was not readily available for dating.

Methods:

Charcoal, calcined bone, and FMR were selected from archived site collections from Central Washington University (Sunrise Ridge Borrow Pit and the Bray Site), the Jamestown S'Klallam (Sequim Bypass), and Mount Rainier National Park (Fryingpan Creek Rockshelter). Both the Sunrise Ridge Borrow Pit and the Bray Site are only temporarily held at Central Washington University. The Sunrise Ridge Borrow Pit Site will eventually be archived and stored at Mount Rainier National Park and the Bray Site will eventually be archived and stored at the Burke Museum.

Radiocarbon dates on charcoal that were not conducted as part of this study are taken as being selected from a discrete cultural context, resulting in these ages being taken as the true age of the feature. Sites that contain previously dated charcoal are the Sequim Bypass Site, Bray Site, and Fryingpan Creek Rockshelter.

All other radiocarbon dates conducted were assayed using standard methods by DirectAMS (See Appendix A for Laboratory Protocol). The protocol used for processing charcoal samples is a standard acid-base-acid pretreatment. For calcined bone samples an acid-acid pretreatment process was developed and applied to all samples (Brown 2014). The limitation of processing calcined bone samples is the necessity for the calcined bone to be fully calcined with no charred core. To identify full calcination of the bone the samples were broken in half.

All FMR luminescence dates were processed at the University of Washington Luminescence Laboratory using standard methods of TL, OSL, and IRSL dating techniques (See Appendices C and D for Laboratory Protocols). FMR samples were submitted as thermoluminescence samples. However, for all samples the ages were calculated using

thermoluminescence, optically-stimulated luminescence, and infrared stimulated luminescence techniques. In all circumstances the thermoluminescence age is the one that is reported. Additionally, luminescence dates are reported as AD/BC calendar system, to make them comparable to radiocarbon dates the luminescence dates were converted to B.P. system.

4. RESULTS

A total of twenty-five dates comprise the charcoal/calcined/FMR triplets, and an additional eight dates make up the charcoal/calcined bone matched-pairs set. All radiocarbon dates were calibrated using IntCal 13 (Reimer et al. 2013). Additionally, the provenance, uncalibrated dates, and calibrated 2-sigma age ranges are provided in Table 6. We discuss the findings on a site-by site basis. Results are most easily compared graphically. Represented in the graphs for each site are the calibrated 2-sigma age ranges of the radiocarbon dates, represented as cal B.P. for the radiocarbon dates. The luminescence dates, which are calculated in years before the measurement took place, are graphed as a normal distribution. In each case, the brackets underlying the graphed distribution range are first the 1-sigma range followed by the lower 2-sigma range bracket.

Table 6. Results of Radiocarbon and Luminescence Dates

Sample Number	Site Number	Unit	Feature	Material	Dated Age B.P.	2-Sigma Range Cal. B.P.	Citation
Charcoal/Calcined Bone/FMR Pairs							
DAMS-007911	45PI408	71.5N/65.5E	AA	Charcoal	1814±24	1636-1821	This Publication
DAMS-3594	45PI408	71.5N/65.5E	AA	Calcined Bone	2246±24	2158-2338	This Publication
DAMS-3596	45PI408	71.5N/65.5E	AA	Charcoal	2410±28	2351-2682	This Publication
DAMS-3597	45PI408	71.5N/65.5E	AA	Calcined Bone	2265±27	2159-2347	This Publication
DAMS-3598	45PI408	71.5N/65.5E	AA	Charcoal	2286±43	2155-2357	This Publication
UW3098	45PI408	71.5N/66.5E	AA	FMR	1828±162	1504-2152	This Publication
UW3101	45PI408	71.5N/65.5E	AA	FMR	1672±80	1542-1832	This Publication
UW2965	45PI408	71.5N/65.5E	AA	FMR	2291±124	2043-2539	This Publication
DAMS-11249	45PI408	AI profile	AD	Charcoal	2583±33	2517-2766	This Publication
DAMS-4803	45PI408	AI profile	AD	Calcined Bone	2484±31	2385-2725	This Publication
UW 2964	45PI408	AI Profile	AD	FMR	3006±276	2454-3528	This Publication
DAMS-4802	45PI408	61.5N/35E	R	Calcined Bone	1683±42	1445-1707	This Publication
DAMS-4800	45PI408	61.5N/35E	R	Charcoal	1652±32	1417-1688	This Publication
UW3088	45PI408	61.5N/35E	R	FMR	1305±180	945-1665	This Publication

Table 6 (Continued)

Sample Number	Site Number	Unit	Feature	Material	Dated Age B.P.	2-Sigma Range Cal. B.P.	Citation
DAMS-007914	45PI408	61.5N/35E	R	Charcoal	1526±24	1350-1521	This Publication
DAMS-007918	45PI408	28N/25E	H	Calcined Bone	2574±29	2520-2758	This Publication
Beta-120520	45PI408	30N/25E	I	Charcoal	2390±80	2207-2729	This Publication
DAMS-007913	45PI408	30N/24E	J	Charcoal	2576±26	2543-2758	This Publication
UW3096	45PI408	29N/25E	J	FMR	2425±180	2065-2785	This Publication
DAMS-3278	45PI1276	Unit 1-gg		Calcined Bone	2690±28	2754-2847	Jolivette and Huber In Press
DAMS-1910	45PI1276	Unit 1-gg	Fea 12-2	Charcoal	2823±25	2862-2992	Jolivette and Huber In Press
DAMS-3279	45PI1276	5N/7E		Calcined Bone	2578±27	2542-2759	Jolivette and Huber In Press
DAMS-1911	45PI1276	5N/7E	Fea 12-3	Charcoal	2734±24	2772-2871	Jolivette and Huber In Press
UW3047	45PI1276	3N7E		FMR	3345± 250	2845-3845	Jolivette and Huber In Press
UW3048	45PI1276	5N7E		FMR	2905 ± 220	2465-3345	Jolivette and Huber In Press

Table 6. (Continued)

Sample Number	Site Number	Unit	Feature	Material	Dated Age B.P.	2-Sigma Range Cal. B.P.	Citation
Charcoal-Calcined Bone Pairs							
DAMS-14290	45CA426	304N/198E		Calcined Bone	2425±25	2354-2691	This Publication
DAMS-14291	45CA426	304N/198E		Calcined Bone	2489±28	2464-2723	This Publication
Beta 107612	45CA426	304N/198E		Charcoal	2480±50	2365-2725	Morgan 1999
Beta 163695	45PI43	Unit A	Feature 1	Charcoal	460±70	236-488	Lubinski and Burtchard 2005
DAMS-3819a	45PI43	Unit A	Feature 1	Calcined Bone	553±27	521-636	This Publication
DAMS-3819b	45PI43	Unit A	Feature 1	Calcined Bone	408±59	314-529	This Publication
Beta 163694	45PI43	Unit A	Feature 1	Charcoal	890±40	730-916	Lubinski and Burtchard 2005
DAMS-3818	45PI43	Unit A	Feature 1	Calcined Bone	578±26	534-646	This Publication

Bray Site:

Figure 7 compares the results of dating charcoal, calcined bone and FMR from two earth oven features at the Bray Site. The distribution of the luminescence dates is markedly different due to being graphed as a normal distribution. The remainder of the dates appears to be close in age. The above graph shows that when calibrated at a 2-sigma range all of the dates significantly overlap, UW3047 appearing to be slightly older than the rest of the dates. This may result from an earlier firing of the FMR used in this feature coupled with a low heating temperature during the last use event.

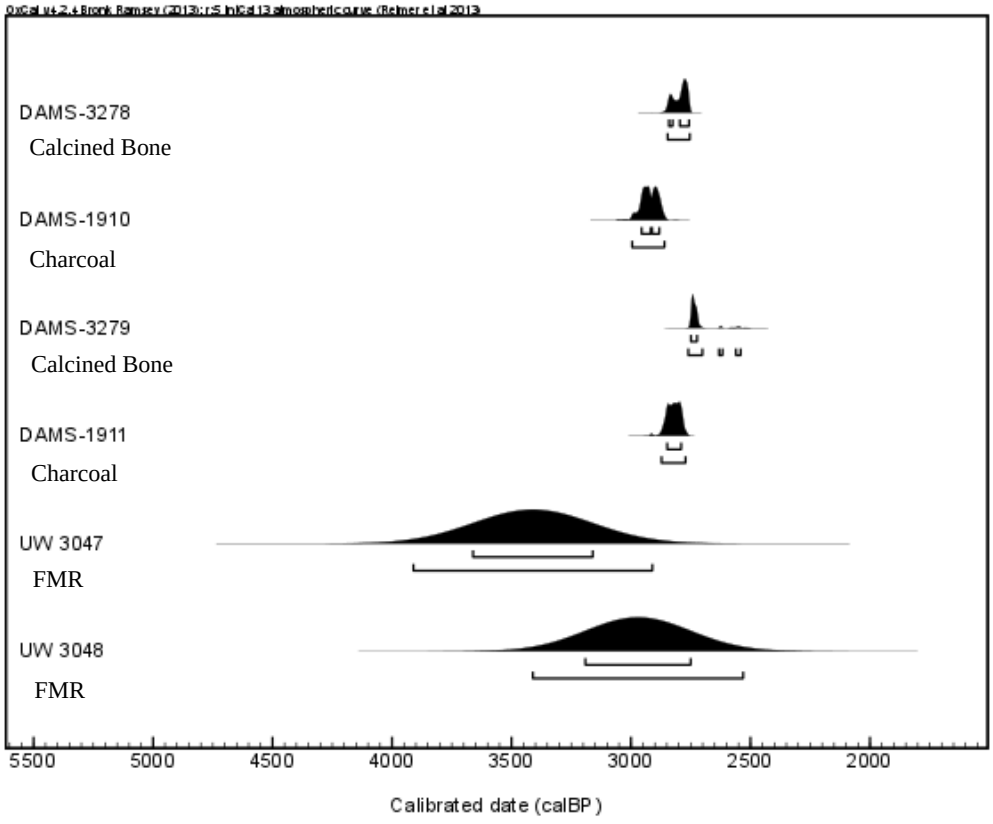

Figure 7. Calibrated Age Ranges of Radiocarbon Dates and Two Sigma Age Ranges of Luminescence Dates from the Bray Site Earth Oven Features

Sunrise Ridge Borrow Pit Site:

Figures 8- 11 compare findings for four features at this site. Figure 8 shows the distribution of the dates from the 30N feature. Based upon the graph it is clear the pairings overlap. It shows that when calibrated at a 2-sigma range all of the dates significantly overlap.

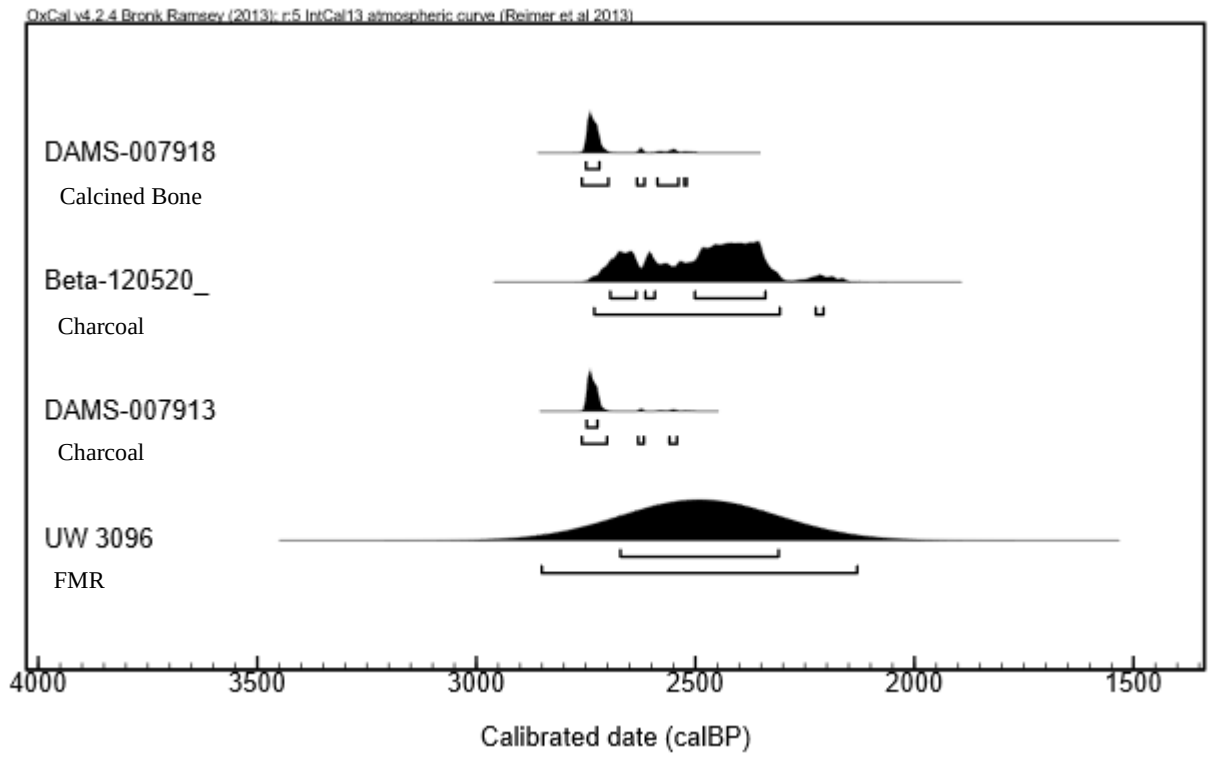

Figure 8. Calibrated Age Ranges of Radiocarbon Dates and Two Sigma Age Range of Luminescence Dates from the Sunrise Ridge Borrow Pit Site 30N Features

Figures 9 shows the distribution of the dates from the Feature AA. Based upon the graph it is clear the pairings overlap, however, based upon the radiocarbon dates, there is a range of dates from 2500-1500 cal. B.P. The above graph shows that when calibrated at a 2-sigma range all of the dates do not significantly overlap, it appears that there are between two to three uses of this feature resulting in a distribution of dates over three separate periods. This is most clearly seen in the distribution of the five radiocarbon dates.

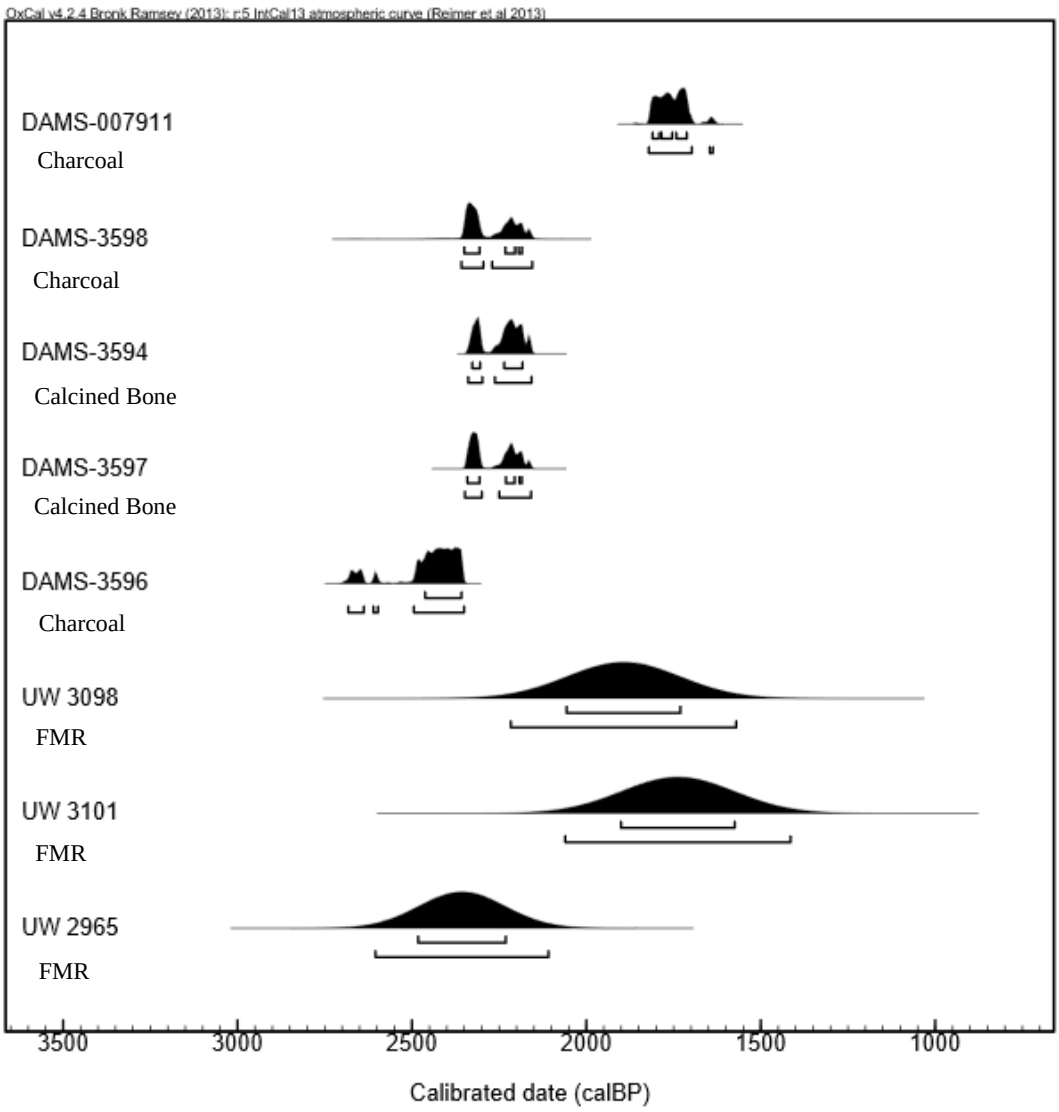

Figure 9. Calibrated Age Ranges of Radiocarbon Dates and Two Sigma Age Range of Luminescence Dates from the Sunrise Ridge Borrow Pit Site Feature AA

Figures 10 shows the distribution of the dates from Feature AD. Based upon the graph it is clear that the pairings overlap. However, it appears that UW 2964 provides a slightly older estimate that either the charcoal or calcined bone radiocarbon samples. The above graph shows that when calibrated at a 2-sigma range all of the dates significantly overlap.

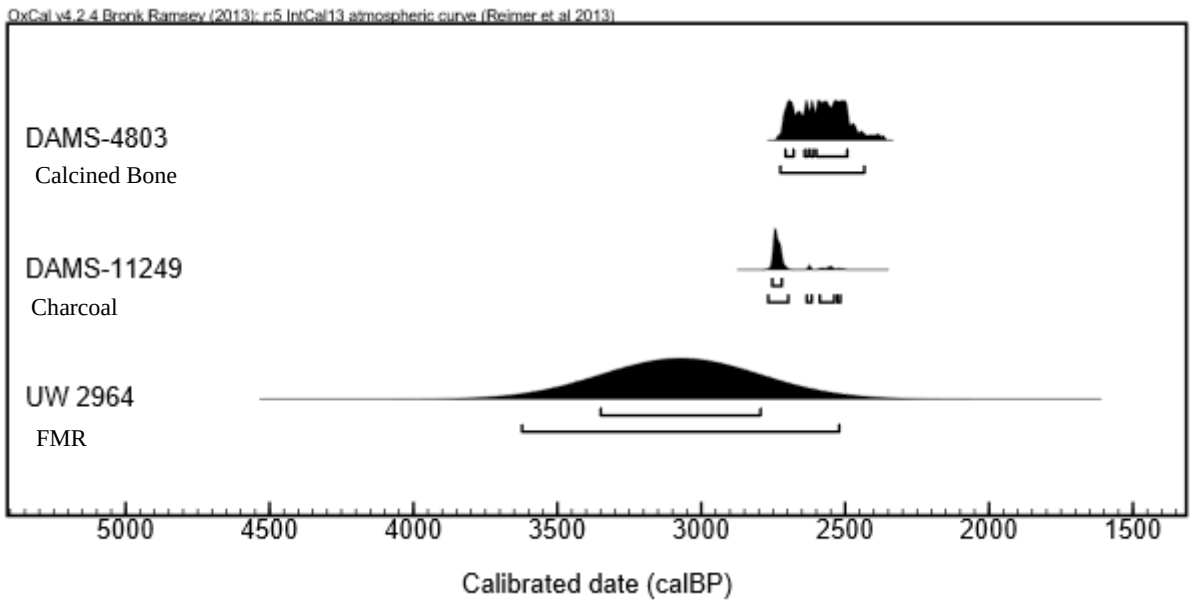

Figure 10. Calibrated Age Ranges of Radiocarbon Dates and Two Sigma Age Range of Luminescence Dates from the Sunrise Ridge Borrow Pit Site Feature AD

Figures 11 shows the distribution of the dates from Feature R. Based upon the graph it is clear the pairings again overlap. The above graph shows that when calibrated at a 2-sigma range all of the dates significantly overlap.

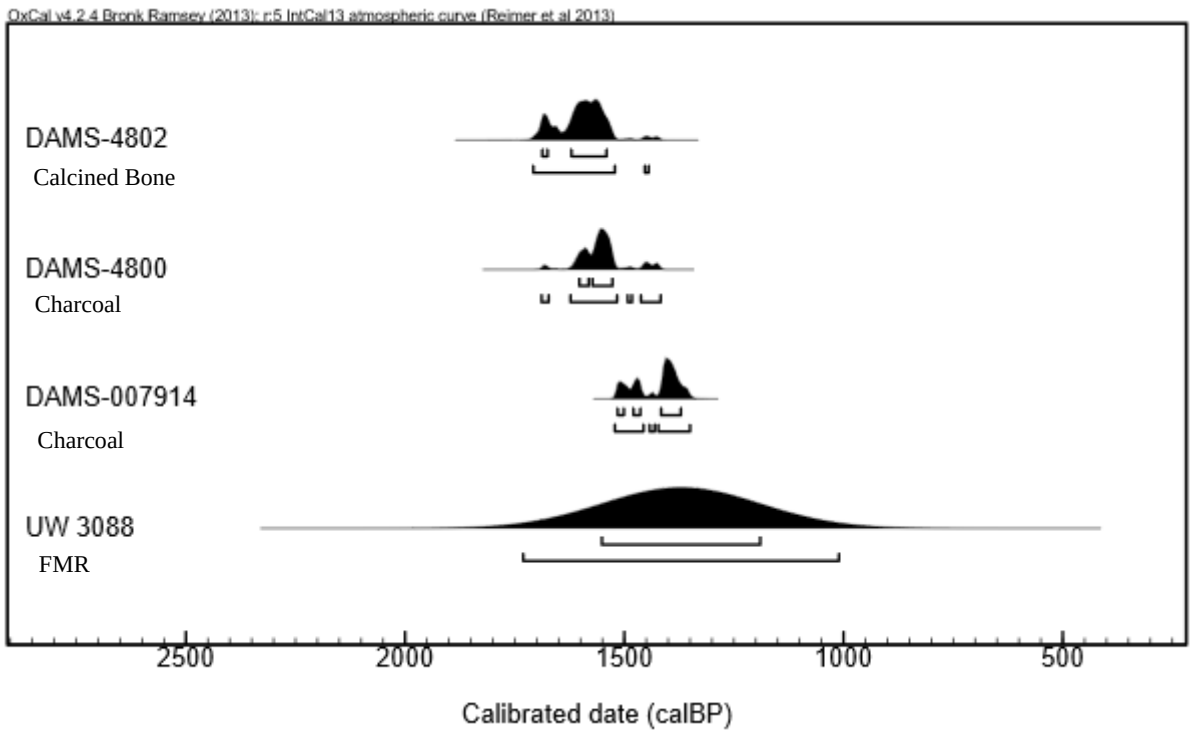

Figure 11. Calibrated Age Ranges of Radiocarbon Dates and Two Sigma Age Range of Luminescence Dates from the Sunrise Ridge Borrow Pit Site Feature R

Fryingpan Creek Rockshelter:

Figures 12 shows the distribution of the dates from Feature 1. The calcined bone samples and one of two charcoal samples indicate that this feature had a single use approximately 600-500 cal. B.P. The above graph shows that when calibrated at a 2-sigma range all but one of the dates significantly overlap. Beta 163694, a charcoal date from a 10 cm level below the other measurements is signifcantly older then the remainder of the dates. This is possibly a result of earlier use of the feature or contamination through the old wood effect.

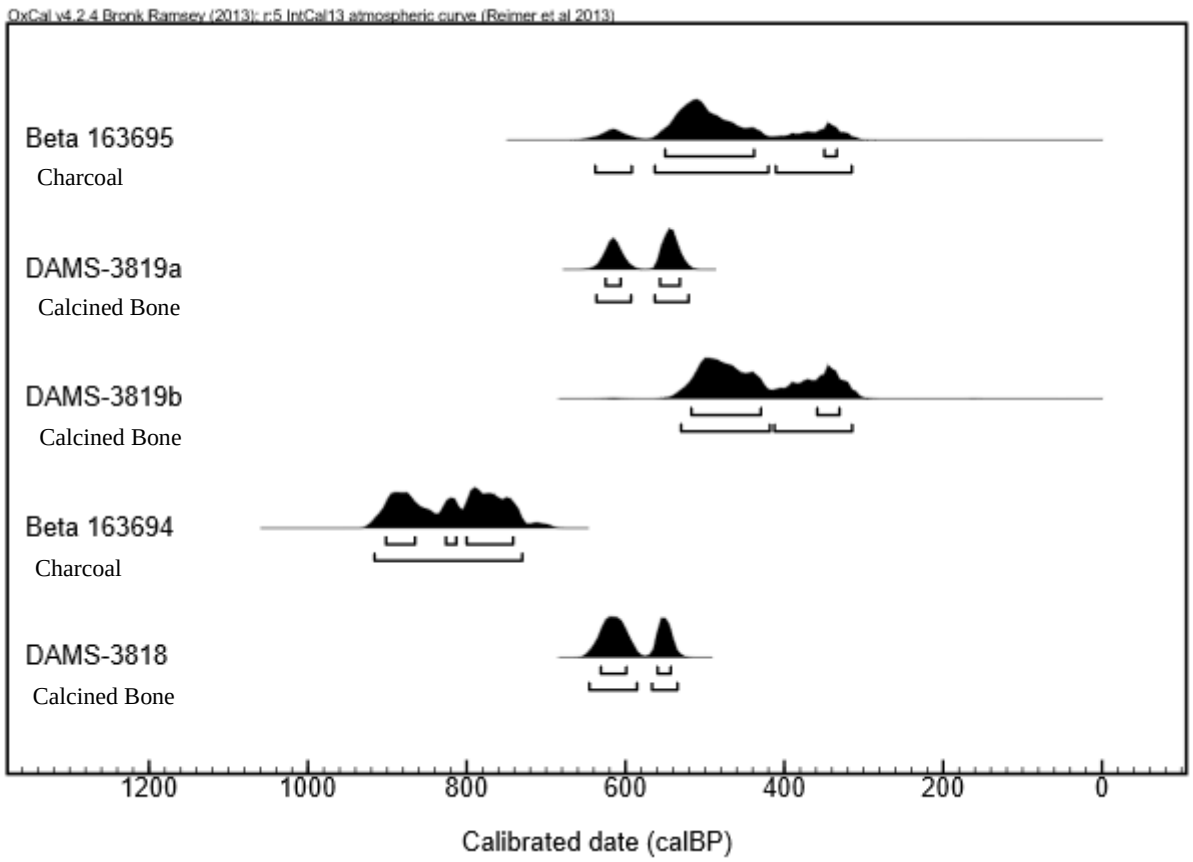

Figure 12. Calibrated Age Ranges of Radiocarbon Dates from the Fryingpan Creek Rockshelter Feature 1

Sequim Bypass:

Figure 13 shows the distribution of the dates from the hearth feature of unit 304N/198E. The calcined bone samples and charcoal sample indicate that this feature had a single use approximately 2350-2730 cal. B.P. The above graph shows that when calibrated at a 2-sigma range all but one of the dates significantly overlap.

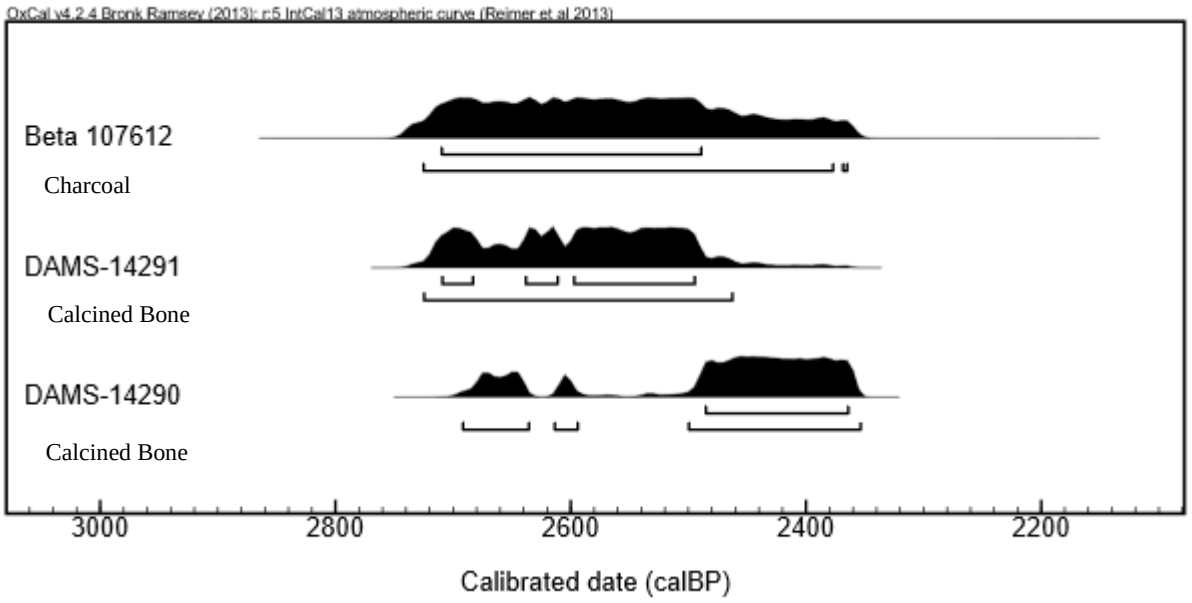

Figure 13. Calibrated Age Ranges of Radiocarbon Dates from the Sequim Bypass Site.

Statistical Test:

To compare the differences between the charcoal, calcined bone, and FMR we employed a series of Wilcoxon Match-Pair tests on the entire data set. These tests broke the dataset down into two sets of match pairs: charcoal/calcined bone and charcoal/FMR. Only the pairings of charcoal/calcined bone and charcoal/FMR were used because charcoal from a distinct cultural context is the standard in radiocarbon dating. Thus, we are trying to validate the use of calcined bone and FMR by comparing to charcoal from a known cultural context. The hypotheses for these tests are:

H_0: The match-pairs are drawn from a similar population of dated events

H_A: The match-pairs are drawn from different populations of dated events

For each of these tests, the median was calculated and compared between the match pairs. To incorporate the 2-sigma range of these dates, a simulation was conducted that drew 100 random samples from within the corresponding date ranges. The alpha values for all tests are 0.05.

A total of ten match-pairs of charcoal and calcined bone were identified (Table 7). The results of the charcoal/calcined bone match pairs are a z-score of 1.48 and a p-value of 0.14. With a p-value of 0.14 we fail to reject the null hypothesis meaning that the date range of charcoal and calcined bone are drawn from a similar population of dated events. In the use of the 100 randomized samples, there were only eleven z-scores that were returned as statistically significant.

Table 7. Identified Charcoal-Calcined Bone Match-Pairs

Pairing	Sample Number	Site Number	Unit	Material	Dated Age B.P.	2-Sigma Range Cal. B.P.
1	DAMS-3594	45PI408	71.5N/65.5E	Calcined Bone	2246±24	2158-2338
	DAMS-3596	45PI408	71.5N/65.5E	Charcoal	2410±28	2351-2682
2	DAMS-3597	45PI408	71.5N/65.5E	Calcined Bone	2265±27	2159-2347
	DAMS-3598	45PI408	71.5N/65.5E	Charcoal	2286±43	2155-2357
3	DAMS-11249	45PI408	AI profile	Charcoal	2583±33	2517-2766
	DAMS-4803	45PI408	AI profile	Calcined Bone	2484±31	2385-2725
4	DAMS-4802	45PI408	61.5N/35E	Calcined Bone	1683±42	1445-1707
	DAMS-4800	45PI408	61.5N/35E	Charcoal	1652±32	1417-1688
5	DAMS-007918	45PI408	28N/25E	Calcined Bone	2574±29	2520-2758
	DAMS-007913	45PI408	30N/24E	Charcoal	2576±26	2543-2758
6	DAMS-14290	45CA426	304N/198E	Calcined Bone	2425±25	2354-2691
	Beta 107612	45CA426	304N/198E	Charcoal	2480±50	2365-2725

Table 7. (Continued)

Pairing	Sample Number	Site Number	Unit	Material	Dated Age B.P.	2-Sigma Range Cal. B.P.
7	DAMS-3278	45PI1276	1-gg	Calcined Bone	2690±28	2754-2847
	DAMS-1910	45PI1276	1-gg	Charcoal	2823±25	2862-2992
8	DAMS-3279	45PI1276	5N/7E	Calcined Bone	2578±27	2542-2759
	DAMS-1911	45PI1276	5N/7E	Charcoal	2734±24	2772-2871
9	Beta 163695	45PI43	Unit A	Charcoal	460±70	236-488
	DAMS-3819b	45PI43	Unit A	Calcined Bone	408±59	314-529
10	Beta 163694	45PI43	Unit A	Charcoal	890±40	730-916
	DAMS-3818	45PI43	Unit A	Calcined Bone	578±26	534-646

A total of eight match-pairs of charcoal and FMR were identified (Table 8). The results of the charcoal/FMR match-pairs are a z-score of 1.69 and a p-value of 0.09. With a p-value of 0.09 we fail to reject the null hypothesis, indicating that the date ranges of charcoal and FMR are drawn from similar populations of dated events. In the use of the 100 randomized samples, there were eighteen z-scores that were returned as statistically significant.

Table 8. Identified Charcoal-FMR Match-Pairs

Pairing	Sample Number	Site Number	Unit	Material	Dated Age B.P.	2-Sigma Range Cal. B.P.
1	DAMS-007911	45PI408	71.5N/65.5E	Charcoal	1814±24	1636-1821
	UW3101	45PI408	71.5N/65.5E	FMR	1672±80	1542-1832
2	DAMS-3596	45PI408	71.5N/65.5E	Charcoal	2410±28	2351-2682
	UW2965	45PI408	71.5N/65.5E	FMR	2291±124	2043-2539
3	DAMS-3598	45PI408	71.5N/65.5E	Charcoal	2286±43	2155-2357
	UW3098	45PI408	71.5N/66.5E	FMR	1828±162	1504-2152
4	DAMS-11249	45PI408	AI profile	Charcoal	2583±33	2517-2766
	UW 2964	45PI408	AI Profile	FMR	3006±276	2454-3528
5	DAMS-4800	45PI408	61.5N/35E	Charcoal	1652±32	1417-1688
	UW3088	45PI408	61.5N/35E	FMR	1305±180	945-1665
6	DAMS-007913	45PI408	30N/24E	Charcoal	2576±26	2543-2758
	UW3096	45PI408	29N/25E	FMR	2425±180	2065-2785
7	DAMS-1910	45PI1276	1-gg	Charcoal	2823±25	2862-2992
	UW3047	45PI1276	3N7E	FMR	3345± 250	2845-3845
8	DAMS-1911	45PI1276	5N/7E	Charcoal	2734±24	2772-2871
	UW3048	45PI1276	5N7E	FMR	2905 ± 220	2465-3345

5. DISCUSSION & CONCLUSION

Based upon the comparison of the charcoal/calcined bone and charcoal/FMR matched pairs, we conclude that both calcined bone and FMR can be used as media for accurately dating archaeological deposits. The results of the statistical tests and the similar distributions of the charcoal/calcined bone pairings make it evident that calcined bone is an accurate medium for the radiocarbon dating of archaeological sites in the PNW of North America. Nearly all of the charcoal/calcined bone pairings overlap significantly when calibrated at 2-sigma. Results indicate that calcined bone would be capable of dating archaeological sites that contain no reliable charcoal for dating. This gives the possibility for dating previously undated sites in the PNW through the means of calcined bone.

Comparisons of the charcoal/calcined bone/FMR triplets show that they share similar distributions when graphed at 2-sigma, however, due to the low precision of luminescence dating the radiocarbon dates fall within the 2-sigma range of all luminescence dates. Many of the charcoal and calcined bone match closely with the FMR. The error associated with luminescence dating is so large that a graphical comparison is not significant. Even though there are large error terms associated with luminescence dating, which makes it lack precision, this does not discredit it as a technique for use in the PNW due to its high accuracy. The high accuracy associated with the luminescence dating of FMR indicates that luminescence dating can be utilized in the Pacific Northwest when neither reliable charcoal nor calcined bone is available.

Research throughout the world (Liritzis et al. 2013) has been attempting to increase the validity of luminescence dating. In the PNW of North America, there has been some use of luminescence dating (Chatters et al. 2011; Mack et al. 2010). Our research shows luminescence dating in the PNW could instead provide an accurate medium, that uses a common artifact

(FMR), requires a substantially shorter bridging argument to be made between the dated and target events, and it closely matches those dated events thought to be tied to target events of interest. Using luminescence dating will increase the accuracy of describing the timing for cultural phenomena. However, due to the lack of precision associated with luminescence dating the technique should not be solely relied upon to understand the cultural change of the PNW when other, more precise media are available.

Limitations of these techniques are that luminescence dating is a costly dating technique that takes a lengthy period of time to have a date returned. Additionally, unless excavation is occurring with the possibility for luminescence dating then the collection of FMR may not have occurred. A limitation of calcined bone is that the sample has to be fully calcined, that there cannot be a charred core left in the bone. This often results in the need to snap the bone to identify if the bone is calcined. Additionally, the calcined bone may not have been collected or properly identified during excavation.

ACKNOWLEDGEMENTS

This study is a research initiative of DirectAMS, which funded the majority of the radiocarbon dating. Additional funding for radiocarbon and luminescence dating came from CWU College of the Sciences, CWU Science Honors Program, CWU School of Graduate Studies and Mount Rainier National Park. We would like to thank the archaeologists that provided samples for this research: Greg Burtchard of Mt. Rainier National Park and the Jamestown S'Klallam. Additional thanks goes to The Bray Family, Edgar Huber and Statistical Research Inc. for the funding of the luminescence dates for the Bray Site. Thanks goes to Dr. James K. Feathers for the internship at the University of Washington Luminescence Laboratory.

BIBLIOGRAPHY

Aitkens, M.J.
1985 *Thermoluminescence Dating.* Academic Press, London.

1998 *An Introduction to Optical Dating.* Oxford University Press, Oxford.

Aiken, M.J., M.S. Tite, and J. Reid
1964 Thermoluminescent Dating of Ancient Ceramics. *Nature*. 202:1032-1033.

Ames, Kenneth M.
1996 Life in the Big House, Household Labor and Dwelling Size on the Northwest Coast. In *People who lived in Big Houses, Archaeological Perspectives on large domestic structures* edited by Gary Coupland and E.B. Banning. Prehistory Press, Madison. Pp. 178 – 200.

1991 The Archaeology of the Longue Duree: Temporal and Spatial Scale in the Evolution of Social Complexity on the Southern Northwest Coast. *Antiquity.*65:935-945.

1994 The Northwest Coast: Complex Hunter-Gatherers, Ecology, and Social Evolution. *Annual Review of Anthropology.* 23:209-229.

1998 Economic Prehistory of the Northern British Columbia Coast. *Arctic Anthropology.* 35(1):68-87

2002 Intensification of Food Production on the Northwest Coast and Elsewhere. In *Keeping it Living: Traditions of Plant Use and Cultivation on the Northwest Coast of North America.* Edited by Douglas Deur and Nancy J. Turner, pp. 67-100. University of Washington Press, Seattle.

Ames, Kenneth M., Don E. Dumond, Jerry Galm, and Rick Minor.
1998 The Prehistory of the Southern Plateau. In *Handbook of North American Indians, Volume 9, The Plateau*. edited by Deward Walker. Smithsonian Institution Press, Washington D.C. pp.: 103 – 119

Ames, Kenneth M., and Herbert D.G. Maschner
1999 *Peoples of the Northwest Coast: Their Archaeology and Prehistory.* Thames and Hudson Ltd. London.

Benea, V., D. Vandenberghe, A. Timar, P. van den Haute, C. Cosma, M. Gligor, and C. Florescu
2007 Luminescence Dating of Neolithic Ceramics from Lumea Noua, Romania. *Geochronometria.* 28:9-16.

Berger, Glenn W.
1988 Dating Quarternary Events by Luminescence. *Geological Society of America Special Papers.* 227:13-50

Bettinger, Robert L., Raven Garvey, and Shannon Tushingham.
2015 *Hunter-gatherers: Archaeological and Evolutionary Theory.* Springer, New York.

Binford, Lewis R.
1980 Willow Smoke and Dog's Tails: Hunter-Gatherer Settlement Systems and Archaeological Site Formation. *American Antiquity* 45:4-20.

Brain, C.K.
1981 *The Hunters or the Hunted? An Introduction to African Cave Taphonomy.* University of Chicago Press, Chicago.

Brown, James W.
2014 Radiocarbon Dating of Calcined Bone: Pacific Northwest. Unpublished Undergraduate Science Honors Thesis, Department of Anthropology, Central Washington University, Ellensburg.

Butler, B. R.
1961 *The Old Cordilleran Culture in the Pacific Northwest* (No. 5). Idaho State College Museum.

Butler, Virginia L.
2000 Resource Depression on the Northwest Coast of North America. *Antiquity* 74:649-661.

Butler, Virginia L. and Sarah K. Campbell
2004 Resource Intensification and Resource Depression in the Pacific Northwest of North America: A Zooarchaeological Review. *Journal of World Prehistory.* 18(4):327-405

Campbell, Sarah K. and Virginia L. Butler
2010 Archaeological Evidence for Resilience of Pacific Northwest Salmon and Socioecological System over the 7,500 Years. *Ecology and Society.* 15(1):1

Carlson, Roy L.
1983 Prehistory of the Northwest Coast. In *Indian Art Traditions of the Northwest Coast,* edited by Roy L. Carlson, pp. 13-32. Simon Fraser University Press, Burnaby.

Chatters, James C.
1987 Hunter-Gatherer Adaptations and Assemblage Structure. *Journal of Anthropological Archaeology* 6:336-375.

1995 Population Growth, Climatic Cooling, and the Development of Collector Strategies on the Southern Plateau, Western North America. *Journal of World Prehistory* 9(3):341-400.

2009 A Macroevolutionary Perspective on the Archaeological Record of North America. In *Macroevolution in Human Prehistory,* edited by A.M. Prentiss, I. Kuijt, and J.C. Chatters, pp. 213-234. Springer, New York.

Chatters, James C., Jason B. Cooper, Phillippe D. LeTourneau, and Lara C. Rooke
2011 *Understanding Olcott: Data Recovery at 45SN28 and 45SN303, Snohomish County, Washington.* AMEC Earth and Environmental. Submitted to Snohomish County Department of Public Works. Manuscript on file, Washington Department of Archaeology and Historic Preservation, Olympia.

Chatters, James C. and William C. Prentiss
2005 A Darwinian Macro-Evolutionary Perspective on the Development of Hunter-Gatherer Systems in Northwestern North America. *World Archaeology.* 37(1): 46-65.

Coupland, Gary
1988 Prehistoric Economic and Social Change in the Tsimshian Area. In *Research in Economic Anthropology Supplement 3: Prehistoric Economies of the Pacific Northwest Coast,* edited by Barry L. Isaac, pp. 231-243. JAI Press, Greenwich, Connecticut.

Croes, Dale R., and Steven Hackenberger
1988 Hoko River Archaeological Complex: Modeling Prehistoric Northwest Coast Economic Evolution. In *Research in Economic Anthropology Supplement 3: Prehistoric Economies of the Pacific Northwest Coast,* edited by Barry L. Isaac, pp. 19-85. JAI Press, Greenwich, Connecticut.

Croes, Dale R., Scott Williams, Larry Ross, Mark Collard, Carolyn Dennler, and Barbara Vargo
2008 The Projectile Point Sequences in the Puget Sound Region. In *Projectile Point Sequences in Northwestern North America,* edited by Roy L. Carlson and Martin P.R. Magne, pp.105-130. Archaeology Press, Simon Fraser University, Burnaby, B.C.

Dean, Jeffrey S.
1978 Independent Dating in Archaeological Analysis. *Advances in Archaeological Method and Theory* 1:223-255.

Dincauze, D.
2000 *Environmental Archaeology: Principles and Practice.* Cambridge University Press, Cambridge.

Dunnell, Robert C.
1980 Evolutionary Theory and Archaeology. *Advances in Archaeological Method and Theory* 3:35-99.

Dunnell, Robert C. and James K. Feathers
1995 Thermoluminescence Dating of Surficial Archaeological Materials. In *Dating in Surface Context,* edited by C. Beck. University of New Mexico Press, Albuquerque. pp. 115-137

Dykeman, D.D., R.H. Towner, J.K. Feathers
2002 Tree-ring and Thermoluminescence Dating: Evaluating Methods for Confidently Dating Protohistoric Navajo Sites. *American Antiquity.* 67:145-164.

Eldredge, Niles
1989 *Macroevolutionary Dynamics.* McGraw-Hill, New York.

Eldredge, Niles and Stephen Jay Gould
1972 Punctuated Equilibria: An Alternative to Phyletic Gradualism. In *Models in Paleobiology,* edited by Thomas J.M. Schopf. Freeman, Cooper and Company, San Francisco. pp. 82-115.

Feathers, James K.
1997 The Application of Luminescence Dating in American Archaeology. *Journal of Archaeological Method and Theory.* 4(1): 1-66.

2003 Use of Luminescence Dating in Archaeology. *Measurement Science and Technology.* 14:1493-1509.

2009 Problems of Ceramic Chronology in the Southeast: Does Shell-Tempered Pottery Appear Earlier than We Think? *American Antiquity.* 74(1):113-142.

Franklin, Jerry F., and Christen T. Dyrness
1988 Natural Vegetation of Oregon and Washington. Oregon State University Press, Corvallis, Oregon.

Gardner, G.J., A.J. Mortlock, D.M. Price, M.L. Readhead, and R.J. Wasson
1987 Thermoluminescence and Radiocarbon Dating of Australian Desert Dunes. *Australian Journal of Earth Sciences: An International Geoscience Journal of the Geological Society of Australia* 34(3):343-357.

Hallett, Douglas J., Dana S. Lepofsky, Rolf W. Mathewes, and Ken P. Lertzman
2003 11,000 Years of Fire History and Climate in the Mountain Hemlock Rain Forests of Southwestern British Columbia Based on Sedimentary Charcoal. *Canadian Journal of Research* 33:292-312.

Hayden, Brian
1995 Pathways to Power. In *Foundations of Social Inequality,* edited by T. Douglas Price and Gary M. Feinman. pp. 15-86. Springer, New York.

2001 Richman, Poorman, Beggarman, Chief: The Dynamics of Social Inequality. In *Archaeology at the Millenium,* edited by Gary M. Feinman and T. Douglas Price, pp. 231-272. Springer, New York.

Huelsbeck, David R.
1988 The Surplus Economy of the Central Northwest Coast. In *Research in Economic Anthropology Supplement 3: Prehistoric Economies of the Pacific Northwest Coast,* edited by Barry L. Isaac, pp. 149-178. JAI Press, Greenwich, Connecticut.

Huls, CM, H. Erlenkeuser, M-J Nadeau, P.M. Grootes, and N. Anderson
2010 Experimental Study on the Origin of Cremated Bone Apatite Carbon. *Radiocarbon* 52(2):587-599.

Hunt, Terry L. and Carl P. Lipo
2007 Chronology, Deforestation, and "Collapse:" Evidence vs. Faith in Rapa Nui Prehistory. *Rapa Nui Journal* 21(2):85-97.

Johnson, E.
1989 Human Modified Bones from Early Southern Plains Sites. In *Bone Modification*. Edited by R. Bonnichsen and M.H. Sorg, pp. 431-471. University of Maine Center for the Study of the First Americans, Orono.

Jolivette, Stephanie, and Edgar K. Huber
In Press *Monitoring of Site Restoration and Analysis of Materials from the Bray Site (45PI1276) under DAHP Excavation Permit No. 2015-31, Pierce County, Washington.* SRI Technical Report 16-27, Lacey, WA.

Kiszley, I.
1973 Derivatographic Examination of Subfossil and Fossil Bones. *Current Anthropology* 14:280-286.

Kramer, Stephenie
2000 Camas Bulbs, the Kalapuya, and Gender: Exploring Evidence of Plant Food Intensification in the Willamette Valley of Oregon. Unpublished Master's Thesis. Department of Anthropology, University of Oregon, Eugene.

Lanting, J.N., and A.L. Brindley
1998 Dating Cremated Bone: The Dawn of a New Era. *The Journal of Irish Archaeology* 9:1-7.

Lanting, J.N., A.T. Aerts-Bijma, J. van der Plicht
2001 Dating Cremated Bone. *Radiocarbon* 43(2A):249-254.

Leonhardy, Frank C., and David G. Rice
1980 Lower Snake River Typology Revision and Evaluation. Paper presented at the 33rd Annual Northwest Anthropological Conference, Bellingham, Washington.

Liritzis, Ioannis, Ashok Kumar Singhvi, James K. Feathers, Gunther A. Wagner, Annette Kadereit, Nikolaos Zacharias, and Sheng-Hua Li
2013 *Luminescence Dating in Archaeology, Anthropology, and Geoarchaeology: An Overview.* Springer, New York.

Lubinski, Patrick M., and Greg C. Burtchard
2005 Fryingpan Rockshelter (45PI43): A Subalpine Fauna in Mount Rainier National Park. *Archaeology in Washington* 11:35-52.

Lupo, Karen D.
2007 Evolutionary Foraging Models in Zooarchaeological Analysis: Recent Applications and Future Challenges. *Journal of Archaeological Research* 15:143-190

Lyman, R. Lee
2003a Pinniped Behavior, Foraging Theory and the Depression of Metapopulations and Nondepression of a Local Population on the Southern Northwest Coast of North America. *Journal of Anthropological Archaeology* 22:376-388.

2003b The Influence of Time Averaging and Space Averaging on the Application of Foraging Theory in Zooarchaeology. *Journal of Archaeological Science* 30:595-610.

Mack, Cheryl A., James C. Chatters, and Anna M. Prentiss
2010 *Archaeological Data Recovery at the Beech Creek Site (45LE415), Gifford Pinchot National Forest, Washington.* Prepared for the Gifford Pinchot National Forest, U.S. National Forest Service. Manuscript on file, Washington Department of Archaeology and Historic Preservation, Olympia.

Maschner, Herbert D.G.
1991 The Emergence of Cultural Complexity on the Northern Northwest Coast. *Antiquity.* 65(249):924-934.

Matson, Richard G.
2008 The Crescent Beach site and the Place of the Locarno Beach Phase. Electronic document, http://www.anth.ubc.ca/fileadmin/user_upload/anso/LOA_PDFs/Matson_Crescent_Beach/FrontMatter.pdf, accessed December 10, 2014.

Matson, R.G. and Gary Coupland
1995 *The Prehistory of the Northwest Coast*. Academic Press, New York.

McCutcheon, Patrick T.
1992 Burned Archaeological Bone. In *Deciphering Shell Middens,* Edited by Julie K. Stein, pp. 347-370.

McCutcheon, Patrick T., Anne B. Parfitt, James W. Brown, David R. Davis, Caitlin Limberg, and Sherri Middleton
In Prep *Investigating Intra-Site Variation for Holocene Epoch Human Land Use at the Sunrise Ridge Borrow Pit Site (45PI408).* Prepared for the National Park Service, Seattle, WA. Department of Anthropology and Museum Studies, Central Washington Archaeological Survey, Central Washington University, Ellensburg.

Mejdahl, V.
1969 Thermoluminescence Dating of Ancient Danish Ceramics. *Archaeometry.*11(1): 99-104

Mitchell, Donald and Leland Donald
1988 Archaeology and the Study of Northwest Coast Economies. In *Research in Economic Anthropology Supplement 3: Prehistoric Economies of the Pacific Northwest Coast,* edited by Barry L. Isaac, pp. 293-351. JAI Press, Greenwich, Connecticut.

Morgan, Vera E. (editor)
1999 *The SR-101 Sequim Bypass Archaeological Project: Mid- to Late-Holocene Occupations on the Northern Olympic Peninsula, Clallam County, Washington.* Submitted to Washington Department of Transportation. Eastern Washington University Reports in Archaeology and History 100-108, Archaeological and Historic Services, Cheney.

Muller, Richard A.
1977 Radioisotope Dating with a Cyclotron. *Science.* 196(4289):489-494.

Naysmith, Philip, E. Marian Scott, Gordon T. Cook, Jane Heinemeier, Johannes can der Plicht, Mark Van Strydonck, Christopher Bronk Ramsey, Pieter M. Grootes, and Stewart P.H.T. Freeman
2007 A Cremated Bone Intercomparison Study. *Radiocarbon.* 49(2):403-408.

Nolan, Kevin C.
2012 Temporal Hygiene: Problems in Cultural Chronology of the Late Prehistoric Period of the Middle Ohio River Valley. *Southeastern Archaeology* 31:187-209.

Olsen, Jesper, Jan Heinemeier, Karen Margrethe Hornstrup, Pia Bennike, and Henrik Thrane
2013 'Old Wood' Effect in Radiocarbon Dating of Prehistoric Cremated Bones? *Journal of Archaeological Science.* 40:30-34

Prentiss, Anna M.
2009 The Emergence of New Socioeconomic Strategies in the Middle and Late Holocene Pacific Northwest Region of North America. In *Macroevolution in Human Prehistory,* edited by A.M. Prentiss, I. Kuijt, and J.C. Chatters, pp. 111-131. Springer, New York.

2011 Social Histories of Complex Hunter-Gatherers Pacific Northwest Prehistory in a Macroevolutionary Framework. In *Hunter-Gatherer Archaeology as Historical Process,* edited by Kenneth E. Sassaman and Donald H. Holly Jr. The University of Arizona Press, Tucson. pp. 17-33.

Prentiss, Anna M., James C. Chatters, Randall R. Skelton, and Matthew Walsh
2014 The Evolution of Old Cordilleran Core Technology. In *Works in Stone: Contemporary Perspectives on Lithic Analysis,* edited by Michael J. Shott, pp. 178-196. University of Utah Press, Salt Lake City, Utah.

Prentiss, Anna M., Nathan Goodale, Lucille E. Harris, and Nicole Crossland
2015 Evolution of the Slate Tool Industry at Bridge River, British Columbia. In *Lithic Technological Systems and Evolutionary Theory,* edited by Nathan Goodale and William Andrefsky Jr. Cambridge University Press, Cambridge. pp. 267-292.

Reimer PJ, Bard E, Bayliss A, Beck JW, Blackwell PG, Bronk Ramsey C, Buck CE, Cheng H, Edwards RL, Friedrich M, Grootes PM, Guilderson TP, Haflidason H, Hajdas I, HattÃ C, Heaton TJ, Hogg AG, Hughen KA, Kaiser KF, Kromer B, Manning SW, Niu M, Reimer RW, Richards DA, Scott EM, Southon JR, Turney CSM, van der Plicht J.
2013 IntCal13 and MARINE13 radiocarbon age calibration curves 0-50000 years cal BP *Radiocarbon* 55(4): 1869-1887

Rice, David G.
1972 *The Windust Phase in Lower Snake River Region Prehistory.* Washington State University Laboratory of Anthropology.

Richter, D.
2007 Advantages and Limitations of Thermoluminescence Dating of Heated Flint from Paleolithic Sites. *Geoarchaeology.* 22:671-683.

Richter, D., G. Tostevin, P. Skrlda, and W. Davies
2009 New Radiometric Ages for the Early and Upper Paleolithic Type Locality of Brno-Bohunice (Czech Republic): Comparison of OSL, IRSL, TL, and 14C Dating Results. *Journal of Archaeological Science.* 36:708-720.

Schalk, Randall and Gregory Cleveland
1983 A Sequence of Adaptations in the Columbia-Fraser Plateau. In *Cultural Resource Investigations for the Lyons Ferry Fish Hatchery Project, Near Lyons Ferry, Washington.* Edited by Randall Schalk, pp 11-56. Project Report Number 8, Laboratory of Archaeology and History, Washington State University, Pullman.

Sheldon, David, James Chatters, Marc Fairbanks, Bruce Gustafson, and James Brown
2013 Early Resource Intensification and Collector Strategies: The Bray Site (45PI1276), Pierce County, WA. Poster Presented at the 2013 Northwest Anthropological Conference.

Shipman, P., G. Foster, and M. Schoeninger
1984 Burnt Bones and Teeth: An Experimental Study of Color, Morphology, Crystal Structure and Shrinkage. *Journal of Archaeological Science* 11:307-325.

Smith, M.A., J.R. Prescott, and M.J. Head
1997 Comparison of ^{14}C and Luminescence Chronologies at Puritjarra Rockshelter, Central Australia. *Quaternary Science Reviews* 16(3-5):299-320.

Snoeck, C., F. Brock, and R.J. Schulting
2014 Carbon Exchanges Between Bone Apatite and Fuels During Cremation: Impact on Radiocarbon Dates. *Radiocarbon.* 56(2):591-602.

Stuiver, Minze
1978 Radiocarbon Timescale Tested Against Magnetic and Other Dating Methods. *Nature* 273: 271-274.

Taylor, R.E.
1997 *Radiocarbon Dating.* Springer, New York.

Taylor, R.E. and Ofer Bar-Yosef
2014 *Radiocarbon Dating: An Archaeological Perspective.* Left Coast Press, Inc., Walnut Creek, California.

Thoms, Alston V.
1989 The Northern Roots of Hunter-Gatherer Intensification: Camas and the Pacific Northwest. Unpublished Ph.D. Dissertation. Department of Anthropology, Washington State University, Pullman.

Van Strydonck, M., M. Boudin, G. De Mulder
2010 The Origin of the Carbon in Bone Apatite of Cremated Bones. *Radiocarbon* 52(2-3): 578-586.

Walsh, Megan K., Jennifer R. Marlon, Simon J. Goring, Kendrick J. Brown, and Daniel G. Gavin
2015 A Regional Perspective on Holocene Fire-Climate-Human Interactions in the Pacific Northwest of North America. *Annals of the Association of American Geographers.* DOI: 10.1080/00045608.2015.1064457

Wessen, Gary C.
1988 The Use of Shellfish Resources on the Northwest Coast: The View from Ozette. In *Research in Economic Anthropology Supplement 3: Prehistoric Economies of the Pacific Northwest Coast,* edited by Barry L. Isaac, pp. 179-210. JAI Press, Greenwich, Connecticut.

Wilmshurst, Janet M., Terry L. Hunt, Carl P. Lipo, and Atholl J. Anderson
2011 High-Precision Radiocarbon Dating Shows Recent and Rapid Initial Human Colonization of East Polynesia. *PNAS* 108(5):1815-1820.

Wintle, A.G.
1993 Recent Developments in Optical Dating of Sediments. *Radiation Protection Dosimetry.* 47(1-4):627-635.

2008 Fifty Years of Luminescence Dating. *Archaeometry.* 50(2):276-312.

Yang, X-Y, A. Kadereit, G.A. Wagner, I. Wagner, J-Z. Zhang.
2005 TL and IRSL Dating of Jiahu Relics and Sediments: Clue of 7th Millennium BC Civilization in Central China. *Journal of Archaeological Science.* 32:1045-1051.

Zazzo, Antoine
2014 Bone and Enamel Carbon Diagenesis: A Radiocarbon Prospective. *Paleogeography, Paleoclimatology, Paleoecology* (in Press)

Zazzo, Antoine and J-F. Saliege
2011 Radiocarbon Dating of Biological Apatites: A Review. *Paleogeography, Paleoclimatology, Paleoecology* 310:52-61.

Zazzo, Antoine, J-F Saliege, A. Person, and H. Boucher
2009 Radiocarbon Dating of Calcined Bone: Where Does the Carbon Come From? *Radiocarbon* 51(2):601-611.

Zazzo, Antoine, Jean-Francois Saliege, Matthieu Lebon, Sebastien Lepetz, and Christophe Moreau
2012 Radiocarbon Dating of Calcined Bones: Insights from Combustion Experiments Under Natural Conditions. *Radiocarbon* 54(3-4):855-866.

Zazzo, Antoine, Matthieu Lebon, Laurent Chiotti, Clothilde Comby, Emmanuelle Delque-Kolic, Roland Nespoulet, and Ina Reiche
2013 Can We Use Calcined Bones for ^{14}C Dating the Paleolithic? *Radiocarbon* 55(2-3):1409-1421.

Zazzo, Antoine, Christophe Lecuyer, and Andre Mariotti
2004 Experimentally-Controlled Carbon and Oxygen Isotope Exchange between Bioapatites and Water Under Inorganic and Microbially-Mediated Conditions. *Geochimica et Cosmochimica Acta.* 68(1):1-12.

APPENDIX A
DIRECTAMS LABORATORY PROTOCOL

Protocol provided and authored by DirectAMS
Bothell, Washington

7.1 Acid-Base-Acid (ABA) Pretreatment of Wood and Charcoal

Charcoal and plant materials were subjected to acid-base-acid (ABA) treatment. The ABA treatment described by Taylor (1987) has been modified as follows:

Samples were immersed in excess 6M HCl (approximately 4 mL) at 65 °C for 12 minutes to remove inorganic carbon and acid soluble compounds. In particular, we monitored for the presence of iron, as indicated by a yellowing of the acid/charcoal solution. Iron can chelate humic acids and decrease their solubility in basic solutions, so the acid step was repeated until the solution was clear. Samples were returned to neutrality by rinsing 3 times with deionized (DI) water.

To remove humic acids, samples were repeatedly immersed in KOH (5% w/w) at 65°C for 12 minutes until the solution remained clear. We observed a curious behavior in some charcoal samples when subjected to this treatment. After repeated alkali treatments yielded a clear solution, the brown coloration indicative of humic acid solutes would sometimes reappear upon rinsing with water. In light of this observation, we changed the procedure to include a DI water rinse and a weak acid rinse (0.05M HCl) between each base treatment (Stafford, personal communication 2012). Decreasing the pH between base treatments appeared to improve the efficiency of humic acid removal, and was adopted as the standard procedure. At this writing, however, this was a qualitative judgment; investigations into best practices continue.

A high temperature and/or high molarity final acid treatment was not necessary because acidification of the sample between base steps minimized the risk of atmospheric carbon fixation. The final acid step consisted of 3 quick rinses with 0.05M HCl at room temperature, after which samples were dried in an 80°C oven or in a centrifuge under heat and vacuum.

7.2 Combustion of Dry Material to CO2

Between 1 and 5 mg of dry, pretreated material was transferred to a 9 x 180 mm quartz combustion tube, along with approximately 80 mg copper (II) oxide. The amount of material used depended on sample availability and its presumed carbon content. Chemical standards and blanks were portioned according to their known proportion of carbon to achieve a carbon mass of between 1 and 2 mg. Oxalic acid standards, IAEA-C7 and NIST Ox-II, were portioned approximately 30% in excess of the calculated mass to account for apparent adsorption of atmospheric water. The combustion tubes were labeled with a high temperature paint pen, then connected to a vacuum line, evacuated to 52

less than 20 mtorr, and sealed with a torch. Sealed tubes were heated to 900 °C for 2 hours and allowed to cool to room temperature.

7.3 Pretreatment and Acid Digestion of Carbonate

Shells were examined for evidence of secondary calcite deposits. If a thin, friable layer was observed on the surface, this was scraped away with a blade before portioning for treatment. If epiphytes were present, these parts of the shell were avoided. We selected the thickest part the shell for dating – the collumella of gastropods or near the hinge of bivalves. The shell was broken near the desired area to obtain a representative piece, weighed, then heated in sufficient 0.1M HCl to etch away approximately 30% of the total mass (1mL acid per 5 mg removed).

Digestion of carbonate involves sequestering the shell in a vessel, evacuating the vessel, and then combining it with phosphoric acid to generate carbon dioxide. We achieved this end by first placing an excess of H2PO4 in a Vacuutainer. We then enclosed a shell fragment (15-25 mg) in a folded 24 mm Whatman™ glass microfiber filter (previously baked at 550 °C for 2 hours) and placed it in the Vacuutainer such that the folded sides flared out against the vial walls and held the sample above the phosphoric acid. The vessel was then sealed, evacuated to less than 5 mtorr, then tipped gently to slosh the acid onto the filter, soaking it and causing it to drop into the acid. The carbonate standard and blank (IAEA-C2 and Icelandic doublespar, respectively) were prepared in the same way.

7.4 Reduction of CO2 to Graphite

DirectAMS uses the septa-seal vial zinc reduction method (Ognibene et al. 2003), adapted from the process used at Accium and licensed from Lawrence Livermore. This reduction method uses the water from combustion to supply the hydrogen needed to reduce carbon dioxide to graphite. The reaction is as follows:

Zn + H2O □□ZnO + H2

CO2 + H2 □□CO + H2O

CO + H2 + catalyst (Fe) + heat (550 °C) □□Cgraphite + H2O

Reduction takes place in individually-prepared septa-sealed vials. Each vial contains zinc powder and an inner vial containing a few mg of iron powder. The inner vial rests upon a 3-4 glass beads, separating it from the zinc below. All glass has been previously baked at 550 °C for 2 hours.
Sealed combustion tubes with a tapered break point are inserted partway into a length of flexible plastic tubing, and the tubing is connected to a 3-way stopcock by slipping over a conical Luer fitting. The remaining ports on the stopcock connect to a vacuum line and a fine-gauge needle that pierces the septum of the reduction vial. All parts are single-use.

The system and reduction vial are first evacuated to 3 mtorr and the bottom 10 mm of the reduction vial is immersed in liquid nitrogen before the tip of the combustion tube is snapped inside the flexible tubing to release the CO2. The flask of liquid nitrogen is raised to immerse approximately half of the vial. After 35 seconds, the stopcock is turned again to expose the reduction vial to the vacuum, removing non-condensable gases. After 30 seconds the needle is removed and the vial is placed in a custom-built heating module at 550 °C. The module is designed to heat only the bottom third of the vial; an insulating layer on the surface protects the rubber septum from the heat. Graphitization is complete in 3 hours.

Reduction of CO2 generated from carbonate proceeds in a similar fashion. A 3-way stopcock is connected to a vacuum line and to a needle which pierces the septum of a reduction vial. A needle attached to a length of flexible tubing connects to the third port. The needle is inserted partway into the rubber seal on a Vaccutainer containing CO2 evolved from carbonate. The vacuum line is opened to evacuate the reduction vial, stopcock and tubing. When the pressure drops below 3 mtorr, the stopcock is turned to close off the vacuum and the needle is pushed through the rubber stopper, releasing the CO2. From this point, reduction proceeds as described above.

APPENDIX B
RADIOCARBON CALIBRATION DATA

RADIOCARBON CALIBRATION PROGRAM*
CALIB REV7.1.0

*To be used in conjunction with:
Stuiver, M., and Reimer, P.J., 1993, Radiocarbon, 35, 215-230.

DAMS 3591a
Lab Code
Sample Description
Radiocarbon Age BP 500 +/- 26
Delta R = 0.0 +/- 0.0
Calibration data set: marine13.14c # Reimer et al. 2013

% area enclosed	cal BP age ranges	relative area under probability distribution
68.3 (1 sigma)	cal BP 0 - 9	0.052
	56 - 148	0.754
	162 - 192	0.167
	216 - 222	0.027
95.4 (2 sigma)	cal BP 0 - 30	0.098
	41 - 236	0.902

Median Probability: 119

DAMS 3593
Lab Code
Sample Description
Radiocarbon Age BP 1425 +/- 26
Delta R = 0.0 +/- 0.0
Calibration data set: marine13.14c # Reimer et al. 2013

% area enclosed	cal BP age ranges	relative area under probability distribution
68.3 (1 sigma)	cal BP 925 - 998	1.000
95.4 (2 sigma)	cal BP 910 - 1043	1.000

Median Probability: 968

DAMS 3281
Lab Code
Sample Description
Radiocarbon Age BP 3027 +/- 28
Calibration data set: intcal13.14c # Reimer et al. 2013

% area enclosed	cal BP age ranges	relative area under probability distribution
68.3 (1 sigma)	cal BP 3174 - 3249	0.860
	3307 - 3321	0.140

95.4 (2 sigma) cal BP 3084 - 3087 0.004
3144 - 3273 0.750
3284 - 3342 0.246
Median Probability: 3225

DAMS 3282
Lab Code
Sample Description
Radiocarbon Age BP 1389 +/- 26
Calibration data set: intcal13.14c # Reimer et al. 2013

% area enclosed	cal BP age ranges	relative area under probability distribution
68.3 (1 sigma)	cal BP 1287 - 1313	1.000
95.4 (2 sigma)	cal BP 1281 - 1341	1.000

Median Probability: 1303

AA23390
Lab Code
Sample Description
Radiocarbon Age BP 1405 +/- 45
Calibration data set: intcal13.14c # Reimer et al. 2013

% area enclosed	cal BP age ranges	relative area under probability distribution
68.3 (1 sigma)	cal BP 1290 - 1342	1.000
95.4 (2 sigma)	cal BP 1268 - 1390	1.000

Median Probability: 1318

DAMS 4799
Lab Code
Sample Description
Radiocarbon Age BP 1342 +/- 32
Calibration data set: intcal13.14c # Reimer et al. 2013

% area enclosed	cal BP age ranges	relative area under probability distribution
68.3 (1 sigma)	cal BP 1263 - 1300	1.000
95.4 (2 sigma)	cal BP 1184 - 1208	0.122
	1232 - 1308	0.878

Median Probability: 1280

Beta 16369
Lab Code
Sample Description
Radiocarbon Age BP 460 +/- 28
Calibration data set: intcal13.14c # Reimer et al. 2013

% area enclosed	cal BP age ranges	relative area under probability distribution

68.3 (1 sigma)	cal BP 502 - 522	1.000
95.4 (2 sigma)	cal BP 488 - 536	1.000

Median Probability: 513

DAMS 3819a
Lab Code
Sample Description
Radiocarbon Age BP 553 +/- 27
Calibration data set: intcal13.14c # Reimer et al. 2013

% area enclosed	cal BP age ranges	relative area under probability distribution
68.3 (1 sigma)	cal BP 532 - 556	0.616
	607 - 624	0.384
95.4 (2 sigma)	cal BP 521 - 562	0.564
	593 - 636	0.436

Median Probability: 556

DAMS 3819b
Lab Code
Sample Description
Radiocarbon Age BP 408 +/- 59
Calibration data set: intcal13.14c # Reimer et al. 2013

% area enclosed	cal BP age ranges	relative area under probability distribution
68.3 (1 sigma)	cal BP 330 - 359	0.213
	429 - 517	0.787
95.4 (2 sigma)	cal BP 314 - 413	0.370
	418 - 529	0.630

Median Probability: 450

Beta 16369
Lab Code
Sample Description
Radiocarbon Age BP 890 +/- 40
Calibration data set: intcal13.14c # Reimer et al. 2013

% area enclosed	cal BP age ranges	relative area under probability distribution
68.3 (1 sigma)	cal BP 741 - 800	0.547
	813 - 826	0.111
	865 - 902	0.342
95.4 (2 sigma)	cal BP 730 - 916	1.000

Median Probability: 814

DAMS 3818
Lab Code
Sample Description

Radiocarbon Age BP 578 +/- 26
Calibration data set: intcal13.14c # Reimer et al. 2013

% area enclosed	cal BP age ranges	relative area under probability distribution
68.3 (1 sigma)	cal BP 543 - 559	0.328
	599 - 631	0.672
95.4 (2 sigma)	cal BP 534 - 566	0.339
	585 - 646	0.661

Median Probability: 605

DAMS 3594
Lab Code
Sample Description
Radiocarbon Age BP 2246 +/- 24
Calibration data set: intcal13.14c # Reimer et al. 2013

% area enclosed	cal BP age ranges	relative area under probability distribution
68.3 (1 sigma)	cal BP 2183 - 2236	0.684
	2305 - 2327	0.316
95.4 (2 sigma)	cal BP 2158 - 2262	0.698
	2298 - 2338	0.302

Median Probability: 2228

DAMS 3596
Lab Code
Sample Description
Radiocarbon Age BP 2410 +/- 28
Calibration data set: intcal13.14c # Reimer et al. 2013

% area enclosed	cal BP age ranges	relative area under probability distribution
68.3 (1 sigma)	cal BP 2358 - 2460	1.000
95.4 (2 sigma)	cal BP 2351 - 2494	0.879
	2598 - 2610	0.021
	2639 - 2682	0.100

Median Probability: 2429

DAMS 3597
Lab Code
Sample Description
Radiocarbon Age BP 2265 +/- 27
Calibration data set: intcal13.14c # Reimer et al. 2013

% area enclosed	cal BP age ranges	relative area under probability distribution
68.3 (1 sigma)	cal BP 2185 - 2192	0.070
	2206 - 2230	0.311
	2306 - 2341	0.619

95.4 (2 sigma)	cal BP 2159 - 2249	0.504
	2300 - 2347	0.496

Median Probability: 2257

DAMS 3598
Lab Code
Sample Description
Radiocarbon Age BP 2286 +/- 43
Calibration data set: intcal13.14c # Reimer et al. 2013

% area enclosed	cal BP age ranges	relative area under probability distribution
68.3 (1 sigma)	cal BP 2184 - 2195	0.079
	2204 - 2232	0.258
	2306 - 2350	0.664
95.4 (2 sigma)	cal BP 2155 - 2270	0.478
	2295 - 2357	0.522

Median Probability: 2305

DAMS 11249
Lab Code
Sample Description
Radiocarbon Age BP 2583 +/- 33
Calibration data set: intcal13.14c # Reimer et al. 2013

% area enclosed	cal BP age ranges	relative area under probability distribution
68.3 (1 sigma)	cal BP 2721 - 2752	1.000
95.4 (2 sigma)	cal BP 2517 - 2527	0.010
	2538 - 2588	0.076
	2617 - 2632	0.036
	2698 - 2766	0.878

Median Probability: 2735

DAMS 4803
Lab Code
Sample Description
Radiocarbon Age BP 2484 +/- 31
Calibration data set: intcal13.14c # Reimer et al. 2013

% area enclosed	cal BP age ranges	relative area under probability distribution
68.3 (1 sigma)	cal BP 2492 - 2601	0.657
	2608 - 2622	0.087
	2627 - 2641	0.083
	2679 - 2708	0.173
95.4 (2 sigma)	cal BP 2385 - 2386	0.001
	2433 - 2725	0.999

Median Probability: 2584

DAMS 4802
Lab Code
Sample Description
Radiocarbon Age BP 1683 +/- 42
Calibration data set: intcal13.14c # Reimer et al. 2013

% area enclosed	cal BP age ranges	relative area under probability distribution
68.3 (1 sigma)	cal BP 1541 - 1620	0.912
	1676 - 1686	0.088
95.4 (2 sigma)	cal BP 1445 - 1453	0.008
	1522 - 1707	0.992

Median Probability: 1592

DAMS 4800
Lab Code
Sample Description
Radiocarbon Age BP 1652 +/- 32
Calibration data set: intcal13.14c # Reimer et al. 2013

% area enclosed	cal BP age ranges	relative area under probability distribution
68.3 (1 sigma)	cal BP 1527 - 1572	0.786
	1581 - 1602	0.214
95.4 (2 sigma)	cal BP 1417 - 1462	0.091
	1482 - 1493	0.010
	1517 - 1622	0.880
	1673 - 1688	0.020

Median Probability: 1555

DAMS 11250
Lab Code
Sample Description
Radiocarbon Age BP 8331 +/- 36
Calibration data set: intcal13.14c # Reimer et al. 2013

% area enclosed	cal BP age ranges	relative area under probability distribution
68.3 (1 sigma)	cal BP 9305 - 9364	0.558
	9368 - 9389	0.175
	9391 - 9421	0.266
95.4 (2 sigma)	cal BP 9262 - 9462	1.000

Median Probability: 9358

DAMS 11251
Lab Code
Sample Description
Radiocarbon Age BP 8680 +/- 40

Calibration data set: intcal13.14c # Reimer et al. 2013

% area enclosed	cal BP age ranges	relative area under probability distribution
68.3 (1 sigma)	cal BP 9555 - 9635	0.783
	9638 - 9661	0.217
95.4 (2 sigma)	cal BP 9542 - 9710	0.973
	9715 - 9736	0.027

Median Probability: 9622

DAMS 14362
Lab Code
Sample Description
Radiocarbon Age BP 5901 +/- 28
Calibration data set: intcal13.14c # Reimer et al. 2013

% area enclosed	cal BP age ranges	relative area under probability distribution
68.3 (1 sigma)	cal BP 6676 - 6741	1.000
95.4 (2 sigma)	cal BP 6664 - 6784	1.000

Median Probability: 6717

DAMS 14363
Lab Code
Sample Description
Radiocarbon Age BP 5871 +/- 30
Calibration data set: intcal13.14c # Reimer et al. 2013

% area enclosed	cal BP age ranges	relative area under probability distribution
68.3 (1 sigma)	cal BP 6664 - 6727	1.000
95.4 (2 sigma)	cal BP 6636 - 6752	0.984
	6765 - 6775	0.016

Median Probability: 6695

WSU 3593
Lab Code
Sample Description
Radiocarbon Age BP 6650 +/- 120
Calibration data set: intcal13.14c # Reimer et al. 2013

% area enclosed	cal BP age ranges	relative area under probability distribution
68.3 (1 sigma)	cal BP 7432 - 7611	1.000
95.4 (2 sigma)	cal BP 7311 - 7724	1.000

Median Probability: 7530

DAMS 14290
Lab Code
Sample Description

Radiocarbon Age BP 2425 +/- 25
Calibration data set: intcal13.14c # Reimer et al. 2013

% area enclosed	cal BP age ranges	relative area under probability distribution
68.3 (1 sigma)	cal BP 2364 - 2472	0.922
	2475 - 2485	0.078
95.4 (2 sigma)	cal BP 2354 - 2499	0.799
	2594 - 2613	0.042
	2636 - 2691	0.159

Median Probability: 2446

DAMS 14291
Lab Code
Sample Description
Radiocarbon Age BP 2489 +/- 28
Calibration data set: intcal13.14c # Reimer et al. 2013

% area enclosed	cal BP age ranges	relative area under probability distribution
68.3 (1 sigma)	cal BP 2495 - 2597	0.694
	2611 - 2622	0.072
	2627 - 2638	0.078
	2683 - 2708	0.156
95.4 (2 sigma)	cal BP 2464 - 2723	1.000

Median Probability: 2586

Beta 10761
Lab Code
Sample Description
Radiocarbon Age BP 2480 +/- 50
Calibration data set: intcal13.14c # Reimer et al. 2013

% area enclosed	cal BP age ranges	relative area under probability distribution
68.3 (1 sigma)	cal BP 2489 - 2623	0.637
	2626 - 2647	0.097
	2650 - 2709	0.266
95.4 (2 sigma)	cal BP 2365 - 2367	0.005
	2377 - 2725	0.995

Median Probability: 2570

DAMS 9408
Lab Code
Sample Description
Radiocarbon Age BP 1364 +/- 28
Calibration data set: intcal13.14c # Reimer et al. 2013

% area enclosed	cal BP age ranges	relative area under probability distribution

68.3 (1 sigma)	cal BP 1280 - 1303	1.000
95.4 (2 sigma)	cal BP 1261 - 1335	1.000

Median Probability: 1292

DAMS 9409
Lab Code
Sample Description
Radiocarbon Age BP 1309 +/- 31
Calibration data set: intcal13.14c # Reimer et al. 2013

% area enclosed	cal BP age ranges	relative area under probability distribution
68.3 (1 sigma)	cal BP 1186 - 1204	0.300
	1241 - 1249	0.094
	1255 - 1287	0.606
95.4 (2 sigma)	cal BP 1182 - 1213	0.288
	1223 - 1294	0.712

Median Probability: 1251

Beta 2798
Lab Code
Sample Description
Radiocarbon Age BP 1570 +/- 90
Calibration data set: intcal13.14c # Reimer et al. 2013

% area enclosed	cal BP age ranges	relative area under probability distribution
68.3 (1 sigma)	cal BP 1373 - 1551	1.000
95.4 (2 sigma)	cal BP 1300 - 1627	0.979
	1667 - 1692	0.021

Median Probability: 1469

Beta 2799
Lab Code
Sample Description
Radiocarbon Age BP 1780 +/- 70
Calibration data set: intcal13.14c # Reimer et al. 2013

% area enclosed	cal BP age ranges	relative area under probability distribution
68.3 (1 sigma)	cal BP 1617 - 1742	0.742
	1754 - 1785	0.158
	1790 - 1810	0.099
95.4 (2 sigma)	cal BP 1555 - 1866	1.000

Median Probability: 1703

Beta 2800
Lab Code
Sample Description

Radiocarbon Age BP 1560 +/- 50
Calibration data set: intcal13.14c # Reimer et al. 2013

% area enclosed	cal BP age ranges	relative area under probability distribution
68.3 (1 sigma)	cal BP 1406 - 1448	0.359
	1451 - 1522	0.641
95.4 (2 sigma)	cal BP 1350 - 1550	1.000

Median Probability: 1459

DAMS 14288
Lab Code
Sample Description
Radiocarbon Age BP 1825 +/- 28
Calibration data set: intcal13.14c # Reimer et al. 2013

% area enclosed	cal BP age ranges	relative area under probability distribution
68.3 (1 sigma)	cal BP 1723 - 1744	0.274
	1752 - 1811	0.726
95.4 (2 sigma)	cal BP 1636 - 1647	0.013
	1697 - 1826	0.976
	1850 - 1860	0.011

Median Probability: 1765

DAMS 14289
Lab Code
Sample Description
Radiocarbon Age BP 1671 +/- 29
Calibration data set: intcal13.14c # Reimer et al. 2013

% area enclosed	cal BP age ranges	relative area under probability distribution
68.3 (1 sigma)	cal BP 1545 - 1605	1.000
95.4 (2 sigma)	cal BP 1525 - 1626	0.944
	1669 - 1691	0.056

Median Probability: 1576

DAMS 3278
Lab Code
Sample Description
Radiocarbon Age BP 2690 +/- 28
Calibration data set: intcal13.14c # Reimer et al. 2013

% area enclosed	cal BP age ranges	relative area under probability distribution
68.3 (1 sigma)	cal BP 2757 - 2795	0.810
	2826 - 2841	0.190
95.4 (2 sigma)	cal BP 2754 - 2847	1.000

Median Probability: 2788

DAMS 1910
Lab Code
Sample Description
Radiocarbon Age BP 2823 +/- 25
Calibration data set: intcal13.14c # Reimer et al. 2013

% area enclosed	cal BP age ranges	relative area under probability distribution
68.3 (1 sigma)	cal BP 2882 - 2911	0.432
	2918 - 2955	0.568
95.4 (2 sigma)	cal BP 2862 - 2992	1.000

Median Probability: 2923

DAMS 3279
Lab Code
Sample Description
Radiocarbon Age BP 2578 +/- 27
Calibration data set: intcal13.14c # Reimer et al. 2013

% area enclosed	cal BP age ranges	relative area under probability distribution
68.3 (1 sigma)	cal BP 2725 - 2748	1.000
95.4 (2 sigma)	cal BP 2542 - 2559	0.024
	2618 - 2630	0.021
	2702 - 2759	0.955

Median Probability: 2736

DAMS 1911
Lab Code
Sample Description
Radiocarbon Age BP 2734 +/- 24
Calibration data set: intcal13.14c # Reimer et al. 2013

% area enclosed	cal BP age ranges	relative area under probability distribution
68.3 (1 sigma)	cal BP 2791 - 2848	1.000
95.4 (2 sigma)	cal BP 2772 - 2871	1.000

Median Probability: 2821

DAMS 9402
Lab Code
Sample Description
Radiocarbon Age BP 1966 +/- 29
Calibration data set: intcal13.14c # Reimer et al. 2013

% area enclosed	cal BP age ranges	relative area under probability distribution
68.3 (1 sigma)	cal BP 1883 - 1945	1.000
95.4 (2 sigma)	cal BP 1865 - 1991	1.000

Median Probability: 1916

DAMS 9403
Lab Code
Sample Description
Radiocarbon Age BP 1848 +/- 28
Calibration data set: intcal13.14c # Reimer et al. 2013

% area enclosed	cal BP age ranges	relative area under probability distribution
68.3 (1 sigma)	cal BP 1736 - 1765	0.358
	1770 - 1821	0.642
95.4 (2 sigma)	cal BP 1714 - 1835	0.915
	1840 - 1864	0.085

Median Probability: 1782

DAMS 3640
Lab Code
Sample Description
Radiocarbon Age BP 7695 +/- 46
Calibration data set: intcal13.14c # Reimer et al. 2013

% area enclosed	cal BP age ranges	relative area under probability distribution
68.3 (1 sigma)	cal BP 8427 - 8484	0.606
	8488 - 8520	0.326
	8530 - 8537	0.068
95.4 (2 sigma)	cal BP 8405 - 8562	0.986
	8569 - 8578	0.014

Median Probability: 8483

DAMS 3641
Lab Code
Sample Description
Radiocarbon Age BP 7603 +/- 39
Calibration data set: intcal13.14c # Reimer et al. 2013

% area enclosed	cal BP age ranges	relative area under probability distribution
68.3 (1 sigma)	cal BP 8380 - 8420	1.000
95.4 (2 sigma)	cal BP 8345 - 8458	0.990
	8498 - 8508	0.010

Median Probability: 8403

DAMS 3642
Lab Code
Sample Description
Radiocarbon Age BP 6976 +/- 36
Calibration data set: intcal13.14c # Reimer et al. 2013

% area enclosed	cal BP age ranges	relative area under probability distribution
68.3 (1 sigma)	cal BP 7753 - 7852	0.961
	7908 - 7913	0.039
95.4 (2 sigma)	cal BP 7704 - 7871	0.894
	7896 - 7927	0.106

Median Probability: 7810

DAMS 3275a
Lab Code
Sample Description
Radiocarbon Age BP 1179 +/- 27
Calibration data set: intcal13.14c # Reimer et al. 2013

% area enclosed	cal BP age ranges	relative area under probability distribution
68.3 (1 sigma)	cal BP 1063 - 1094	0.358
	1106 - 1148	0.450
	1158 - 1173	0.192
95.4 (2 sigma)	cal BP 1003 - 1027	0.063
	1051 - 1180	0.937

Median Probability: 1113

DAMS 3276a
Lab Code
Sample Description
Radiocarbon Age BP 1395 +/- 32
Calibration data set: intcal13.14c # Reimer et al. 2013

% area enclosed	cal BP age ranges	relative area under probability distribution
68.3 (1 sigma)	cal BP 1289 - 1320	1.000
95.4 (2 sigma)	cal BP 1277 - 1352	1.000

Median Probability: 1308

DAMS 3276b
Lab Code
Sample Description
Radiocarbon Age BP 1220 +/- 49
Calibration data set: intcal13.14c # Reimer et al. 2013

% area enclosed	cal BP age ranges	relative area under probability distribution
68.3 (1 sigma)	cal BP 1070 - 1184	0.844
	1209 - 1231	0.156
95.4 (2 sigma)	cal BP 1007 - 1024	0.026
	1053 - 1276	0.974

Median Probability: 1149

DAMS 3277a
Lab Code
Sample Description
Radiocarbon Age BP 1250 +/- 28
Calibration data set: intcal13.14c # Reimer et al. 2013

% area enclosed	cal BP age ranges	relative area under probability distribution
68.3 (1 sigma)	cal BP 1176 - 1191	0.182
	1198 - 1261	0.818
95.4 (2 sigma)	cal BP 1083 - 1160	0.186
	1172 - 1273	0.814

Median Probability: 1212

DAMS 3277b
Lab Code
Sample Description
Radiocarbon Age BP 1295 +/- 46
Calibration data set: intcal13.14c # Reimer et al. 2013

% area enclosed	cal BP age ranges	relative area under probability distribution
68.3 (1 sigma)	cal BP 1183 - 1210	0.327
	1228 - 1283	0.673
95.4 (2 sigma)	cal BP 1087 - 1111	0.029
	1123 - 1159	0.040
	1172 - 1301	0.930

Median Probability: 1233

DAMS 9404
Lab Code
Sample Description
Radiocarbon Age BP 5290 +/- 33
Calibration data set: intcal13.14c # Reimer et al. 2013

% area enclosed	cal BP age ranges	relative area under probability distribution
68.3 (1 sigma)	cal BP 5995 - 6027	0.265
	6043 - 6068	0.189
	6076 - 6117	0.340
	6151 - 6176	0.206
95.4 (2 sigma)	cal BP 5950 - 5965	0.032
	5989 - 6183	0.968

Median Probability: 6079

DAMS 9405
Lab Code
Sample Description
Radiocarbon Age BP 5972 +/- 34

Calibration data set: intcal13.14c # Reimer et al. 2013

% area enclosed	cal BP age ranges	relative area under probability distribution
68.3 (1 sigma)	cal BP 6748 - 6805	0.585
	6812 - 6851	0.415
95.4 (2 sigma)	cal BP 6695 - 6701	0.006
	6718 - 6898	0.994

Median Probability: 6807

DAMS 9406
Lab Code
Sample Description
Radiocarbon Age BP 7013 +/- 69
Calibration data set: intcal13.14c # Reimer et al. 2013

% area enclosed	cal BP age ranges	relative area under probability distribution
68.3 (1 sigma)	cal BP 7788 - 7934	1.000
95.4 (2 sigma)	cal BP 7696 - 7958	1.000

Median Probability: 7846

DAMS 9407
Lab Code
Sample Description
Radiocarbon Age BP 5475 +/- 35
Calibration data set: intcal13.14c # Reimer et al. 2013

% area enclosed	cal BP age ranges	relative area under probability distribution
68.3 (1 sigma)	cal BP 6218 - 6236	0.283
	6273 - 6304	0.717
95.4 (2 sigma)	cal BP 6202 - 6319	0.984
	6374 - 6388	0.016

Median Probability: 6282

References for calibration datasets:
Reimer PJ, Bard E, Bayliss A, Beck JW, Blackwell PG, Bronk Ramsey C, Buck CE Cheng H, Edwards RL, Friedrich M, Grootes PM, Guilderson TP, Haflidason H, Hajdas I, HattÃ© C, Heaton TJ, Hogg AG, Hughen KA, Kaiser KF, Kromer B, Manning SW, Niu M, Reimer RW, Richards DA, Scott EM, Southon JR, Turney CSM, van der Plicht J.
IntCal13 and MARINE13 radiocarbon age calibration curves 0-50000 years calBP Radiocarbon 55(4). DOI: 10.2458/azu_js_rc.55.16947
Reimer PJ, Bard E, Bayliss A, Beck JW, Blackwell PG, Bronk Ramsey C, Buck CE Cheng H, Edwards RL, Friedrich M, Grootes PM, Guilderson TP, Haflidason H, Hajdas I, HattÃ© C, Heaton TJ, Hogg AG, Hughen KA, Kaiser KF, Kromer B, Manning SW, Niu M, Reimer RW, Richards DA, Scott EM, Southon JR, Turney CSM, van der Plicht J.

IntCal13 and MARINE13 radiocarbon age calibration curves 0-50000 years calBP
Radiocarbon 55(4). DOI: 10.2458/azu_js_rc.55.16947

Comments:
* This standard deviation (error) includes a lab error multiplier.
** 1 sigma = square root of (sample std. dev.^2 + curve std. dev.^2)
** 2 sigma = 2 x square root of (sample std. dev.^2 + curve std. dev.^2)
where ^2 = quantity squared.
[ ] = calibrated range impinges on end of calibration data set
0* represents a "negative" age BP
1955* or 1960* denote influence of nuclear testing C-14

NOTE: Cal ages and ranges are rounded to the nearest year which may be too precise in many instances. Users are advised to round results to the nearest 10 yr for samples with standard deviation in the radiocarbon age greater than 50 yr.

APPENDIX C
Procedures for Thermoluminescence Analysis of Pottery

Protocol provided and authored by James K. Feathers
University of Washington Luminescence Dating Laboratory

Sample preparation -- fine grain

The sherd is broken to expose a fresh profile. Material is drilled from the center of the cross-section, more than 2 mm from either surface, using a tungsten carbide drill tip. The material retrieved is ground gently by an agate mortar and pestle, treated with HCl, and then settled in acetone for 2 and 20 minutes to separate the 1-8 μm fraction. This is settled onto a maximum of 72 stainless steel discs.

Glow-outs

Thermoluminescence is measured by a Daybreak reader using a 9635Q photomultiplier with a Corning 7-59 blue filter, in N_2 atmosphere at 1°C/s to 450°C. A preheat of 240°C with no hold time precedes each measurement. Artificial irradiation is given with a ^{241}Am alpha source and a ^{90}Sr beta source, the latter calibrated against a ^{137}Cs gamma source. Discs are stored at room temperature for at least one week after irradiation before glow out. Data are processed by Daybreak TLApplic software.

Fading test

Several discs are used to test for anomalous fading. The natural luminescence is first measured by heating to 450°C. The discs are then given an equal alpha irradiation and stored at room temperature for varied times: 10 min, 2 hours, 1 day, 1 week and 8 weeks. The irradiations are staggered in time so that all of the second glows are performed on the same day. The second glows are normalized by the natural signal and then compared to determine any loss of signal with time (on a log scale). If the sample shows fading and the signal versus time values can be reasonably fit to a logarithmic function, an attempt is made to correct the age following procedures recommended by Huntley and Lamothe (2001). The fading rate is calculated as the g-value, which is given in percent per decade, where decade represents a power of 10.

Equivalent dose

The equivalent dose is determined by a combination additive dose and regeneration (Aitken 1985). Additive dose involves administering incremental doses to natural material. A growth curve plotting dose against luminescence can be extrapolated to the dose axis to estimate an equivalent dose, but for pottery this estimate is usually inaccurate because of errors in extrapolation due to nonlinearity. Regeneration involves zeroing natural material by heating to 450°C and then rebuilding a growth curve with incremental doses. The problem here is sensitivity change caused by the heating. By constructing both curves, the regeneration curve can be used to define the extrapolated area and can be corrected for sensitivity change by

comparing it with the additive dose curve. This works where the shapes of the curves differ only in scale (i.e., the sensitivity change is independent of dose). The curves are combined using the "Australian slide" method in a program developed by David Huntley of Simon Fraser University (Prescott et al. 1993). The equivalent dose is taken as the horizontal distance between the two curves after a scale adjustment for sensitivity change. Where the growth curves are not linear, they are fit to quadratic functions. Dose increments (usually five) are determined so that the maximum additive dose results in a signal about three times that of the natural and the maximum regeneration dose about five times the natural. If the regeneration curve has a significant negative intercept, which is not expected given current understanding, the additive dose intercept is taken as the best, if not fully reliable approximation.

A plateau region is determined by calculating the equivalent dose at temperature increments between 240° and 450°C and determining over which temperature range the values do not differ significantly. This plateau region is compared with a similar one constructed for the b-value (alpha efficiency), and the overlap defines the integrated range for final analysis.

Alpha effectiveness

Alpha efficiency is determined by comparing additive dose curves using alpha and beta irradiations. The slide program is also used in this regard, taking the scale factor (which is the ratio of the two slopes) as the b-value (Aitken 1985).

Radioactivity

Radioactivity is measured by alpha counting in conjunction with atomic emission for ^{40}K. Samples for alpha counting are crushed in a mill to flour consistency, packed into plexiglass containers with ZnS:Ag screens, and sealed for one month before counting. The pairs technique is used to separate the U and Th decay series. For atomic emission measurements, samples are dissolved in HF and other acids and analyzed by a Jenway flame photometer. K concentrations for each sample are determined by bracketing between standards of known concentration. Conversion to ^{40}K is by natural atomic abundance. Radioactivity is also measured, as a check, by beta counting, using a Risø low level beta GM multicounter system. About 0.5 g of crushed sample is placed on each of four plastic sample holders. All are counted for 24 hours. The average is converted to dose rate following Bøtter-Jensen and Mejdahl (1988) and compared with the beta dose rate calculated from the alpha counting and flame photometer results.

Both the sherd and an associated soil sample are measured for radioactivity. Additional soil samples are analyzed where the environment is complex, and gamma contributions determined by gradients (after Aitken 1985: appendix H). Cosmic radiation is determined after Prescott and Hutton (1994). Radioactivity concentrations are translated into dose rates following Guérin et al. (2011).

Moisture Contents

Water absorption values for the sherds are determined by comparing the saturated and dried weights. For temperate climates, moisture in the pottery is taken to be 80 ± 20 percent of total absorption, unless otherwise indicated by the archaeologist. Again for temperate climates, soil moisture contents are taken from typical moisture retention quantities for different textured soils (Brady 1974: 196), unless otherwise measured. For drier climates, moisture values are determined in consultation with the archaeologist.

Procedures for Optically Stimulated or Infrared Stimulated Luminescence of Fine-grained pottery.

Optically stimulated luminescence (OSL) and infrared stimulated luminescence (IRSL) on fine-grain (1-8μm) pottery samples are carried out on single aliquots following procedures adapted from Banerjee et al. (2001) and Roberts and Wintle (2001. Equivalent dose is determined by the single-aliquot regenerative dose (SAR) method (Murray and Wintle 2000).

The SAR method measures the natural signal and the signal from a series of regeneration doses on a single aliquot. The method uses a small test dose to monitor and correct for sensitivity changes brought about by preheating, irradiation or light stimulation. SAR consists of the following steps: 1) preheat, 2) measurement of natural signal (OSL or IRSL), L(1), 3) test dose, 4) cut heat, 5) measurement of test dose signal, T(1), 6) regeneration dose, 7) preheat, 8) measurement of signal from regeneration, L(2), 9) test dose, 10) cut heat, 11) measurement of test dose signal, T(2), 12) repeat of steps 6 through 11 for various regeneration doses. A growth curve is constructed from the L(i)/T(i) ratios and the equivalent dose is found by interpolation of L(1)/T(1). Usually a zero regeneration dose and a repeated regeneration dose are employed to insure the procedure is working properly. For fine-grained ceramics, a preheat of 240°C for 10s, a test dose of 3.1 Gy, and a cut heat of 200°C are currently being used, although these parameters may be modified from sample to sample.

The luminescence, L(i) and T(i), is measured on a Risø TL-DA-15 automated reader by a succession of two stimulations: first 100 s at 60°C of IRSL (880nm diodes), and then 100s at 125°C of OSL (470nm diodes). Detection is through 7.5mm of Hoya U340 (ultra-violet) filters. The two stimulations are used to construct IRSL and OSL growth curves, so that two estimations of equivalent dose are available. Anomalous fading usually involves feldspars and only feldspars are sensitive to IRSL stimulation. The rationale for the IRSL stimulation is to remove most of the feldspar signal, so that the subsequent OSL (post IR blue) signal is free from anomalous fading. However, feldspar is also sensitive to blue light (470nm), and it is possible that IRSL does not remove all the feldspar signal. Some preliminary tests in our laboratory have suggested that the OSL signal does not suffer from fading, but this may be sample specific. The procedure is still undergoing study.

A dose recovery test is performed by first zeroing the sample by exposure to light and then administering a known dose. The SAR protocol is then applied to see if the known dose can be obtained.

The laboratory is currently investigating using pulsed OSL to measure equivalent dose on ceramics. In pulsed mode, the stimulating light is turned off and on in a series of pulses with the

luminescence only measured during the off-time. Because the time between stimulation and emission is much longer for quartz than feldspar, an appropriate pulse width can be chosen to eliminate any feldspar signal. Previous work has suggested that a 10 μs on-time and 240 μs off-time for each pulse, and also using an initial infrared exposure (as in double SAR), will minimize the feldspar signal during the off-time, so that the signal stems mainly from quartz. Pulsed OSL is measured on a Risø DA-20 using similar parameters as in the double SAR. Detection is for 100 s total (both on- and off-time) which includes 400,000 pulses for a total on-time of 4 seconds. This procedure is currently undergoing study because it is not certain 4 seconds is sufficient exposure to deplete the signal.

Alpha efficiency will surely differ among IRSL, OSL and TL on fine-grained materials. It does differ between coarse-grained feldspar and quartz (Aitken 1985). Research is currently underway in the laboratory to determine how much b-value varies according to stimulation method. Results from several samples from different geographic locations show that OSL b-value is less variable and centers around 0.5. IRSL b-value is more variable and is higher than that for OSL. TL b-value tends to fall between the OSL and IRSL values. We currently are measuring the b-value for IRSL and OSL by giving an alpha dose to aliquots whose luminescence have been drained by exposure to light. An equivalent dose is determined by SAR using beta irradiation, and the beta/alpha equivalent dose ratio is taken as the b-value. A high OSL b-value is indicative that feldspars might be contributing to the signal and thus subject to anomalous fading.

.

Age and error terms

The age and error for both OSL and TL are calculated by a laboratory constructed spreadsheet, based on Aitken (1985). All error terms are reported at 1-sigma.

References

Adamiec, G., and Aitken, M. J., 1998, Dose rate conversion factors: update. *Ancient TL* 16:37-50.

Aitken, M. J., 1985, *Thermoluminescence Dating*, Academic Press, London.

Banerjee, D., Murray, A. S., Bøtter-Jensen, L., and Lang, A., 2001, Equivalent dose estimation using a single aliquot of polymineral fine grains. *Radiation Measurements* 33:73-93.

Bøtter-Jensen, L, and Mejdahl, V., 1988, Assessment of beta dose-rate using a GM multi-counter system. *Nuclear Tracks and Radiation Measurements* 14:187-191.

Brady, N. C., 1974, *The Nature and Properties of Soils*, Macmillan, New York.

Guérin, G., Mercier, N., and Adamiec, G., 2011, Dose-rate converstion factors: update. *Ancient TL* 29:5-8.

Huntley, D. J., and Lamothe, M., 2001, Ubiquity of anomalous fading in K-feldspars, and measurement and correction for it in optical dating. *Canadian Journal of Earth Sciences* 38:1093-1106.

Mejdahl, V., 1983, Feldspar inclusion dating of ceramics and burnt stones. *PACT* 9:351-364.

Murray, A. S., and Wintle, A. G., 2000, Luminescence dating of quartz using an improved single-aliquot regenerative-dose protocol. *Radiation Measurements* 32:57-73.

Prescott, J. R., Huntley, D. J., and Hutton, J. T., 1993, Estimation of equivalent dose in thermoluminescence dating – the *Australian slide* method. *Ancient TL* 11:1-5.

Prescott, J. R., and Hutton, J. T., 1994, Cosmic ray contributions to dose rates for luminescence and ESR dating: large depths and long time durations. *Radiation Measurements* 23:497-500.

Roberts, H. M., and Wintle, A. G., 2001, Equivalent dose determinations for polymineralic fine-grains using the SAR protocol: application to a Holocene sequence of the Chinese Loess Plateau. *Quaternary Science Reviews* 20:859-863.

For a general review of luminescence dating by the director of this laboratory, see:

Feathers, J. K, 2003, Use of luminescence dating in archaeology. *Measurement Science and Technology* 14:1493-1509

APPENDIX D
Procedures for Thermoluminescence Analysis of Burned Chert

Protocol provided and authored by James K. Feathers
University of Washington Luminescence Dating Laboratory

Sample preparation

A diamond-tipped bit is used to drill cores from the center of the pieces. The outer 2 mm of these cores are burred off, so that only an inner portion, not subject to light exposure or external beta radiation, is used for luminescence measurements. The inner core is broken apart with a steel mortar and pestle. After initial breaking, the material is screened through a 125µm screen, and only that portion caught in the screen is subject to additional grinding. Screening is repeated often to minimize mechanical stress. The less than 125µm fraction is treated with HCl and then either screened further to isolate the 90-125µm (for larger samples), or settled in acetone for 2 and 20 minutes to separate the 1-8 µm fraction (for smaller samples). These are settled onto stainless steel discs.

Glow-outs

Thermoluminescence is measured by a Daybreak reader using a 9635Q photomultiplier using either a Corning 7-59 blue filter, or a Melles-Griot 03FIV046 orange filter in N_2 atmosphere at 1°C/s to 450°C. A preheat of 240°C with no hold time precedes each measurement. Artificial irradiation is given with a ^{241}Am alpha source and a ^{90}Sr beta source, the latter calibrated against a ^{137}Cs gamma source. Discs are stored at room temperature for at least one week after irradiation before glow out. Data are processed by Daybreak TLApplic software.

Equivalent dose

For most samples, equivalent dose is determined by a multi-aliquot combination additive dose and regeneration (Aitken 1985), using the blue filter. Additive dose involves administering incremental doses to natural material. A growth curve plotting dose against luminescence can be extrapolated to the dose axis to estimate an equivalent dose, but for pottery this estimate is usually inaccurate because of errors in extrapolation due to nonlinearity. Regeneration involves zeroing natural material by heating to 450°C and then rebuilding a growth curve with incremental doses. The problem here is sensitivity change caused by the heating. By constructing both curves, the regeneration curve can be used to define the extrapolated area and can be corrected for sensitivity change by comparing it with the additive dose curve. This works where the shapes of the curves differ only in scale (i.e., the sensitivity change is independent of dose). The curves are combined using the "Australian slide" method in a program developed by David Huntley of Simon Fraser University (Prescott et al. 1993). The equivalent dose is taken as the horizontal distance between the two curves after a scale adjustment for sensitivity change. Where the growth curves are not linear, they are fit to quadratic functions. Dose increments (usually five) are determined so that the maximum additive dose results in a signal about three times that of the natural and the maximum regeneration dose about five times the natural. If the

regeneration curve has a significant negative intercept, which is not expected given current understanding, the additive dose intercept is taken as the best, if not fully reliable approximation.

A plateau region is determined by calculating the equivalent dose at temperature increments between 240° and 450°C and determining over which temperature range the values do not differ significantly. This plateau region is compared with a similar one constructed for the b-value (alpha efficiency), and the overlap defines the integrated range for final analysis.

For smaller samples, the laboratory is experimenting with a single-aliquot technique developed by Richter and Krbetschek (2006) using the orange filter. This involves measuring the natural signal and then subsequent signals from regeneration doses on the same aliquot. Usually single-aliquot techniques require a test dose to correct for sensitivity change from repeated heating, but Richter and Krbetschek found that sensitivity changes were slight and could be monitored by a repeated regeneration dose of the same magnitude. They recommended using only two regeneration doses (of different magnitude) to produce signals that bracket the natural signal and thereby determine the equivalent dose by interpolation. We have found that additional regeneration doses are necessary for samples where bracketing doses are not known in advance. Dose recovery experiments by Richter and Temming (2006) found that the multi-aliquot procedure with the blue emission produced the most accurate results, but it requires a large sample. The single-aliquot procedure should be suitable for smaller samples, but is still undergoing study.

Alpha effectiveness

Alpha efficiency is determined by comparing additive dose curves using alpha and beta irradiations. The slide program is also used in this regard, taking the scale factor (which is the ratio of the two slopes) as the b-value (Aitken 1985).

Radioactivity

Radioactivity is measured by alpha counting in conjunction with atomic emission for ^{40}K. Samples for alpha counting are crushed in a mill to flour consistency, packed into plexiglass containers with ZnS:Ag screens, and sealed for one month before counting. The pairs technique is used to separate the U and Th decay series. For atomic emission measurements, samples are dissolved in HF and other acids and analyzed by a Jenway flame photometer. K concentrations for each sample are determined by bracketing between standards of known concentration. Conversion to ^{40}K is by natural atomic abundance. Radioactivity is also measured, as a check, by beta counting, using a Risø low level beta GM multicounter system. About 0.5 g of crushed sample is placed on each of four plastic sample holders. All are counted for 24 hours. The average is converted to dose rate following Bøtter-Jensen and Mejdahl (1988) and compared with the beta dose rate calculated from the alpha counting and flame photometer results.

Both the lithic and an associated soil sample are measured for radioactivity. Additional soil samples are analyzed where the environment is complex, and gamma contributions determined by gradients (after Aitken 1985: appendix H). Cosmic radiation is determined after Prescott and Hutton (1994). Radioactivity concentrations are translated into dose rates following

Guérin et al. (2011). Because internal radioactivity of lithics is generally low, *in situ* dosimeters are also recommended. The laboratory currently uses high purity copper capsules containing $CaSO_4$:Dy. The capsules are left in the ground for one year, and their luminescence then calibrated against laboratory beta irradiation.

Moisture Contents

Water absorption values for the lithics are determined by comparing the saturated and dried weights. For temperate climates, moisture in the lithics is taken to be 80 ± 20 percent of total absorption, unless otherwise indicated by the archaeologist. Again for temperate climates, soil moisture contents are taken from typical moisture retention quantities for different textured soils (Brady 1974: 196), unless otherwise measured. For drier climates, moisture values are determined in consultation with the archaeologist.

References

Aitken, M. J., 1985, *Thermoluminescence Dating*, Academic Press, London.

Bøtter-Jensen, L, and Mejdahl, V., 1988, Assessment of beta dose-rate using a GM multi-counter system. *Nuclear Tracks and Radiation Measurements* 14:187-191.

Brady, N. C., 1974, *The Nature and Properties of Soils*, Macmillan, New York.

Guérin, G., Mercier, N., and Adamiec, G., 2011, Dose-rate converstion factors: update. *Ancient TL* 29:5-8.

Prescott, J. R., Huntley, D. J., and Hutton, J. T., 1993, Estimation of equivalent dose in thermoluminescence dating – the *Australian slide* method. *Ancient TL* 11:1-5.

Prescott, J. R., and Hutton, J. T., 1994, Cosmic ray contributions to dose rates for luminescence and ESR dating: large depths and long time durations. *Radiation Measurements* 23:497-500.

Richter, D., and Krbetschek, M., 2006, A new thermoluminescence dating technique for heated flint. *Archaeometry* 48:695-705.

Richter, D., and Temming, H., 2006, Testing heated flint palaeodose protocols using dose recovery procedures. *Radiation Measurements* 41:819-825.

For a general review of luminescence dating by the director of this laboratory, see:

Feathers, J. K, 2003, Use of luminescence dating in archaeology. *Measurement Science and Technology* 14:1493-1509

APPENDIX E
LUMINESCENCE ANALYSIS OF FIRE-MODIFIED ROCK FROM WESTERN WASHINGTON

18 January 2016
James K. Feathers
Luminescence Dating Laboratory
University of Washington
Seattle, WA 98195-3412
Email: jimf@u.washington.edu

This report presents the results of luminescence analysis on two fire-modified rocks from the Bray site, 45PI1276 near Sumner, Washington. The samples were submitted by David Sheldon of Central Washington University. The site contains several intact features believe to be pit hearths. Two of them have radiocarbon dates of about 2700-2800 BP (uncalibrated). Table 1 lists the samples, proveniences and depths. Laboratory procedures are given in the appendix.

Table 1. Samples

UW lab #	Provenience	Feature	Depth (cm)
UW3047	3N7E	12-2	10-36
UW3048	5N7E	12-3	50-61

Dose rate

The dose rate was measured on each rock and an associated sediment. Dose rates were mainly determined using alpha counting and flame photometry. The beta dose rate calculated from these measurements on the rocks was compared with the beta dose rate measured directly by beta counting. These were within 1-sigma error terms for both samples. Moisture content was estimated as 80 ± 20 % of saturated value (about 3%) for the rocks and 20 ± 5 % for the sediments. Cosmic dose radiation was calculated as explained in the appendix. Table 2 gives the radioactivity data and comparison of the beta dose rate calculated in the two ways mentioned. Table 3 gives total dose rates for each sample.

Table 2. Radionuclide concentrations

Sample	^{238}U *(ppm)*	^{233}Th *(ppm)*	*K (%)*	*Beta dose rate (Gy/ka)*	
				ß-counting	α-counting/flame photometry
UW3047	1.29±0.10	2.71±0.64	2.54±0.06	2.29±0.20	2.34±0.06
sediment	0.88±0.07	1.35±0.40	0.77±0.03		
UW3048	1.75±0.15	8.23±1.06	2.55±0.06	2.72±0.24	2.58±0.06
Sediment	0.73±0.09	3.93±0.76	0.96±0.03		

Table 3. Dose rates (Gy/ka)*

Sample	*alpha*	*beta*	*gamma*	*cosmic*	*total*
UW3047	0.44±0.03	2.27±0.06	0.38±0.03	0.20±0.04	3.29±0.08

UW3048	0.96±0.11	2.51±0.06	0.62±0.04	0.18±0.04	4.27±0.13

* Dose rates for rocks are calculated for fine-grained OSL. They will be higher for TL and IRSL due to higher b-values, and lower for coarse-grained samples Also the beta dose rate is lower than that given in Table 2 due to moisture correction. Dose rate will be smaller for coarse-grain dating because of reduced influence of alpha irradiation.

Equivalent Dose – fine grain

Equivalent dose on 1-8μm grains was measured for TL, OSL and IRSL as described in the appendix. TL plateau (Table 4) was broad for UW3047, rather narrow for UW3048. Sensitivity change with heat was observed for UW3047. It is unknown if the sensitivity changed for UW3048 because an additive dose curve was not constructed due to a laboratory error. Scatter in the growth curves was high for UW3047, low for the regeneration curve for UW3048. TL anomalous fading was evident in both samples. Age correction followed Huntley and Lamothe (2001).

Table 4. TL parameters

Sample	*Plateau (°C)*	*1st/2nd ratio**	*fit*	*Fading g-value***
UW3047	250-360	0.50±0.21	linear	4.56±3.82
UW3048	300-350		linear	6.94±0.85

*Refers to slope ratio between the first and second glow growth curves. A glow refers to luminescence as a function of temperature; a second glow comes after heating to 450°C.
** A g-value is a rate of anomalous fading, measured as percent of signal loss per decade, where a decade is a power of 10.

OSL/IRSL was measured on 5-6 aliquots per sample (Table 5). Scatter was low for both samples – less than 2% over-dispersion. The IRSL signal was about 5 to 20 times less intense than the OSL signal. Weak IRSL signals are not uncommon for heated materials. IRSL stems from feldspars, which are prone to anomalous fading. A relatively large IRSL signal may suggest the OSL signal partly stems from feldspars and therefore may fade, so a weak IRSL suggests the OSL is dominated by quartz. However, the OSL b-value, which is a measure of the efficiency of alpha radiation in producing luminescence as compared to beta and gamma radiation, is for neither sample in the range of quartz; in fact it is more than the IRSL b-value, which reflects feldspar. It is possible, therefore, that feldspar contributes to the OSL signal, which therefore it might fade.

As a test of the SAR procedures, a dose recovery test was performed on UW3048. The recovered dose was within two sigma of the given dose. Equivalent dose and b-values for TL and OSL are given in Table 6.

Table 5. OSL/IRSL data

Sample	# aliquots*		OSL Over-dispersion (%)	Dose Recovery (OSL)	
	OSL	IRSL		Given Dose (sß)	Recovered Dose (sß)
UW3047	5	5	1.6 ± 4.8		
UW3048	5	6	0	100	95 ± 4

*Denotes aliquots with measurable signals

Table 6. Equivalent dose and b-value – fine grains

Sample	*Equivalent dose (Gy)*			*b-value (Gy μm^2)*		
	TL	*IRSL*	*OSL*	*TL*	*IRSL*	*OSL*
UW3047	14.0±6.35	9.31±0.35	7.35±0.16	3.89±1.59	1.16±0.04	1.28±0.04
UW3048	12.0±0.48	4.55±0.37	5.64±0.12	2.56±0.16	1.02±0.08	1.42±0.14

Ages – fine-grains

Ages from the fine-grain analysis are given in Table 7. For UW3047, the TL age agreed with the OSL age but had very high error. The OSL is considered the best estimate. For UW3048, the OSL age was much younger than the fading-corrected TL age. It is possible the OSL signal suffers from fading, but it is not likely the discrepancy can be fully attributed to that. At this point the young OSL age seems anomalous

Table 7. Ages – fine-grains

Sample	Age (ka)	% error	Basis for age	Calendar date
UW3047	2.23±0.10	4.5	OSL	BC 220 ± 100
UW3048	1.32±0.06	4.9	OSL	AD 690 ± 65
	3.63±0.33	9.1	Corrected TL	BC 1620 ± 330

Equivalent dose/Age – coarse grains

IRSL was measured on 180-212μm potassium feldspar single-grains, as described in the appendix. Of 200 grains measured on each sample, 66 produced usable data for UW3047 and 58 for UW3048. The coarse grain dose rates were 3.24 ± 014 and 3.74 ± 0.16 Gy/ka respectively. Internal K content was estimated at 10 ± 3 %. The central tendency for the fading-corrected ages, calculated by the central age model, are given in Table 8, along with the over-dispersion. The over-dispersion is not particularly high for single-grain data. This is shown in Figure 1, which presents radial graphs for the age distribution for each sample. A radial graph plots precision against a standardized age with more precise points plotted to the right. The standardization is the number of standard errors each point is from a reference, in this case the central age. The shaded area encompasses all points within two standard errors of the reference. Lines drawn from the origin through any point intersects the right hand scale at the estimated age. As can be seen, few points fall outside the two standard error limit.

Table 8. Ages – coarse grains

Sample	Age (ka)	% error	Over-dispersion (%)	Calendar date
UW3047	3.47±0.25	7.2	27.1±9.3	BC 1460 ± 250
UW3048	3.03±0.22	7.2	13.1±13.8	BC 1020 ± 220

Figure 1.

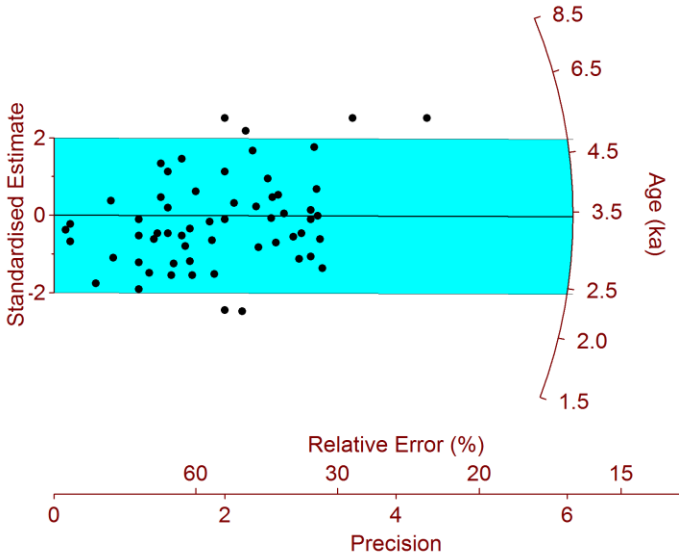

UW3047

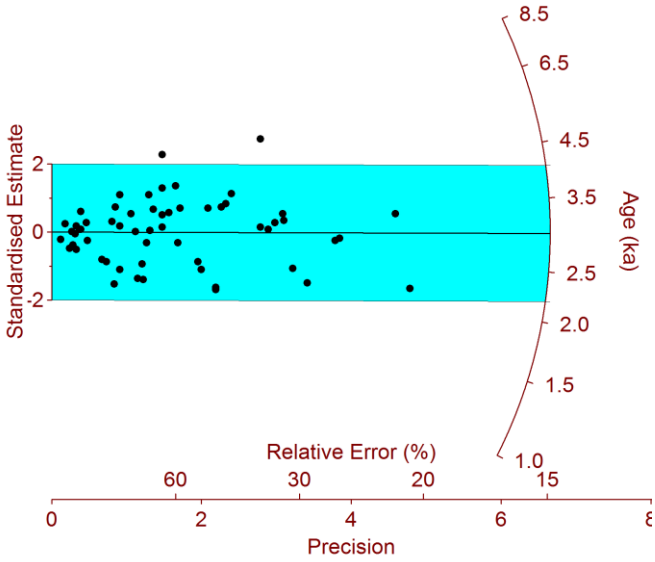

UW3048

Summary

The coarse-grain age for UW3048 is slightly younger than the fine-grain TL age, although they agree at two sigma. The coarse-grain age for UW3047 is much older than the fine-grain age, but the fine-grain age, based on OSL, may fade. The coarse grain ages are therefore probably the best estimates. Note that these are in the ballpark of the uncalibrated radiocarbon dates.

Appendix

Procedures for Thermoluminescence Analysis of Fire Modified Rock

Sample preparation -- fine grain

The outer surfaces of the rocks were removed with a diamond saw. The inner part, more than 2 mm from any surface, was crushed with a steel mortar and pestle, and sieved to separate grains smaller and larger than 90 µm. The coarse material is discussed in the next section on K-feldspar. The fine grains were treated with HCl, and then settled in acetone for 2 and 20 minutes to separate the 1-8 µm fraction. This is settled onto a maximum of 72 stainless steel discs.

Glow-outs

Thermoluminescence is measured by a Daybreak reader using a 9635Q photomultiplier with a Corning 7-59 blue filter, in N_2 atmosphere at 1°C/s to 450°C. A preheat of 240°C with no hold time precedes each measurement. Artificial irradiation is given with a ^{241}Am alpha source and a ^{90}Sr beta source, the latter calibrated against a ^{137}Cs gamma source. Discs are stored at room temperature for at least one week after irradiation before glow out. Data are processed by Daybreak TLApplic software.

Fading test

Several discs are used to test for anomalous fading. The natural luminescence is first measured by heating to 450°C. The discs are then given an equal alpha irradiation and stored at room temperature for varied times: 10 min, 2 hours, 1 day, 1 week and 8 weeks. The irradiations are staggered in time so that all of the second glows are performed on the same day. The second glows are normalized by the natural signal and then compared to determine any loss of signal with time (on a log scale). If the sample shows fading and the signal versus time values can be reasonably fit to a logarithmic function, an attempt is made to correct the age following procedures recommended by Huntley and Lamothe (2001). The fading rate is calculated as the g-value, which is given in percent per decade, where decade represents a power of 10.

Equivalent dose

The equivalent dose is determined by a combination additive dose and regeneration (Aitken 1985). Additive dose involves administering incremental doses to natural material. A

growth curve plotting dose against luminescence can be extrapolated to the dose axis to estimate an equivalent dose, but for pottery this estimate is usually inaccurate because of errors in extrapolation due to nonlinearity. Regeneration involves zeroing natural material by heating to 450°C and then rebuilding a growth curve with incremental doses. The problem here is sensitivity change caused by the heating. By constructing both curves, the regeneration curve can be used to define the extrapolated area and can be corrected for sensitivity change by comparing it with the additive dose curve. This works where the shapes of the curves differ only in scale (i.e., the sensitivity change is independent of dose). The curves are combined using the "Australian slide" method in a program developed by David Huntley of Simon Fraser University (Prescott et al. 1993). The equivalent dose is taken as the horizontal distance between the two curves after a scale adjustment for sensitivity change. Where the growth curves are not linear, they are fit to quadratic functions. Dose increments (usually five) are determined so that the maximum additive dose results in a signal about three times that of the natural and the maximum regeneration dose about five times the natural.

A plateau region is determined by calculating the equivalent dose at temperature increments between 240° and 450°C and determining over which temperature range the values do not differ significantly. This plateau region is compared with a similar one constructed for the b-value (alpha efficiency), and the overlap defines the integrated range for final analysis.

Alpha effectiveness

Alpha efficiency is determined by comparing additive dose curves using alpha and beta irradiations. The slide program is also used in this regard, taking the scale factor (which is the ratio of the two slopes) as the b-value (Aitken 1985).

Radioactivity

Radioactivity is measured by alpha counting in conjunction with atomic emission for ^{40}K. Samples for alpha counting are crushed in a mill to flour consistency, packed into plexiglass containers with ZnS:Ag screens, and sealed for one month before counting. The pairs technique is used to separate the U and Th decay series. For atomic emission measurements, samples are dissolved in HF and other acids and analyzed by a Jenway flame photometer. K concentrations for each sample are determined by bracketing between standards of known concentration. Conversion to ^{40}K is by natural atomic abundance. Radioactivity is also measured, as a check, by beta counting, using a Risø low level beta GM multicounter system. About 0.5 g of crushed sample is placed on each of four plastic sample holders. All are counted for 24 hours. The average is converted to dose rate following Bøtter-Jensen and Mejdahl (1988) and compared with the beta dose rate calculated from the alpha counting and flame photometer results.

Both the rock and an associated soil sample are measured for radioactivity. Additional soil samples are analyzed where the environment is complex, and gamma contributions determined by gradients (after Aitken 1985: appendix H). Cosmic radiation is determined after Prescott and Hutton (1994). Radioactivity concentrations are translated into dose rates following Guérin et al. (2011).

Moisture Contents

Water absorption values for the rocks are determined by comparing the saturated and dried weights. For temperate climates, moisture in the pottery is taken to be 80 ± 20 percent of total absorption, unless otherwise indicated by the archaeologist. Again for temperate climates, soil moisture contents are taken from typical moisture retention quantities for different textured soils (Brady 1974: 196), unless otherwise measured. For drier climates, moisture values are determined in consultation with the archaeologist.

Procedures for Optically Stimulated or Infrared Stimulated Luminescence of Fine-grained pottery.

Optically stimulated luminescence (OSL) and infrared stimulated luminescence (IRSL) on fine-grain (1-8μm) samples are carried out on single aliquots following procedures adapted from Banerjee et al. (2001) and Roberts and Wintle (2001. Equivalent dose is determined by the single-aliquot regenerative dose (SAR) method (Murray and Wintle 2000).

The SAR method measures the natural signal and the signal from a series of regeneration doses on a single aliquot. The method uses a small test dose to monitor and correct for sensitivity changes brought about by preheating, irradiation or light stimulation. SAR consists of the following steps: 1) preheat, 2) measurement of natural signal (OSL or IRSL), L(1), 3) test dose, 4) cut heat, 5) measurement of test dose signal, T(1), 6) regeneration dose, 7) preheat, 8) measurement of signal from regeneration, L(2), 9) test dose, 10) cut heat, 11) measurement of test dose signal, T(2), 12) repeat of steps 6 through 11 for various regeneration doses. A growth curve is constructed from the L(i)/T(i) ratios and the equivalent dose is found by interpolation of L(1)/T(1). Usually a zero regeneration dose and a repeated regeneration dose are employed to insure the procedure is working properly. For fine-grained ceramics, a preheat of 240°C for 10s, a test dose of 3.1 Gy, and a cut heat of 200°C are currently being used, although these parameters may be modified from sample to sample.

The luminescence, L(i) and T(i), is measured on a Risø TL-DA-15 automated reader by a succession of two stimulations: first 100 s at 60°C of IRSL (880nm diodes), and then 100s at 125°C of OSL (470nm diodes). Detection is through 7.5mm of Hoya U340 (ultra-violet) filters. The two stimulations are used to construct IRSL and OSL growth curves, so that two estimations of equivalent dose are available. Anomalous fading usually involves feldspars and only feldspars are sensitive to IRSL stimulation. The rationale for the IRSL stimulation is to remove most of the feldspar signal, so that the subsequent OSL (post IR blue) signal is free from anomalous fading. However, feldspar is also sensitive to blue light (470nm), and it is possible that IRSL does not remove all the feldspar signal. Some preliminary tests in our laboratory have suggested that the OSL signal does not suffer from fading, but this may be sample specific. The procedure is still undergoing study.

A dose recovery test is performed by first zeroing the sample by exposure to light and then administering a known dose. The SAR protocol is then applied to see if the known dose can be obtained.

Alpha efficiency will surely differ among IRSL, OSL and TL on fine-grained materials. It does differ between coarse-grained feldspar and quartz (Aitken 1985). Research is currently underway in the laboratory to determine how much b-value varies according to stimulation method. Results from several samples from different geographic locations show that OSL b-value is less variable and centers around 0.5. IRSL b-value is more variable and is higher than that for OSL. TL b-value tends to fall between the OSL and IRSL values. We currently are measuring the b-value for IRSL and OSL by giving an alpha dose to aliquots whose luminescence have been drained by exposure to light. An equivalent dose is determined by SAR using beta irradiation, and the beta/alpha equivalent dose ratio is taken as the b-value. A high OSL b-value is indicative that feldspars might be contributing to the signal and thus subject to anomalous fading.

Laboratory procedures for IRSL dating of K-feldspar grains

The >90 µm fraction was treated with HCl, and then dry-sieved to isolate the 180-212 µm fraction. These grains were density separated using lithium metatungstate set at 2.58 specific gravity. Luminescence measurements were made on the <2.58 fraction. With feldspars, correction for anomalous fading, which is athermal loss of trapped charge through time, is required.

Single-grain dating was employed for all samples. Single-grain measurements were made using Risø TL/OSL DA-20 reader, with an IR single-grain attachment. Stimulation used a 150 mW 830 nm IR laser, set at 30% power and passed through an RG 780 filter. Emission was collected by the photomultiplier through a blue-filter pack, allowing transmission in the 350-450nm range. IRSL measurements were made at 50°C, and a preheat of 250°C for 1 minute at 5°C/s proceeded each measurement. Exposure for single-grains was for 0.8 s, using the first 0.06 s for analysis and the last 0.15 s for background.

Equivalent dose (De) was determined using the single-aliquot regenerative dose (SAR) protocol (Murray and Wintle 2000), and as applied to feldspars by Auclair et al. (2003). The SAR method measures the natural signal and the signal from a series of regeneration doses on a single aliquot. The method uses a small test dose to monitor and correct for sensitivity changes brought about by preheating, irradiation or light stimulation. SAR consists of the following steps: 1) preheat, 2) measurement of natural signal (OSL or IRSL), L(1), 3) test dose, 4) preheat, 5) measurement of test dose signal, T(1), 6) regeneration dose, 7) preheat, 8) measurement of signal from regeneration, L(i), 9) test dose, 10) preheat, 11) measurement of test dose signal, T(i), 12) repeat of steps 6 through 11 for i regeneration doses. A growth curve is constructed from the L(i)/T(i) ratios and the equivalent dose is found by interpolation of L(1)/T(1). A zero regeneration dose and a repeated regeneration dose are employed to insure the procedure is working properly.

Test doses for the SAR were about 5-6 Gy. Doses were delivered by a ^{90}Sr beta source, which provides about 0.11 Gy/s to 180-212 µm grains, and which was calibrated using quartz irradiated by a gamma source at Battelle Laboratory in Hanford, Washington. The dose delivered to different grains in single-grain disks varied by an order of magnitude from one end of the disk to the other. This variation was taken into account when determining doses to individual grains.

An advantage of single-grain dating is the opportunity to remove from analysis grains with unsuitable characteristics by establishing a set of criteria grains must meet. Grains are eliminated from analysis if they (1) had poor signals (as judged from net natural signals not at least three times above the background standard deviation), (2) did not produce, within 20 percent, the same signal ratio (often called recycle ratio) from identical regeneration doses given at the beginning and end of the SAR sequence, suggesting inaccurate sensitivity correction, (3) yielded natural signals that did not intersect saturating growth curves, or (4) had a signal larger than 10 percent of the natural signal after a zero.

Anomalous fading was measured using the procedures of Auclair et al. (2003) on single grains. Age was corrected following Huntley and Lamothe (2001). Storage times after irradiation of up to 3-5 days were employed.

A fading-corrected age was obtained for each suitable grain. Because of varying precision and other factors, the same value is not obtained for each grain even if all are of the same true age. Instead a distribution is produced. The common age model and central age model of Galbraith (Galbraith and Roberts 2012) are statistical tools that were used in evaluation of age distributions. The common age model controls for differential precision by computing a weighted average using log values. The central age model is similar except rather than assuming a single true value it assumes a natural distribution of estimated age values, even for true single-aged samples, because of non-statistical sources of variation that are not accounted for in the estimations, such as variation of luminescence properties among grains or heterogeneity in dose rate. It computes an over-dispersion parameter (σ_b) interpreted as the relative standard deviation (or coefficient of variance) of the true age estimates, or, in other words, that deviation beyond what can be accounted for by measurement error. Empirical evidence suggests that σ_b of between 10 to 20 percent for single-grains are typical. Over-dispersion will be higher for samples that are not single-aged because of partial bleaching or post-depositional mixing.

For the single-grain age distributions, a finite mixture model was employed for evaluation. This model (Galbraith and Roberts 2012) uses maximum likelihood to separate the grains into single-aged components based on the input of a given σ_b value and the assumption of a log normal distribution of each component. The model estimates the number of components, the weighted average of each component, and the proportion of grains assigned to each component. The model provides two statistics for estimating the most likely number of components, maximum log likelihood (llik) and Bayes Information Criterion (BIC). The finite mixture model is most useful for samples that have discrete rather than continuous age populations due to mixing. A minimum age model was also employed (Galbraith and Roberts 2012). This is designed to isolate statistically well-bleached grains from a distribution that includes partially bleached grains. The method assumes a truncated normal distribution, where the truncation represents the fully bleached grains. The over-dispersion estimated to represent a single-age sample is added to the error for each grain in quadrature.

.

Age and error terms

The age and error for both OSL and TL are calculated by a laboratory constructed spreadsheet, based on Aitken (1985). All error terms are reported at 1-sigma.

References

Adamiec, G., and Aitken, M. J., 1998, Dose rate conversion factors: update. *Ancient TL* 16:37-50.

Aitken, M. J., 1985, *Thermoluminescence Dating*, Academic Press, London.

Auclair, M., et al., 2003. Measurement of anomalous fading for feldspar IRSL using SAR. *Radiation Measurements*, 37: 487-492.

Banerjee, D., Murray, A. S., Bøtter-Jensen, L., and Lang, A., 2001, Equivalent dose estimation using a single aliquot of polymineral fine grains. *Radiation Measurements* 33:73-93.

Bøtter-Jensen, L, and Mejdahl, V., 1988, Assessment of beta dose-rate using a GM multi-counter system. *Nuclear Tracks and Radiation Measurements* 14:187-191.

Brady, N. C., 1974, *The Nature and Properties of Soils*, Macmillan, New York.

Galbraith, R. F., and Roberts, R. G., 2012. Statistical aspects of equivalent dose and error calculation and display in OSL dating: an overview and some recommendations. *Quaternary Geochronology* 11:1-27.

Guérin, G., Mercier, N., and Adamiec, G., 2011, Dose-rate converstion factors: update. *Ancient TL* 29:5-8.

Huntley, D. J., and Lamothe, M., 2001, Ubiquity of anomalous fading in K-feldspars, and measurement and correction for it in optical dating. *Canadian Journal of Earth Sciences* 38:1093-1106.

Mejdahl, V., 1983, Feldspar inclusion dating of ceramics and burnt stones. *PACT* 9:351-364.

Murray, A. S., and Wintle, A. G., 2000, Luminescence dating of quartz using an improved single-aliquot regenerative-dose protocol. *Radiation Measurements* 32:57-73.

Prescott, J. R., Huntley, D. J., and Hutton, J. T., 1993, Estimation of equivalent dose in thermoluminescence dating – the *Australian slide* method. *Ancient TL* 11:1-5.

Prescott, J. R., and Hutton, J. T., 1994, Cosmic ray contributions to dose rates for luminescence and ESR dating: large depths and long time durations. *Radiation Measurements* 23:497-500.

Roberts, H. M., and Wintle, A. G., 2001, Equivalent dose determinations for polymineralic fine-grains using the SAR protocol: application to a Holocene sequence of the Chinese Loess Plateau. *Quaternary Science Reviews* 20:859-863.